

INFORMATION TO USERS

This dissertation was produced from a microfilm copy of the original document. While the most advanced technological means to photograph and reproduce this document have been used, the quality is heavily dependent upon the quality of the original submitted.

The following explanation of techniques is provided to help you understand markings or patterns which may appear on this reproduction.

1. The sign or "target" for pages apparently lacking from the document photographed is "Missing Page(s)". If it was possible to obtain the missing page(s) or section, they are spliced into the film along with adjacent pages. This may have necessitated cutting thru an image and duplicating adjacent pages to insure you complete continuity.
2. When an image on the film is obliterated with a large round black mark, it is an indication that the photographer suspected that the copy may have moved during exposure and thus cause a blurred image. You will find a good image of the page in the adjacent frame.
3. When a map, drawing or chart, etc., was part of the material being photographed the photographer followed a definite method in "sectioning" the material. It is customary to begin photoing at the upper left hand corner of a large sheet and to continue photoing from left to right in equal sections with a small overlap. If necessary, sectioning is continued again – beginning below the first row and continuing on until complete.
4. The majority of users indicate that the textual content is of greatest value, however, a somewhat higher quality reproduction could be made from "photographs" if essential to the understanding of the dissertation. Silver prints of "photographs" may be ordered at additional charge by writing the Order Department, giving the catalog number, title, author and specific pages you wish reproduced.

University Microfilms

300 North Zeeb Road
Ann Arbor, Michigan 48106
A Xerox Education Company

MASTERS THESIS

M-3974

STEVENS, Carolyn Clark
A PROVENANCE STUDY OF THE TERTIARY SANDSTONES
IN THE HEALY CREEK AND LIGNITE CREEK COAL
BASINS, NENANA COAL FIELD, ALASKA.

University of Alaska, M.S., 1971
Geology

University Microfilms, A XEROX Company, Ann Arbor, Michigan

© 1973

CAROLYN CLARK STEVENS

ALL RIGHTS RESERVED

A PROVENANCE STUDY OF THE TERTIARY SANDSTONES
IN THE HEALY CREEK AND LIGNITE CREEK COAL BASINS,
NENANA COAL FIELD, ALASKA

A
THESIS

Presented to the Faculty of the
University of Alaska in Partial Fulfillment
of the Requirements
for the Degree of
MASTER OF SCIENCE

By

Carolyn Clark Stevens, B.S.

College, Alaska

May 16, 1971

A PROVENANCE STUDY OF THE TERTIARY SANDSTONES
IN THE HEALY CREEK AND LIGNITE CREEK COAL BASINS,
NENANA COAL FIELD, ALASKA

APPROVED:

Richard L. Allison

Florence R. Weber

Dean M. Triplehorn
Chairman

Carl S. Benson
Department Head

APPROVED: *Carl S. Benson* DATE: 1/20/70
Dean of the College of Earth Sciences
and Mineral Industry

Carl S. Benson
Vice President for Research and
Advanced Study

PLEASE NOTE:

Some pages may have

indistinct print.

Filmed as received.

University Microfilms, A Xerox Education Company

ABSTRACT

Forty-eight pebble samples, six sand samples, and 135 crossbed measurements from nine stratigraphic sections were utilized to determine paleodrainage patterns and source area(s) for the sediments of the "Tertiary coal-bearing group" in the Healy Creek and Lignite Creek coal basins. Directional data indicate that the major source of the sandstones in the Suntrana and Lignite Creek Formations is north of the depositional basins. Petrographic studies of 101 pebbles and six heavy mineral samples indicate complex low- to medium-grade metamorphic and granitic igneous source terranes for the sediments. The petrographic data, coupled with the paleocurrent data, suggest the northwestern part of the Yukon-Tanana Upland and adjacent areas as the most likely source terranes.

The depositional history of the Healy Creek and Lignite Creek coal basins was partially controlled by tectonic activity in the basins. This activity may have been directly related to tectonism in the source areas. Factor analysis of pebble data aided in tentative identification of north-south and west-northwest trending structural components active in the basin of deposition during Suntrana time.

The sediments of the Healy Creek Formation were locally derived from surrounding highlands of low- to medium-grade metamorphic terrane as moderate tectonic activity occurred in the central Alaska Range in late Oligocene or early Miocene time. Uplift in the Yukon-Tanana Upland and adjacent areas in the middle Miocene caused a reversal of paleodrainage directions and the Upland supplied most of the sediments to the basins during the deposition of the Suntrana and Lignite Creek Formations.

Abrupt increases in complexity of pebble and heavy mineral assemblages in the Lignite Creek Formation from those of the underlying Healy Creek and Suntrana Formations as well as the more arkosic nature of the Lignite Creek sediments seems to indicate rejuvenation of the Yukon-Tanana source land in the middle Miocene. Differing standard deviations from the grand means of the directional data in these formations apparently indicate an increase in paleoslope and resulting stream gradients at about the same time. These data also suggest rejuvenation of the source area.

TABLE OF CONTENTS

	<u>Page</u>
ABSTRACT	iii
CHAPTER I, INTRODUCTION	1
Purpose	1
Plan of Investigation	1
Acknowledgments	2
Location and Description of the Area	3
Geology	3
Preliminary Statement	3
Structure	6
Stratigraphy	6
Previous Works	12
CHAPTER II, METHODS OF INVESTIGATION	13
Directional Data	13
Field Methods	13
Laboratory Methods	15
Pebble Data	15
Field Methods	15
Laboratory Methods	17
Heavy Minerals	24
Field Methods	24
Laboratory Methods	26
CHAPTER III, RESULTS OF ANALYSES	30
Directional Data	30
Vector Means	30
Standard Deviations	30
Pebble Data	34
Factor Analysis	34
Petrography	34
Igneous extrusives	39
Igneous intrusives	41
Sedimentary rocks	42
Metamorphic rocks	43
Altered rocks	44
Heavy Mineral Data	46
CHAPTER IV, INTERPRETATION OF PROVENANCE AND DEPOSITIONAL AREA	49
Metamorphic Rocks	49
Sedimentary Rocks	51
Igneous Intrusives	53
Igneous Extrusives	55

	<u>Page</u>
Pebble Types versus Geology of the Proposed Source Area	55
Heavy Minerals versus Geology of the Proposed Source Area	55
Healy Creek Formation	57
Suntrana Formation	59
Lignite Creek Formation	59
Tectonics of the Source Land	60
Tectonics of the Depositional Site	65
Environment of Deposition	66
Paleoclimate	68
 CHAPTER V, GENESIS OF THE SANDSTONES AND SEDIMENTARY HISTORY	 69
Healy Creek Formation	69
Suntrana Formation	70
Lignite Creek Formation	75
Sedimentary History and Brief Tectonic Synthesis	77
Conclusions	80
Suggested Areas of Future Research	81
 REFERENCES CITED	 84
 APPENDIX I, DIRECTIONAL DATA	 88
 APPENDIX II, PETROGRAPHY OF PEBBLES	 91
 APPENDIX III, FACTOR ANALYSIS	 101

LIST OF TABLES

<u>Table</u>		<u>Page</u>
1	Frequencies of Rock Types in Pebble Samples of the Tertiary Sandstones (Hand Specimen Identification)	18
2	Percentages of Heavy Mineral Species in Six Sand Samples	28
3	"End Member" Samples for Q-Mode Factors 1 and 7	37
4	Sources of Derivation for Heavy Mineral Species	58
5	Heavy Minerals in Sandstones	62
6	Resumé of Prominent Characteristics of the "Tertiary Coal-Bearing Group" Strata	76
7	Resumé of Interpretations for the "Tertiary Coal-Bearing Group" Strata	78
8	Frequency Distribution of Corrected Crossbed Readings	89
9	Tabulation of Vector Means for Calculation of the Grand Mean	90
10	R-Mode Correlation Matrix of 49 Samples	104
11	Unrotated Factor Matrix (R-Mode)	109
12	Varimax Rotated Matrix Accounting for 75.5% of Total Problem Variance	113
13	List of R-Mode Factor Scores	115
14	Q-Mode Varimax Factor Maxtrix on Ten R-Mode Factors	117
15	Groups of Samples Having 75% Total Variance Accounted for by Eacy Q-Mode Factor	119
16	The 10 Single Samples Which Are Most Representative of Each Q-Mode Factor	120

LIST OF FIGURES

<u>Figure</u>		<u>Page</u>
1	Location of study area	4
2	Map showing locations of sampled stratigraphic sections in the Healy D-4 15' quadrangle	5
3	Geologic map of the study area	7
4	Map of coal fields in the northern foothills of the Alaska Range	10
5	Method of measuring dip directions of foreset beds	14
6	Flow chart of procedures used in treatment of crossbed data for each formation	16
7	Flow chart of procedures used in treatment of pebble samples and subsequent factor analysis	25
8	Flow chart illustrating methods used in preparing heavy minerals	29
9	Regional map of central Alaska with a composite rose diagram of all crossbed readings from the study area	31
10	Vector means for crossbed measurements from outcrops of the Suntrana Formation	32
11	Vector means for crossbed measurements from outcrops of the Lignite Creek Formation	33
12	Stratigraphic intervals covered by "isopach" maps of Q-mode factors 1 and 7	35
13	Isopach map of Q-mode factor 1	36
14	Isopach map of Q-mode factor 7	38
15	Classification of igneous rocks	40
16	Correlation between hand specimen and thin section identification of 101 pebbles	45

LIST OF FIGURES, Cont.

<u>Figure</u>	<u>Page</u>
17	Pebble assemblage determined from thin section 45
18	Heavy mineral assemblages, based on six samples, from the Healy Creek, Suntrana, and Lignite Creek Formations 47
19	Physiographic provinces of east-central Alaska 50
20	General geologic map of the Yukon-Tanana Upland 52
21	Major faults of east-central Alaska and alignment of alkalic intrusives 54
22	Coal fields of central and south-central Alaska 67
23	"Isopach" map of factor 7 compared to regional distribution of coal basins in the Nenana coal field 72
24	Nenana coal field basins showing northern limits of the coal-bearing formations 73
25	Highlands and basins of Mesozoic and Early Cenozoic time 74
26	Isopach map of Q-mode factor 2 122

LIST OF PLATES

<u>Plate</u>		<u>Page</u>
I	Healy Creek Stratigraphic Sections	In Pocket
II	Lignite Creek Stratigraphic Sections	In Pocket

CHAPTER I INTRODUCTION

Purpose

The purpose of this study is to investigate the paleodrainage patterns of the Healy Creek and Lignite Creek coal basins using data collected from the Tertiary fluvial sandstones. An attempt has been made: (1) to establish a regional paleocurrent direction for the stratigraphic interval studied; (2) to determine the number of source areas which contributed to the sediments in the study area; (3) to determine the location and nature of the source area or areas; and (4) to reconstruct a sedimentary history of the northern foothills of the central Alaska Range. To accomplish these objectives, crossbed analyses, pebble analyses, and heavy mineral analyses were utilized. Crossbed analyses were used primarily to reconstruct the major character of the regional drainage pattern; heavy mineral analyses and pebble analyses were used to determine the general lithologic character of the source area(s).

Plan of Investigation

The present study results from both field work and laboratory research. Field work was completed in July, August, and September of 1969 and included field measurements of crossbeds, sand sample collection, and pebble collection of selected sections located in the Healy Creek and Lignite Creek areas (see Plates I and II in the pocket). Sections were specifically selected to achieve maximum areal distribution and vertical exposure. Sample selection was necessarily influenced by accessibility and exposure. Some well-documented, accessible sections of coal-bearing sandstone have been partially or totally destroyed by recent mining operations; others are in the cutbanks of swift streams or on precipitous slopes where they were not possible to sample. Approximately 160 sand samples were collected, of which six have been utilized in heavy mineral separations and determinations. Forty-eight pebble samples of 100 pebbles each were collected and

analyzed. Thin sections of 101 selected pebbles were studied for the purpose of more accurate determination of rock types. One hundred thirty-five crossbed measurements were recorded, corrected for tectonic tilt, and then utilized in the construction of rose diagrams for paleocurrent studies.

Acknowledgments

I am deeply indebted to the following people who aided in the preparation of this thesis.

Mr. Joe Usibelli of the Usibelli Coal Mines graciously provided housing for me and my assistant during the course of the field work. Dr. Richard C. Allison of the Geology Department provided the field check and patiently devoted his time to criticizing the manuscript and offering helpful suggestions. Dr. Don M. Triplehorn of the Geology Department and Mrs. Florence R. Weber of the U.S. Geological Survey also made many valuable suggestions during the research and manuscript preparation.

Special thanks are due to Dr. D. B. Hawkins of the Geology Department who unselfishly devoted much time and effort in helping me prepare the parts of the thesis concerned with factor analysis. Dr. Clyde Wahrhaftig of the U. S. Geological Survey provided much useful information about the general area of study through discussions during a field trip in the Alaska Range and adjacent areas, including the study area. Much of the information in this report is based upon years of research in the area by Dr. Wahrhaftig and his colleagues.

Dr. C. M. Hoskin, Dr. D. K. Ray, Dr. Roger Slatt, and Jack Kerin, all of the Geology Department, made many helpful suggestions on various aspects of the problem. Dr. Marvin Andresen of Geonomics and Dr. A. S. Naidu of the Institute of Marine Science provided constructive criticisms of some interpretations of the data.

Miss Martha Aiken of the University of Alaska proved to be a very able and willing field assistant without whose help field work would have been difficult. David E. Livingston accompanied the field party during the excursion into the Lignite Creek area.

The summer field work and part of the thesis expenses were financed through

a National Science Foundation Summer Traineeship grant and an Alaska Business Council Scholarship. The Geology Department of the University of Alaska met some of the other necessary expenses of the project.

My husband, Don, made numerous suggestions in most areas of the research and manuscript preparation. In addition, he has done nothing but encourage me in my work. His complete support is deeply appreciated. Del Stevens provided drafting skills and Elaine Sachse freely contributed her time and talents during the photographic reproduction of the thesis illustrations. Virginia Heiner typed the final manuscript.

Location and Description of the Area

The Healy Creek and Lignite Creek coal basins are situated in the southwestern portion of the Nenana coal field, an area located in the northern foothills of the central Alaska Range between latitudes $63^{\circ} 45'$ and $64^{\circ} 15'$ N. and longitudes $147^{\circ} 30'$ and $149^{\circ} 15'$ W. The area of this study is entirely contained within the Healy D-4 15' quadrangle (1963) as defined by latitudes $63^{\circ} 45'$ and $60^{\circ} 00'$ N. and longitudes $148^{\circ} 30'$ and $149^{\circ} 00'$ W. (Fig 1, p. 4) and is confined to sections located within the drainage basins of Healy and Lignite creeks (Fig. 2, p. 5). The Healy Creek and Lignite Creek drainage basins are essentially parallel and are characterized by asymmetrical valleys drained by westward-flowing streams. Structural control of the topography results in steep valley walls to the north of the streams, and more gentle slopes to the south. The Healy Creek basin lies directly east of Healy Station on the Nenana River and is presently accessible by road. The Lignite Creek basin is located east of Lignite and, at the time of this study, was accessible only by foot.

Geology

Primary Statement

The following general summaries of the structure and stratigraphy

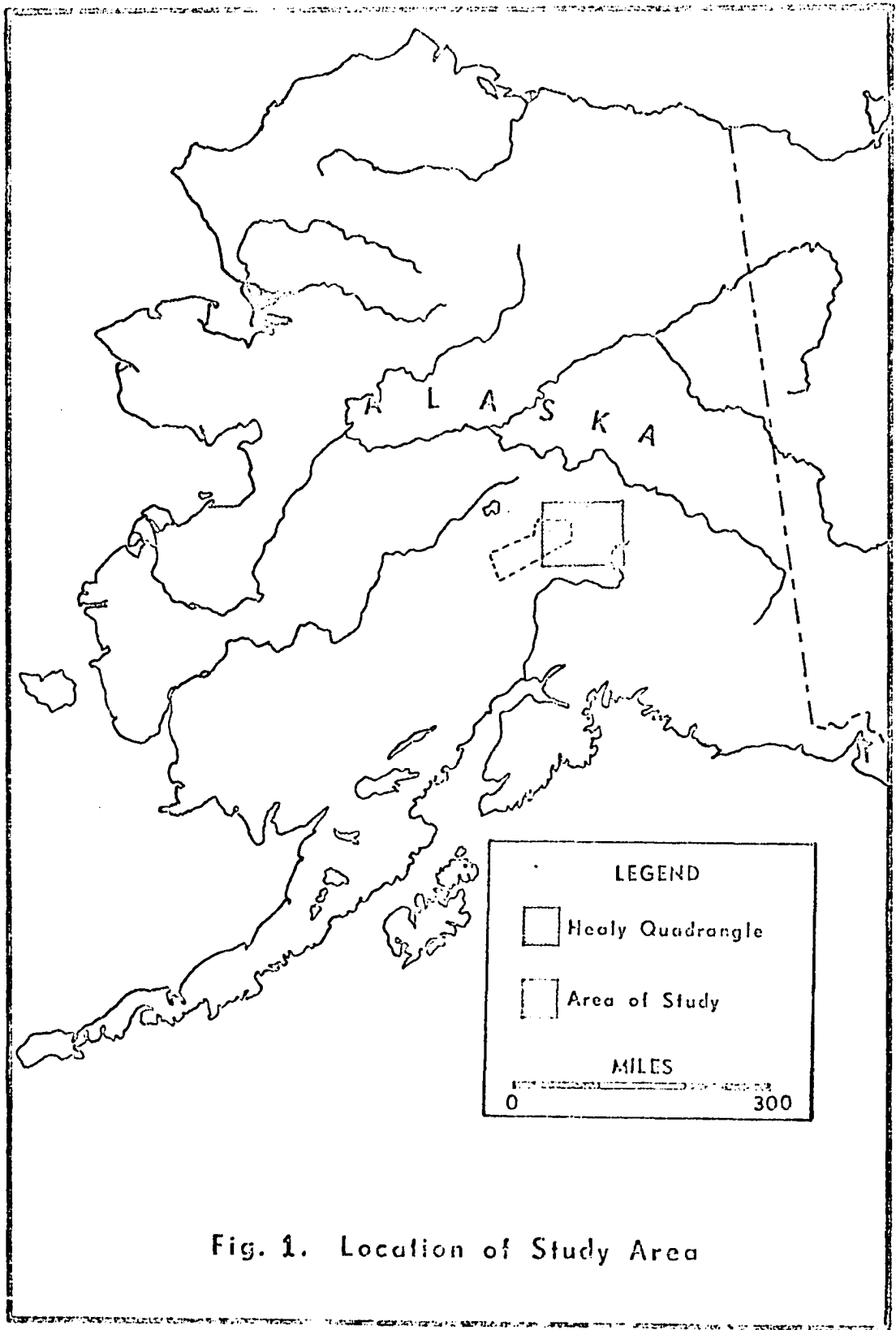


Fig. 1. Location of Study Area



FIGURE 2. Map showing locations of sampled stratigraphic sections in the Healy D-4 15' quadrangle (1963).

of the study area are abstracted from the literature. For further details, the reader is referred to Wahrhaftig, Hickcox, and Freedman (1951, pp. 154-156; and Wahrhaftig, Wolfe, Leopold, and Lanphere (1969).

Structure

Tertiary rocks of the Healy Creek and Lignite Creek areas lie in two asymmetrical plunging synclines whose axes trend east-west parallel to the Alaska Range (Fig. 3, p. 7). The Healy Creek syncline plunges approximately 20° to the west, while the Lignite Creek syncline is exposed in the eastern part of Lignite Creek where it plunges to the east. The two synclines are separated by a belt of Birch Creek Schist which is bounded on the south by a fault having a vertical displacement of more than 5000 feet according to Wahrhaftig and others (1951, p. 154). In Healy Creek, the Tertiary rocks dip 25° to 40° N. and strike N. 65° E. to due east on the south limb of the syncline. The north limb is characterized by beds striking N. 65° to 70° W. and dipping 65° S. to vertical with local overturning. In general, Tertiary rocks on the south limb of the Lignite Creek syncline strike N. 70° E. and dip 10° to 15° N.W. A westward-plunging anticline cored by Birch Creek Schist is exposed near the mouth of Lignite Creek. Minor flexures superimposed upon the major structures include a dome exposed on the east bank of the Nenana River two miles north of the mouth of Lignite Creek. The beds in the eastern half of Lignite Creek valley generally dip northward and are cut by three zones of traverse hinge faults (Wahrhaftig and others, 1951, pp. 154-156).

Stratigraphy

The Tertiary coal-bearing rocks of the Nenana coal field were first informally designated "Tertiary coal-bearing formation" by Capps in 1919. This term was in general use until 1969 when Wahrhaftig and others informally designated the Tertiary coal-bearing formation (Tcb) as the "Tertiary coal-bearing group" and formally divided it into five formations: The Healy Creek, Sanctuary, Suntrana, Lignite Creek, and Grubstake formations (Wahrhaftig and others, 1969). The Tertiary coal-bearing group rests nonconformably on Birch Creek Schist and

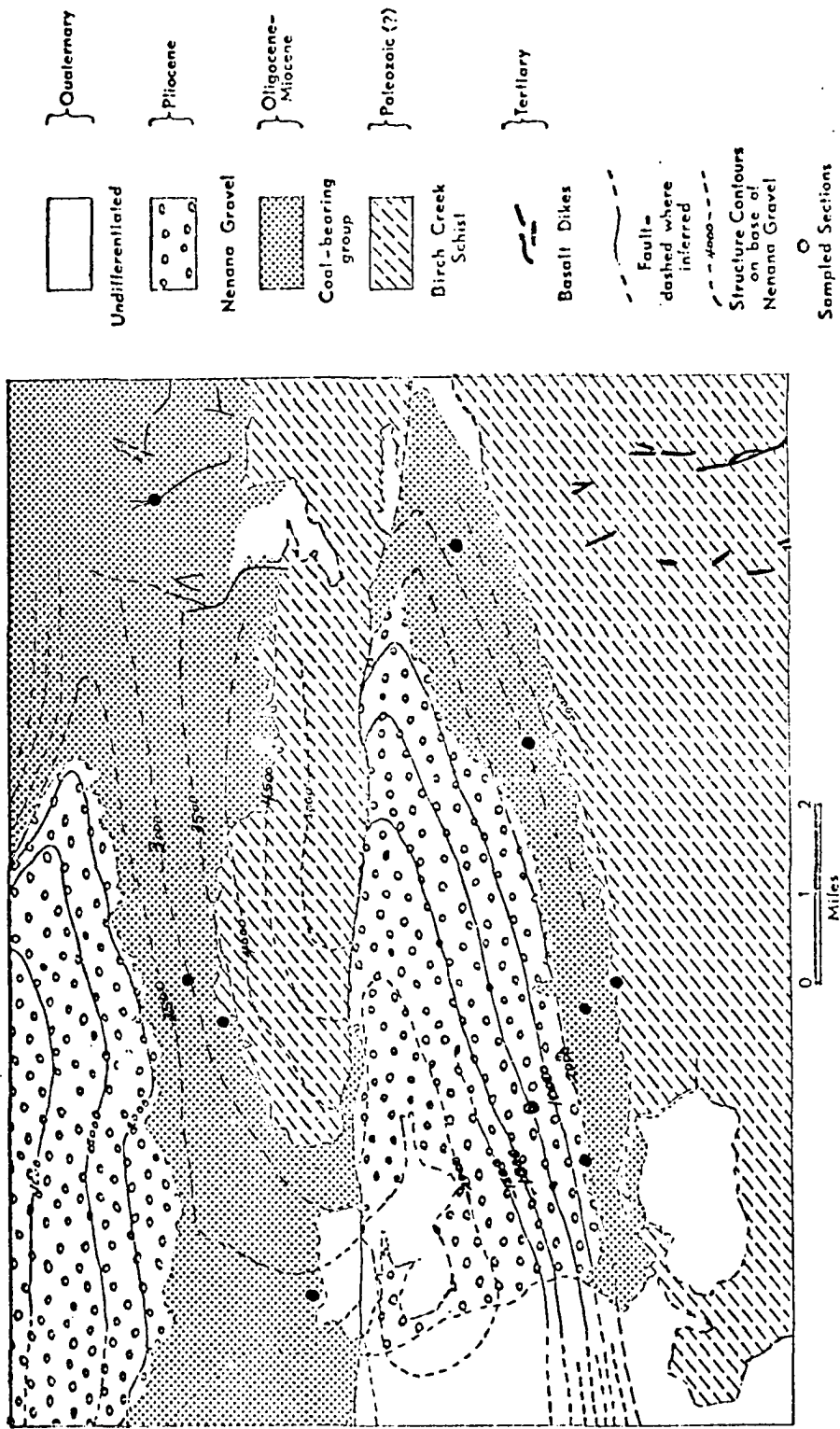


Figure 3. General geologic map of the study area (after Wahrhaftig, 1970).

is conformably overlain by the Nenana Gravel.

The Birch Creek Schist in the study area is, according to Wahrhaftig (1968, p. E10) "...predominantly quartz-sericite schist, quartzite, sericite schist, and quartz-sericite-calcite schist, with minor amounts of carbonaceous schist and marble." Mineral assemblages derived from metamorphosed bodies of intrusives and volcanics within the schist establish the metamorphic grade as greenschist. The Birch Creek Schist is exposed in a belt along the northern flank of the Alaska Range and apparently is correlative with the crystalline basement schist of similar metamorphic grade and general description of the Yukon-Tanana region (Capps, 1940, p. 95). Thickness of the schist is impossible to measure, but it is believed to be at least 10,000 feet (Wahrhaftig, 1968, p. E10). No fossils have yet been found in the Birch Creek Schist, but recent investigations have led some workers to believe that it may be Late Precambrian to Early Paleozoic in age (Foster and Weber, *abs.*, 1970). In the study area, the oldest formation of the Tertiary coal-bearing group, the Healy Creek Formation, rests directly on the Birch Creek Schist.

The Healy Creek Formation consists of poorly consolidated conglomeratic sandstone, claystone, and subbituminous coal. Lenticularity of the beds and general mixing of sediment types within the beds are characteristic of this formation. The Healy Creek is recognized in the Sushana River area to the west and in the Jarvis Creek coal field to the east, a distance of 125 miles, and is probably correlative with other isolated patches of coal-bearing rocks in the Alaska Range and adjacent regions. The formation is approximately 800 feet thick at the eastern extremity of the Healy Creek coal basin. It thickens to 1150 feet to the west in the Lignite Creek coal basin and to 2000 feet to the east in the Jarvis Creek coal field. Plant megafossils and pollen indicate that the Healy Creek Formation is late Oligocene to early Miocene in age (Wolfe in Wahrhaftig, *et al.*, 1969, pp. D9-D12). The formation is overlain conformably by the Sanctuary Formation.

The Sanctuary Formation typically consists of a brown-weathering, finely-banded gray shale. At the type section, the upper half of the formation contains thin sand beds and is generally silty, a characteristic which is common to the formation in other areas of the Nenana coal field. In the Healy Creek coal basin, the formation ranges in thickness from about 120 feet at the type section at Suntrana to 350 feet at the eastern edge of the coal basin. In the Lignite Creek coal basin, the Sanctuary Formation increases in thickness from 5 to 250 feet from west to east.

It is present in the Rex Creek coal basin (Fig. 4 , p. 10) on Kansas Creek, on the Coal Creek tributary of Wood River, on Tatlanika Creek, and in an area southwest of the Sanctuary River. It may also be present in the Mt. Hayes D-4 quadrangle on the east bank of the Delta River just west of Donnelly Dome. Plant fossils suggest an early to middle Miocene age for the Sanctuary Formation (Wolfe in Wahrhaftig et al., 1969, pp. D15-D16). In the study area, the formation is conformably overlain by the Suntrana Formation.

The Suntrana Formation consists of repeated sequences of coarse pebbly sandstone grading upward into medium- and fine-grained sandstone, claystone, and coal. The major coal reserves and most of the thicker, more continuous coal beds of the Nenana coal field are contained within the Suntrana Formation. The poorly consolidated sandstones are generally clean, well-sorted, and crossbedded; the coal has a dark-brown streak and tends to break into equidimensional blocks. The formation is widely exposed along both Healy and Lignite creeks and may also be present in the Rex Creek coal basin. It also appears at the heads of Tatlanika Creek and Coal Creek, a tributary of the Wood River (Fig. 4 , p. 10). The Suntrana Formation is assigned an age of middle Miocene on the basis of plant fossils (Wolfe in Wahrhaftig et al., 1969, pp. D18-D19). The formation is conformable with the overlying Lignite Creek Formation within the study area.

The Lignite Creek Formation is composed of two facies: a coal-bearing facies, and a non-coal-bearing facies. The coal-bearing facies is exposed in the Wood River coal basin, on Tatlanika Creek, and in the Healy Creek and Lignite Creek coal basins (Fig. 4 , p. 10), whereas the non-coal-bearing facies is exposed in the northern and western areas of the Nenana coal field. The coal-bearing facies is similar to the Suntrana Formation with respect to the repeated sequences of sandstone, claystone, and coal, but differs in some respects. For example, the upper portions of the individual cyclic sequences contain thin coal beds interbedded with claystone, whereas in the Suntrana Formation, the upper parts of these cyclic sequences are composed of thicker coal beds. The coal-bearing facies of the Lignite Creek Formation thickens southward and eastward from a minimum thickness of 500 feet in the northwestern part of the Lignite Creek coal basin to a maximum of 800 feet in the Wood River coal basin. The sandstones are similar to those of the Suntrana Formation in that they are often pebbly, poorly consolidated, generally clean, well-sorted, and crossbedded. However, vari-colored heavy minerals and rock fragments in the sandstones of the Lignite Creek Formation are in marked contrast

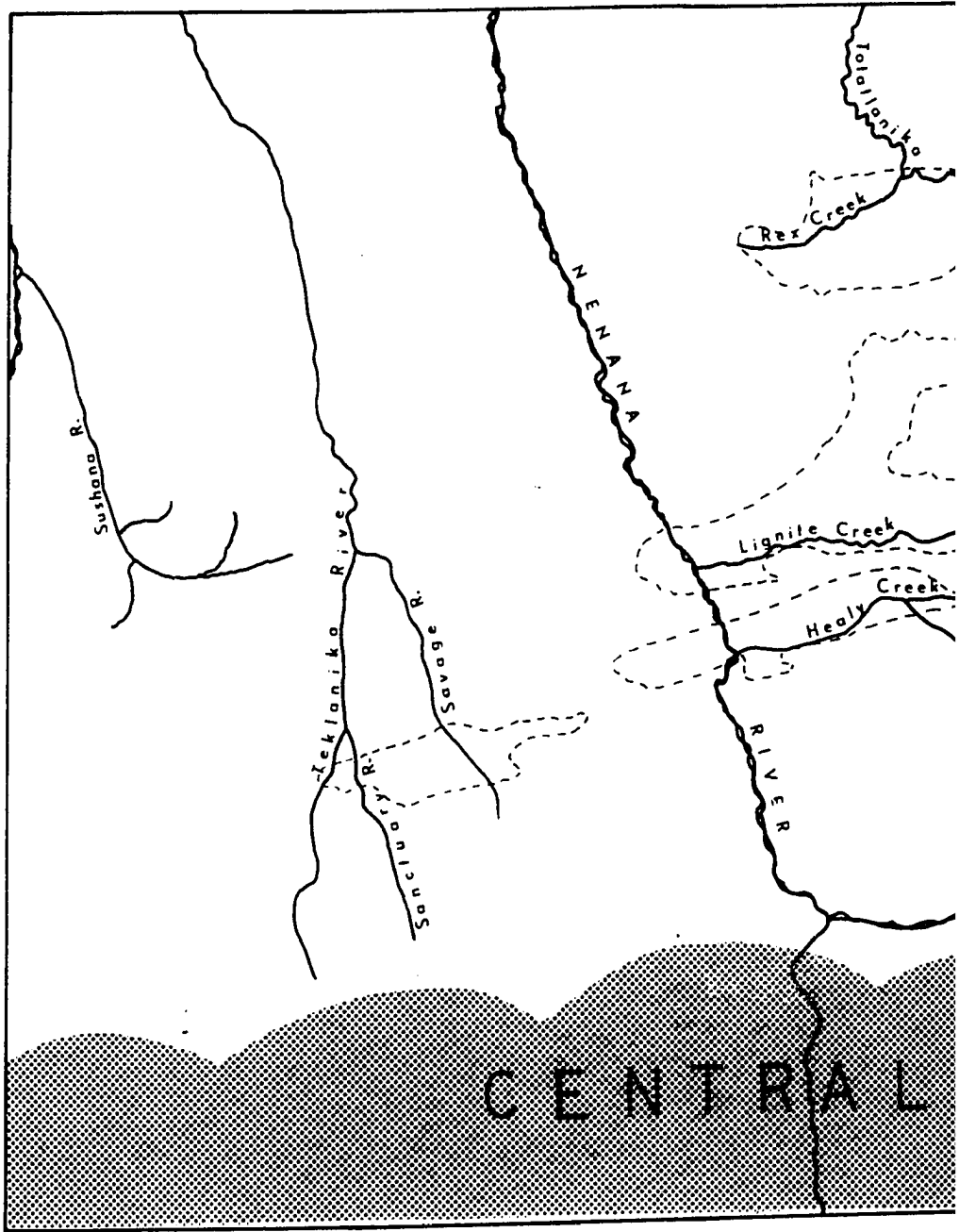
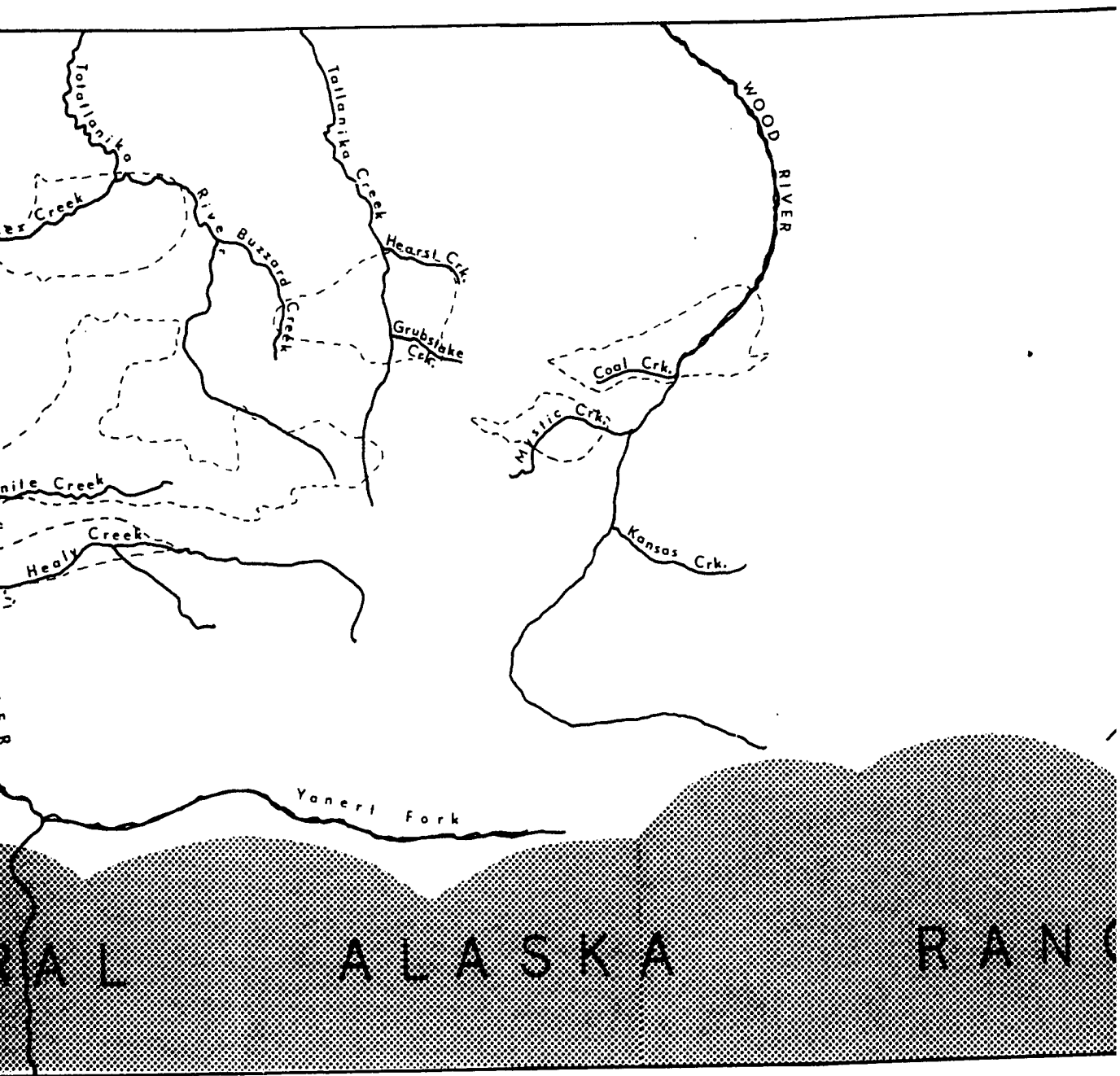
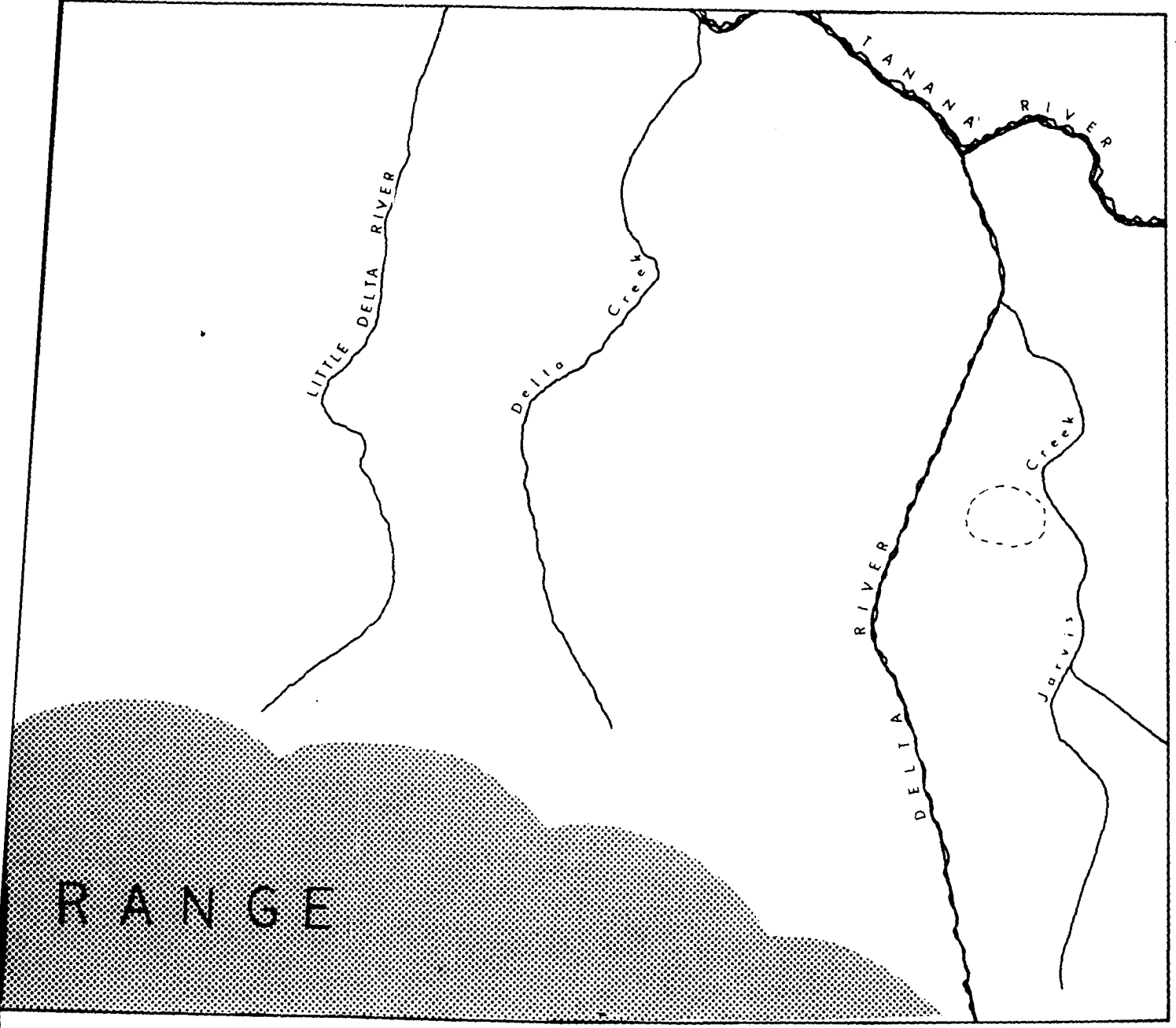


Figure 4. Coal fields in the northern foothills of the



Hills of the Alaska Range (after Wahrhaftig, et al., 1969).



----- Approximate boundary
of coal basin

to the "salt-and-pepper" sandstone of the underlying Suntrana Formation. Upon weathering, the coals break up into masses of long narrow flakes parallel to the bedding, whereas Suntrana coals are blocky. The non-coal-bearing facies inter-fingers with the coal-bearing facies along Tatlanika Creek north of Hearst Creek. The non-coal-bearing facies thickens to the northeast from 250 feet to a maximum of about 1300 feet along the northern edge of the foothills. On the basis of a few plant fossils, the Lignite Creek Formation is assigned to the middle Miocene (Wolfe in Wahrhaftig, et al., 1969, pp. D21-D22). The formation is conformably overlain by the Grubstake Formation in this area.

The Grubstake Formation is typically composed of interbedded dark claystone, dark sandstone, and fine conglomerate. In the Healy Creek and Lignite Creek basins, the formation is composed of a thin-bedded shale and siltstone with a thin bony coal bed at the base. The upper part of the unit contains sandstone and siltstone interbedded. Volcanic glass shards occur at a horizon about one-fourth to one-third of the thickness above the base. At the type section along the east bank of Tatlanika Creek (Fig. 4, p. 10), near the mouth of Grubstake Creek, the formation is about 600 to 1000 feet thick. Maximum thickness of about 1500 feet is attained at a point north of the Coal Creek tributary of the Wood River. It is about 250 feet thick in the eastern end of the Healy Creek coal basin. The megafossil flora of the basal Grubstake Formation indicates that it cannot be older than late Miocene (Wolfe in Wahrhaftig, et al., 1969, pp. D26-D27). The contact of the Nenana Gravel with the underlying Grubstake Formation is generally conformable although local discordance has been noted (Wahrhaftig, et al., 1969).

The Nenana Gravel consists of unconsolidated or loosely cemented, well-rounded pebbles and cobbles. Subordinate amounts of sand are present, and some large cobbles and boulders occur locally. A great variety of rock types are represented; the most common being quartz, quartzite, schist, conglomerate, and a large suite of igneous rock clasts. The gravel characteristically weathers to a buff or yellow color which distinguishes it from younger, less oxidized bluish-colored gravels. The Nenana Gravel is widely exposed in the northern foothills of the central Alaska Range and, although the maximum thickness is not known, it reaches local thicknesses of almost 2000 feet. The age of the Nenana Gravel is not definitely known, but is presumed to be late Miocene or Pliocene, owing to its stratigraphic relationship with the underlying Grubstake Formation and with the younger, unoxidized Pleistocene gravels which occur in deep erosional valleys within the Nenana

Gravel. The formation is considered to be conformable with the underlying Grubstake Formation in most places, but is apparently unconformable in a few scattered localities (Capps, 1940, pp. 123-127).

Previous Works

The Nenana coal field was probably discovered about 1898 but no geological reconnaissance studies were conducted until 1902, when A. H. Brooks and L. M. Prindle made brief observations which were reported by A. J. Collier (1903, p. 46). Further mentions of studies in the Nenana coal field were made by Prindle (1907, pp. 223-225) and Brooks (1911, pp. 95-103), who correlated the coal-bearing rocks with those of the Kenai Formation and suggested an Eocene (?) age for them. In 1910, S. R. Capps (1912) outlined the coal basins approximately as they are known today. G. C. Martin (1919) made a detailed study of the Lignite Creek area of the coal field in 1918 and measured many sections.

No further investigations of significance were made in the area until 1944 and 1945 when U. S. Geological Survey field parties mapped the Healy Creek and Lignite Creek coal basins in detail (Wahrhaftig, et al., 1951, pp. 141-165). Further studies by U. S. G. S. personnel have continued, notably investigations made by Wahrhaftig and others. A comprehensive U. S. Geological Survey publication is forthcoming on the area and a series of geological maps is now published. The Tertiary coal-bearing group was recently divided into five formations, the Healy Creek Formation, the Sanctuary Formation, the Suntrana Formation, the Lignite Creek Formation, and the Grubstake Formation (Wahrhaftig, et al., 1969). These stratigraphic units are reviewed above in the geologic section of this report.

CHAPTER II METHODS OF INVESTIGATION

Crossbedding directional data and petrographic data from pebbles and heavy minerals were employed as analytical tools. Field and laboratory techniques used in collecting and preparing data are presented in this chapter.

Directional Data

Field Methods

The study of directional sedimentary rock features was confined to the measurement and interpretation of foreset dip azimuths of both planar and concave crossbedding. In terms of Allen's (1963) classification, these structures are both grouped and solitary, grouped structures apparently being more common.

Crossbedding in the Lignite Creek and Suntrana formations is common, generally accessible, and easily measured. In the Healy Creek formation, crossbeds are often inaccessible or could not be measured by the method employed, owing to the coarseness and degree of induration of the conglomeratic sandstones. In the thicker sandstone units of the Lignite Creek and Suntrana formations, at least three sets of crossbeds were measured. Generally these measurements were taken near the base, middle, and top of each unit to obtain a uniform distribution of measurements. In sandstone units where crossbedding was sparse or poorly exposed, measurements were taken at all available exposures.

Only one reading was recorded for each individual set of crossbeds. The determinations were made with the Brunton compass using a variation of the measuring technique described in Potter and Pettijohn (1963, pp. 77-78; also Pryor, 1958). Figure 5 illustrates the method of measuring crossbeds.



Figure 5. Method of measuring dip directions of foreset beds. A) Dip direction indicator is placed in the plane of the crossbed and rotated until the bubble in the level is centered. This defines the strike of the foreset bed. B) An aluminum needle or rod is then forced into the unconsolidated sand perpendicular to the defined strike, thus defining the direction of true dip. C) The Brunton compass is then placed perpendicular to the aluminum rod and the azimuth of the strike is determined. D) The back of the compass is then placed parallel to the aluminum rod in the direction of true dip. Alignment of the compass parallel to the apparent dip of the beds behind the rod gives the angle of true dip.

A total of 135 readings were taken of foreset beds from nine sections (location map, Fig. 2). Sixty-eight of these readings were taken in the Suntrana Formation and 64 readings were taken in the Lignite Creek Formation. Only three readings are available from the Healy Creek Formation.

Control for correction of tectonic tilt of the crossbedded units was acquired by determining the strike and dip of the numerous well-exposed coal seams distributed throughout the sections.

Laboratory Methods

Crossbed measurements were corrected for tectonic tilt by means of the Wulff stereonet. Corrections of crossbed measurements taken in sedimentation units close to coal seams were controlled by the attitude of the coal seams, whereas corrections of measurements taken near the middle of sandstone units were controlled by the average strike and dip values of the two bounding coal seams.

After tilt correction, vector means for each formation at each locality were calculated, then the grand mean for each formation was calculated from the vector means (Royse, 1970, pp. 137-149) and rose diagrams for each formation were constructed from all the readings in that formation. Figure 6 is a flow chart illustrating treatment of crossbed data.

Pebble Data

Field Methods

A major part of this investigation concerns selection and analysis of pebble suites from the different sandstone units. A limited size range of 16 to 32 mm. (-4 phi to -5 phi) was arbitrarily chosen for the pebble samples; thus the number of pebble counts was determined in part by the number and distribution of pebble horizons containing sufficient pebbles of this size. A brief reconnaissance indicated

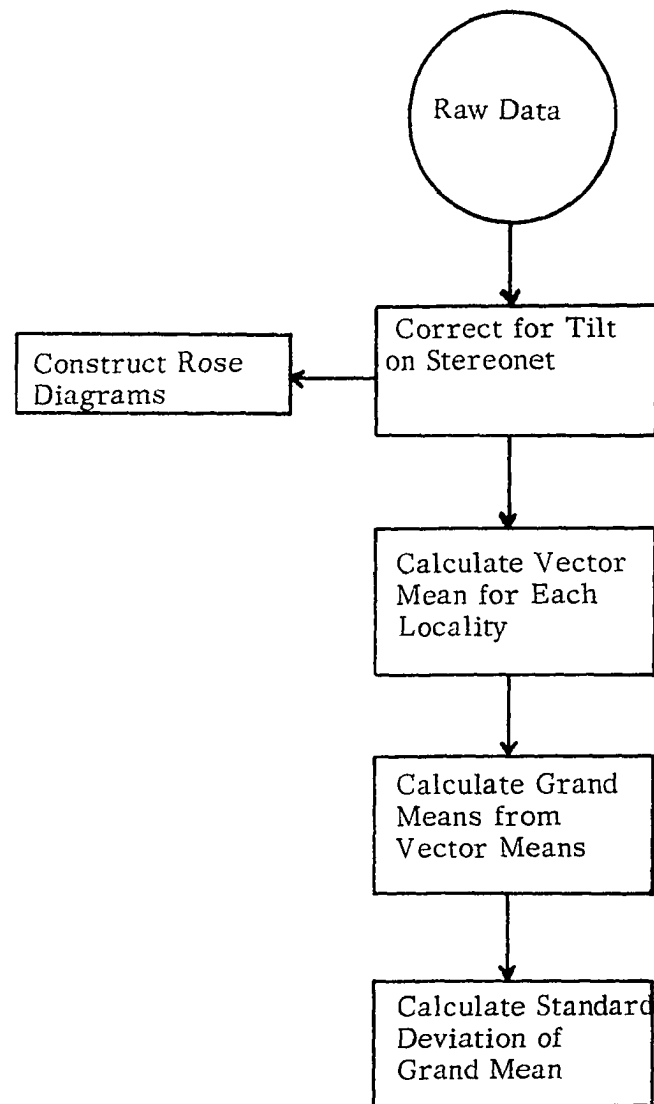


FIGURE 6

Flow Chart of Procedures Used in Treatment of Crossbed Data for Each Formation

that sufficient samples within the 16-32 mm size range could be obtained with good areal and vertical distribution (Wahrhaftig *et al.*, 1969, pp. D17 and D20). This size range was selected because such pebbles are large enough for visual petrologic classification, convenient for thin sectioning, and an adequate sample is not large or heavy. Also, Wahrhaftig (in Wahrhaftig *et al.*, 1969, pp. D17 and D20) indicated that the average size of pebbles in the Suntrana and Lignite Creek formations is 1/4 to 2 inches in diameter.

Pronounced pebble horizons were sampled, and particular efforts were made to sample those occurring immediately above marked lithologic changes. The first 100 pebbles taken within the given size range constituted the pebble sample. One hundred pebbles were chosen for each sample because this number is adequately large, simplifies percentage calculations (when pebble breakage does not occur), and does not constitute a bulky sample. Forty-eight pebble samples were collected and analyzed in the laboratory.

Laboratory Methods

The pebbles in each of the samples were examined under a binocular microscope and sorted into general rock types. These types were grouped into two major divisions: "nondiagnostic" and "diagnostic," based upon their usefulness in determining source areas. "Nondiagnostic" types included quartz, chert, argillite, quartzite, sandstone, conglomerate, breccia, low-grade schist, and others. "Diagnostic" types included all kinds of igneous rocks, higher grade schist, and unknowns (Table 1, p. 19).

Diagnostic pebbles were stained to differentiate feldspar types. Each pebble was etched in concentrated HF acid, rinsed in water, and then immersed in a saturated solution of sodium cobaltinitrite (Chayes, 1952). After drying, the pebbles were immersed in a 5% solution of barium chloride, rinsed in water, dried again, and then immersed in amaranth (F.D. and C. red #2) solution (Laniz *et al.*, 1963). After final rinsing and drying, yellow-stained potassium feldspar and pink-stained plagioclase were readily discriminated. The feldspar stains then permitted classification of the "diagnostic" pebbles into more specific rock types. Representatives of most common igneous rock types were tentatively identified.

Following staining and identification, the tabulated results were stated as

TABLE 1
 Frequencies of Rock Types in Pebble Samples of the Tertiary Sandstones
 (Hand Specimen Identification)

Healy Creek Formation

Pebble Counts	Sr-A-11	Sr-A-1	4-3	4-2
Total No. Pebbles	103	111	98	104
Total Percent	100.0	99.9	99.9	99.8
Unknown	---	---	---	---
Schist	1.0	---	---	---
Diabase	---	---	---	---
Quartz Diorite	---	---	---	---
Dacite	---	---	---	---
Diorite	---	---	---	---
Andesite	---	---	---	---
Granodiorite	---	---	---	---
Rhyodacite	---	---	---	---
Monzonite	---	---	---	---
Latite	---	---	---	---
Quartz Latite	---	---	---	---
Quartz Monzonite	---	---	---	---
Trachyte	---	---	---	---
Syenite	---	---	---	---
Rhyolite	---	---	---	---
Granite	---	---	---	---
Others	---	---	---	---
Schist	---	.9	---	---
Breccia	---	---	---	---
Conglomerate	---	---	1.0	---
Sandstone	---	---	1.0	---
Quartzite	7.8	7.2	9.2	17.3
Argillite	2.9	9.9	5.1	3.8
Chert	27.2	17.1	21.4	25.9
Quartz	61.1	64.8	62.2	52.8

TABLE 1, Cont.
 Frequencies of Rock Types in Pebble Samples of the Tertiary Sandstones
 (Hand Specimen Identification)

Suntrana Formation

Pebble Counts	A-C-2	A-C-8	A-C-11	A-C-14	Sc-C-14	Sc-C-6	Sc-C-1	UV-C-6	UV-C-2
Total No. Pebbles	107	100	101	101	104	113	116	101	112
Total Percent	99.4	(100)	100	(100.2)	99.9	99.3	99.8	100	99.7
Unknown	1.9	3	---	---	---	---	---	---	.9
Schist	.9	1	---	4.0	1.0	---	---	---	1.8
Diabase	---	---	---	---	---	---	---	---	---
Quartz Diorite	---	---	---	---	---	---	---	---	---
Dacite	---	---	---	---	---	---	---	---	---
Diofite	.9	---	---	---	---	---	---	---	---
Andesite	---	---	---	---	---	---	---	---	---
Granodiorite	---	---	---	---	---	---	---	---	.9
Rhyodacite	---	---	---	---	---	---	---	---	---
Monzonite	---	---	---	---	---	---	---	---	---
Latite	---	---	1.0	---	---	---	---	---	2.7
Quartz Latite	---	---	---	---	---	---	---	---	2.7
Quartz Monzonite	.9	---	3.0	1.0	1.9	---	---	2.0	---
Trachyte	---	---	---	1.0	1.9	---	---	---	---
Syenite	---	---	---	---	---	---	---	---	---
Rhyolite	1.9	---	2.0	---	1.9	---	---	2.0	---
Granite	3.7	1	2.0	2.0	---	---	---	1.0	---
Others	.9	---	---	2.0	---	---	---	---	---
Schist	5.6	1	2.0	---	---	---	---	---	.9
Breccia	.9	---	1.0	---	---	---	---	---	.9
Conglomerate	.9	4	---	---	1.9	3.5	---	---	---
Sandstone	2.8	5	5.9	3.0	1.0	2.6	---	3.0	2.7
Quartzite	32.6	25	26.7	29.7	34.6	27.3	12.9	37.6	32.9
Argillite	3.7	3	5.9	5.0	7.7	12.3	6.9	7.9	6.2
Chert	16.7	7	8.9	8.9	10.6	15.8	31.0	11.9	4.4
Quartz	25.1	50	41.6	43.6	37.4	37.8	49.0	34.6	42.7

TABLE 1, Cont.
 Frequencies of Rock Types in Pebble Samples of the Tertiary Sandstones
 (Hand Specimen Identification)

Suntrana Formation, Cont.

Pebble Counts	UV-C-13	2-13	2-8	5-20	5-24	5-31	5-34	5-37	5-39	11-10a
Total No. Pebbles	105	101	108	98	100	101	99	106	103	105
Total Percent	100.0	100.1	99.2	99.7	(100)	100.1	99.9	99.6	99.9	99.9
Unknown	1.9	---	---	---	---	---	---	---	---	1.9
Schist	---	---	---	---	---	---	---	---	---	---
Diabase	---	---	---	---	---	---	---	---	---	---
Quartz Diorite	---	---	---	---	---	---	---	---	---	---
Dacite	---	---	---	---	---	---	---	---	---	---
Diorite	---	---	---	---	---	---	---	---	---	1.9
Andesite	---	---	---	---	---	---	---	---	---	1.0
Granodiorite	---	---	---	---	---	1.0	---	---	---	---
Rhyodacite	---	---	---	---	---	---	---	---	---	---
Monzonite	---	---	---	---	---	---	---	---	---	---
Latite	---	---	---	2.0	---	---	---	---	---	---
Quartz Latite	---	---	---	---	---	1.0	1.0	---	---	---
Quartz Monzonite	---	1.0	1.8	1.0	---	1.0	---	.9	---	1.0
Trachyte	---	---	---	1.0	---	1.0	---	.9	---	---
Syenite	---	---	---	---	---	---	---	---	---	---
Rhyolite	1.0	1.0	---	2.0	2	---	---	---	---	1.0
Granite	1.0	---	.9	1.0	1	1.0	---	---	---	2.8
Others	---	---	---	---	---	---	---	---	---	1.9
Schist	1.0	---	---	---	1	---	1.0	---	---	1.0
Breccia	---	---	---	1.0	2	---	1.0	---	---	4.8
Conglomerate	1.9	---	---	---	---	---	2.0	---	1.0	---
Sandstone	1.0	5.0	.9	2.0	1	2.0	2.0	2.8	---	---
Quartzite	39.9	29.7	23.9	11.2	27	27.7	22.2	34.8	11.6	30.4
Argillite	12.4	8.9	14.7	6.1	6	9.9	7.1	10.3	16.5	7.6
Chert	7.6	10.9	19.3	22.4	10	10.9	21.2	17.9	31.0	14.2
Quartz	32.3	43.6	37.7	50.0	50	44.6	42.4	32.0	39.8	30.4

TABLE 1, Cont.
 Frequencies of Rock Types in Pebble Samples of the Tertiary Sandstones
 (Hand Specimen Identification)

Lignite Creek Formation

Pebble Counts	A-D-3	A-D-8	A-D-12	A-D-14	A-D-16	Sc-D-11	Sc-D-14	Sc-D-17	Sc-D-19
Total No. Pebbles	102	108	104	103	103	113	113	110	111
Total Percent	100.2	99.3	99.9	99.8	100.8	99.7	99.6	100.0	99.9
Unknown	8.8	.9	1.9	1.9	1.9	1.8	---	3.6	1.8
Schist	2.0	.9	2.9	1.9	1.9	5.3	---	1.8	.9
Diabase	---	---	---	---	---	---	.9	---	---
Quartz Diorite	---	---	---	---	---	---	---	---	---
Dacite	2.0	2.8	---	---	---	---	1.8	---	---
Diorite	1.0	---	---	---	---	---	---	---	---
Andesite	2.0	---	---	---	---	.9	2.6	---	---
Granodiorite	---	---	---	1.0	---	---	.9	---	---
Rhyodacite	---	---	---	---	---	---	.9	---	---
Monzonite	1.0	---	---	---	---	---	---	---	---
Latite	---	---	---	---	---	---	---	---	---
Quartz Latite	1.0	---	---	---	1.0	--	1.8	1.8	---
Quartz Monzonite	2.0	3.7	---	2.9	1.0	.9	5.3	1.8	2.7
Trachyte	---	.9	1.9	---	---	1.8	---	2.7	---
Syenite	---	---	---	---	---	---	---	---	.9
Rhyolite	1.0	1.8	3.8	2.9	1.0	2.6	.9	2.7	1.8
Granite	2.0	2.8	1.9	1.9	1.9	3.5	5.3	1.8	2.7
Others	---	---	---	---	---	5.3	1.8	---	---
Schist	1.0	.9	---	---	1.0	---	---	2.7	---
Breccia	2.0	---	2.9	---	---	1.8	---	---	---
Conglomerate	1.0	---	1.0	1.9	3.4	---	---	2.7	.9
Sandstone	4.9	1.8	---	---	1.9	.9	---	5.5	---
Quartzite	12.7	24.8	22.1	25.2	28.1	19.4	13.2	17.3	18.0
Argillite	3.9	10.1	7.7	10.7	4.8	14.1	11.4	5.5	15.3
Chert	28.4	26.7	20.2	23.3	26.2	19.4	25.5	23.7	31.5
Quartz	23.5	21.2	33.6	26.2	26.2	22.0	27.3	26.4	23.4

TABLE 1, Cont.
 Frequencies of Rock Types in Pebble Samples of the Tertiary Sandstones
 (Hand Specimen Identification)

Lignite Creek Formation, Cont.

Pebble Counts	Sc-D-7	Sc-D-5	Sc-D-4	Sc-D-2	G-2	G-7	G-11	2-5	5-2
Total No. Pebbles	111	117	117	102	101	106	100	103	105
Total Percent	99.9	99.4	99.4	100.1	100.1	99.5	(100)	100.0	100.0
Unknown	4.5	---	2.6	---	1.0	---	6	2.9	1.0
Schist	---	6.0	.8	---	---	4.7	2	---	1.0
Diabase	---	---	---	---	---	---	---	---	---
Quartz Diorite	---	---	.8	---	---	---	---	---	---
Dacite	---	---	---	---	---	---	---	1.0	---
Diorite	.9	.8	---	---	---	---	---	---	---
Andesite	---	---	2.6	---	---	---	---	---	---
Granodiorite	---	.8	---	---	---	---	---	---	---
Rhyodacite	---	.8	2.6	---	---	.9	---	---	---
Monzonite	---	---	---	2.0	1.0	---	---	---	---
Latite	---	---	---	---	---	---	1	---	---
Quartz Latite	---	---	2.6	---	1.0	---	---	---	1.0
Quartz Monzonite	.9	2.6	.8	1.0	---	---	1	1.0	---
Trachyte	---	.8	.8	2.0	---	---	---	---	---
Syenite	---	---	---	---	---	---	---	---	---
Rhyolite	.9	3.4	2.6	8.8	4.0	1.9	2	1.9	1.0
Granite	4.5	2.6	4.2	2.0	2.0	3.8	7	3.9	1.9
Others	---	---	---	3.9	---	.9	2	---	---
Schist	.9	2.6	---	1.0	2.0	.9	---	1.0	1.0
Breccia	---	.8	---	---	---	.9	---	---	---
Conglomerate	---	2.6	---	1.0	3.0	.9	2	2.9	---
Sandstone	5.4	1.7	6.0	1.0	---	---	2	8.7	5.7
Quartzite	32.4	39.1	15.3	14.7	18.8	16.9	32	27.2	23.8
Argillite	5.4	3.4	8.5	15.7	8.9	8.5	4	10.7	12.4
Chert	18.0	17.0	28.0	17.6	23.8	26.3	14	23.3	22.8
Quartz	26.1	14.4	21.2	29.4	34.6	32.9	25	15.5	28.5

TABLE 1, Cont.
 Frequencies of Rock Types in Pebble Samples of the Tertiary Sandstones
 (Hand Specimen Identification)

Lignite Creek Formation, Cont.

Pebble Counts	5-6	5-9	5-14	5-17	11-2	11-16a	11-5a
Total No. Pebbles	100	102	101	104	100	104	105
Total Percent	(100)	100.1	100.2	99.9	(100)	100.0	99.7
Unknown	4	4.9	5.0	1.0	1	3.8	2.8
Schist	2	2.0	2.0	---	---	1.0	1.9
Diabase	---	---	---	---	---	---	---
Quartz Diorite	---	---	---	---	---	1.9	---
Dacite	---	---	---	---	---	---	---
Diorite	2	1.0	---	---	---	1.0	---
Andesite	---	---	---	---	---	---	---
Granodiorite	---	---	---	---	---	---	---
Rhyodacite	---	---	3.0	---	---	---	---
Monzonite	---	---	---	---	---	---	---
Latite	1	---	---	---	---	---	---
Quartz Latite	---	1.0	---	---	---	---	1.0
Quartz Monzonite	---	1.0	1.0	4.8	1	1.9	3.8
Trachyte	---	---	5.0	1.0	3	1.9	1.0
Syenite	---	---	---	---	---	---	---
Rhyolite	1	3.9	---	3.8	---	4.8	3.8
Granite	3	2.0	3.0	2.9	2	5.8	3.8
Others	---	---	---	---	---	1.0	---
Schist	---	---	1.0	2.9	1	2.9	1.9
Breccia	---	---	---	3.8	1	1.0	---
Conglomerate	---	1.0	2.0	1.9	---	---	---
Sandstone	3	4.9	3.0	2.9	2	5.8	1.9
Quartzite	24	23.5	18.8	18.2	12	24.0	18.0
Argillite	15	5.9	10.9	5.8	17	11.5	11.4
Chert	25	23.5	15.8	25.9	26	14.4	26.6
Quartz	20	25.5	29.7	25.9	34	17.3	21.8

percentages and factor-analyzed on the IBM 360 computer using the GEOFACT program (Cameron, 1967). First, the data were grouped by R-mode factor analysis into 26 factors. Of these 26 factors, ten factors were rotated, using the Varimax criterion. Ten factors were chosen because the eigenvalues of these factors were greater than 1.0. Approximately 75% of the total variance of the pebble samples is explained in terms of the ten new variables or factors. Factor scores representing the amount of each factor present in each sample were calculated. These factor scores were then utilized in the Q-mode analysis (Klovan, 1968) to group similar samples quantitatively. The Q-mode Varimax factor loadings of the samples from the Q-mode factor analysis were subsequently contoured on vertical cross sections. The resulting vertical sections then provided data points necessary for construction of isopach maps of the pebble facies.

R-mode factor scores of the various sample localities provided a means of selecting pebbles to be sectioned for petrographic analysis. The greatest positive and the greatest negative loadings among the first ten factors were used to determine which sample would provide the representative pebbles for a given factor. Approximately ten pebbles were then chosen to represent each of the ten factors. Standard thin sections were made of a total of 101 pebbles.

Petrographic analysis of the thin sections with a standard binocular polarizing microscope permitted assignment of specific rock names. Mineral species and approximate percentages present in each thin section formed the basis for final rock classification. Where feldspar ratios were difficult or impossible to estimate (e. g., in fine-grained volcanics), the original stained pebble from which the slide was made proved beneficial in approximating the ratio. (Figure 7 is a flow chart illustrating treatment of pebble samples.)

Heavy Minerals

Field Methods

Approximately 167 sand samples were collected from the several stratigraphic sections for detailed heavy mineral analysis. However, Wahrhaftig (personal communication, 1970) stated that Blake of the U. S. G. S. has already made

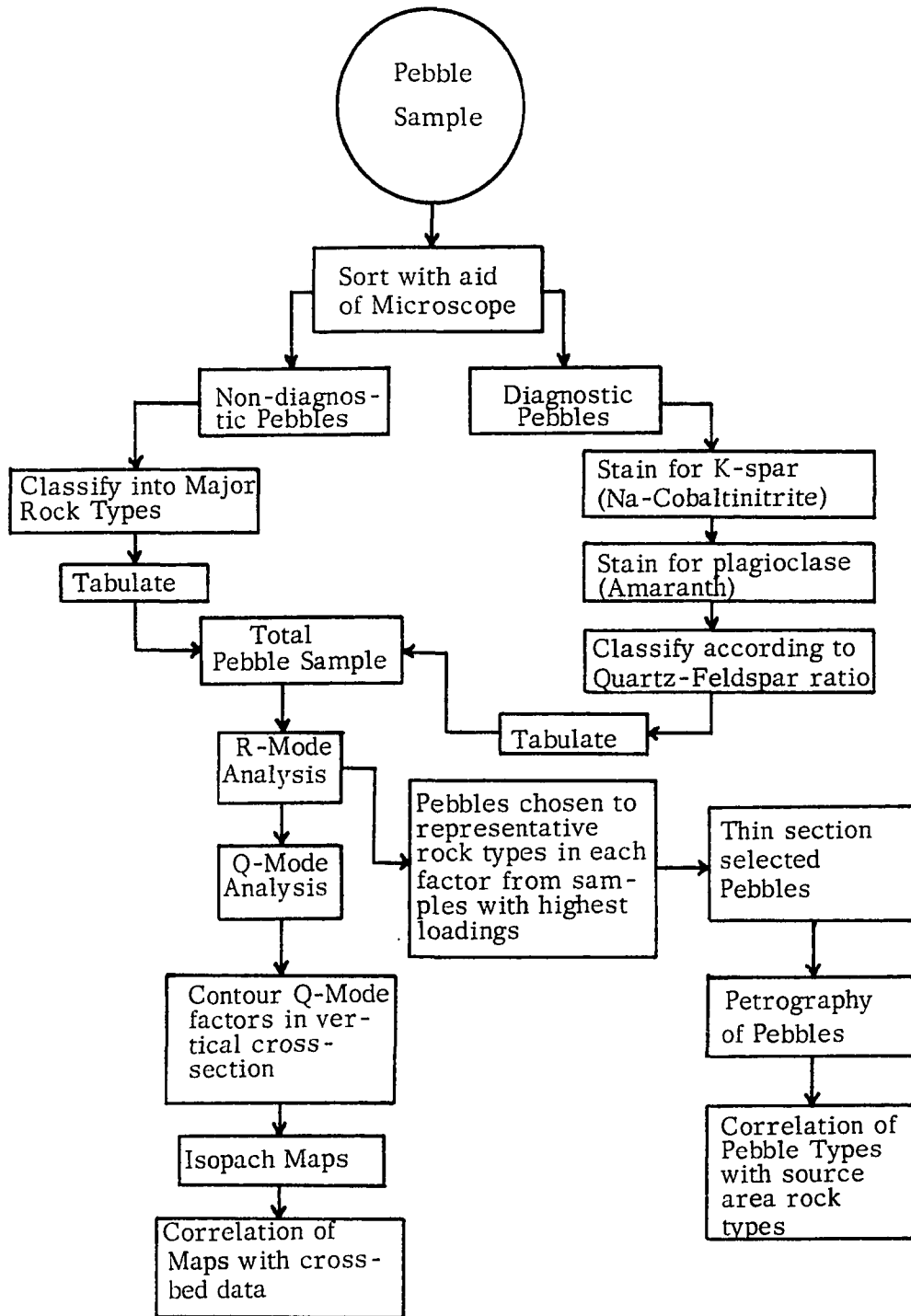


FIGURE 7

Flow Chart for Procedures Used in Treatment of Pebble Samples and Subsequent Factor Analysis

heavy mineral studies in this area. The results are currently awaiting publication in a comprehensive report on the Nenana Coal Field by Wahrhaftig and others. Accordingly, heavy minerals are de-emphasized in this study and restricted to a spot check of six samples.

Samples were collected from most of the exposed sand bodies in each of the representative sections selected for this report. In sandstone units thicker than 100 feet, three spot samples were usually collected--one near the top, one near the middle, and one near the base of the unit. In thinner sandstones, generally two samples were collected--one near the top and one near the base of each unit. Only one sample was taken from units less than about ten feet thick.

Care was taken to collect from homogeneous sedimentation units, i. e., not to sample across stratigraphic boundaries. Particular care was exercised in keeping sampling tools and bags free from contaminants.

Laboratory Methods

Six samples were selected for separation and petrographic analysis. One sample was selected from approximately the middle of each formation in each of the type stratigraphic sections in order to make an estimate of the heavy mineral content of the sands. No particular effort to correlate mineral suites between sections was attempted.

One hundred grams of each of the six sand samples were sieved for 15 minutes on the Ro-Tap machine in Tyler Standard 8-inch diameter wire mesh screens and the 2 phi to 3 phi fraction was then removed and weighed. Disaggregation of the samples was usually not necessary since the sands are largely unconsolidated. The weighed 2 phi to 3 phi fraction was then split in a sample splitter until approximately 7 grams of sample were obtained. The 7 gram fractions of the samples were then chemically cleaned of free iron oxides (see Black, 1965). Heavy and light minerals were separated by centrifuging in tetrabromoethane (specific gravity = 2.96) (Royse, 1970, pp. 93-96). The magnetic fraction was extremely small and no attempts were made to remove it. After the separated samples were washed and dried, heavy and light fractions were stored in separate glass vials. Heavy fractions were then mounted on standard glass slides in Canada balsam (caedex) (R. I. = 1.54) with cover slips.

Point counting was performed during linear traverses until a total of 300 heavy minerals were counted. The results are tabulated in Table 2, p. 28. Fig. 8 is a flow chart illustrating treatment of heavy mineral samples.

TABLE 2
Percentages of Heavy Mineral Species in Six Sand Samples

MINERALS	SAMPLES					
	SC-D-16		SC-C-3		SR-A-7	
	5-7	5-7	5-32	5-32	4-1	4-1
Biotite	1.0	2.66	2.0	.33	7.0	9.0
Muscovite	--	4.0	--	--	.66	.33
Chlorite	4.0	4.0	9.33	1.0	10.0	2.66
Andalusite	1.66	.33	7.33	5.0	1.33	8.66
Sillimanite	1.66	.66	.33	--	.66	--
Kyanite	--	1.0	--	.33	1.33	.66
Staurolite	1.66	1.66	.66	4.66	1.33	.33
Epidote	19.66	9.66	10.0	22.33	2.0	4.0
Clinozoisite	1.33	1.0	2.66	2.66	.33	.33
Garnet	3.0	4.0	11.33	15.33	45.0	8.66
Tremolite	1.33	1.0	.33	.33	.33	.66
Actinolite	3.33	2.0	--	.33	--	.33
Green Hornblende	9.0	6.33	.33	.33	--	.66
Blue-green Hornblende	5.33	3.0	--	--	--	.33
Brown Hornblende	5.0	3.66	--	--	--	--
Enstatite	.66	.33	--	--	--	--
Hypersthene	.66	--	.33	--	--	.33
Diopside	2.33	.66	.33	.33	--	3.0
Augite	--	--	--	--	.33	.66
Spodumene	--	--	--	.33	--	--
Zircon	.33	.33	4.0	3.33	--	1.0
Sphene	3.33	2.0	4.66	4.0	2.66	.33
Rutile	2.0	2.0	--	.66	2.0	2.33
Brookite	--	--	.33	--	.33	--
Anatase	--	--	--	--	--	.33
Apatite	--	.33	.33	.66	2.66	--
Blue Tourmaline	--	--	--	.33	--	.33
Brown Tourmaline	--	.33	1.66	2.66	1.33	.66
Alterites + rock fragments	30.66	40.0	33.66	23.0	16.66	49.66
Opakes	2.0	2.66	10.33	11.0	2.33	1.33
Feldspar + Quartz	--	6.33	--	1.33	1.66	3.33
	Lignite Creek Formation		Suntrana Formation		Healy Creek Formation	

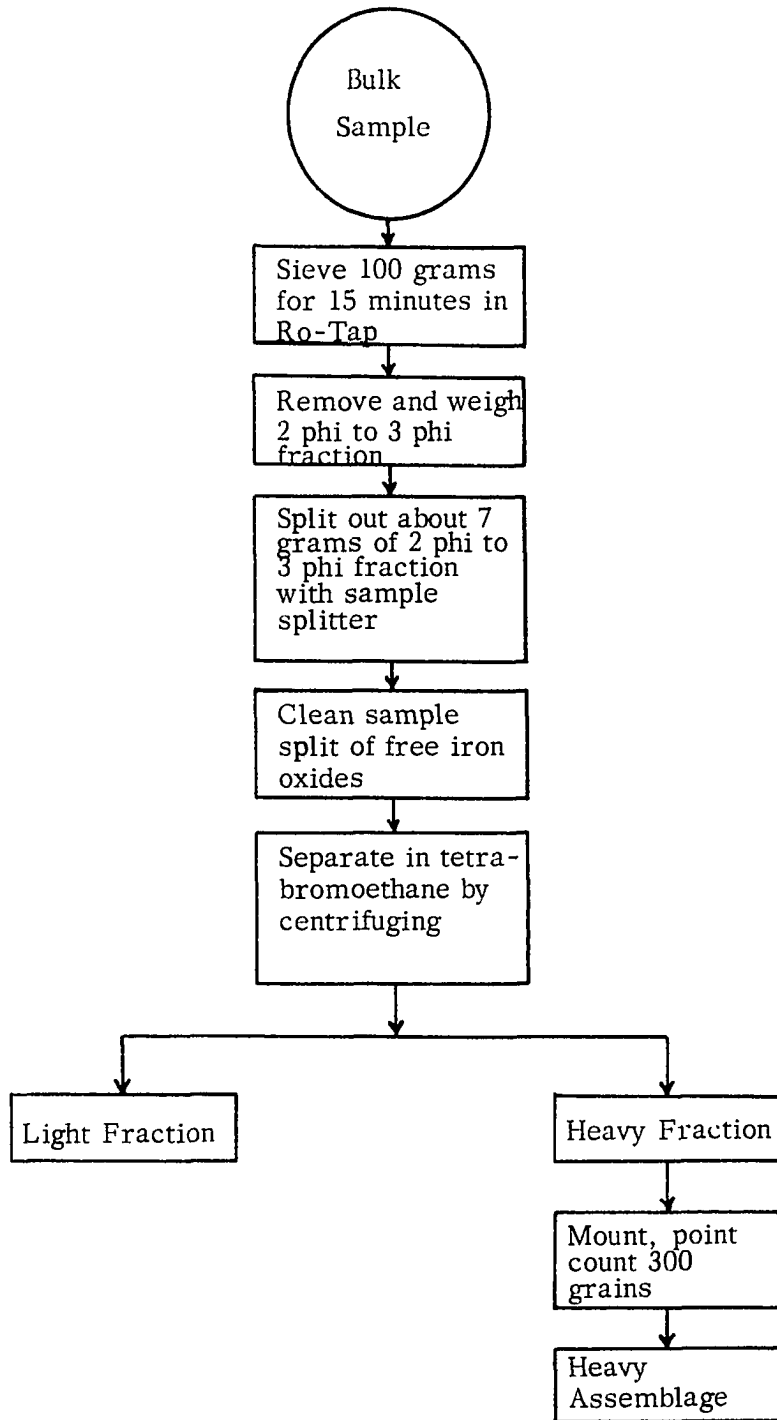


FIGURE 8

Flow Chart Illustrating Methods Used in Preparing Heavy Minerals

CHAPTER III RESULTS OF ANALYSES

Data gleaned from the various analyses performed during the investigations are summarized in the following pages. Included are results of the directional data analysis, petrographic analysis, and heavy mineral analysis.

Directional Data

Directional data measurements indicate that sediments were supplied to the basin from the north during Suntrana and Lignite Creek time and possibly during the deposition of the Healy Creek Formation (Fig. 9, p. 31). The vectoral data are not sufficient to define the source area of the sediments precisely; however, they eliminate the Alaska Range to the south and indicate instead the Yukon-Tanana Upland as a source.

Vector Means

Vector means at each locality for the Suntrana and Lignite Creek Formations are significant. They imply that dispersal within the basin was much less uniform during the deposition of the Suntrana Formation than during the deposition of the Lignite Creek Formation (Figs. 10 and 11, pp. 32-33). This difference may result from increased inclination of the paleoslope and/or may indicate greater tectonic stability in the basin during the Lignite Creek time.

Standard Deviations

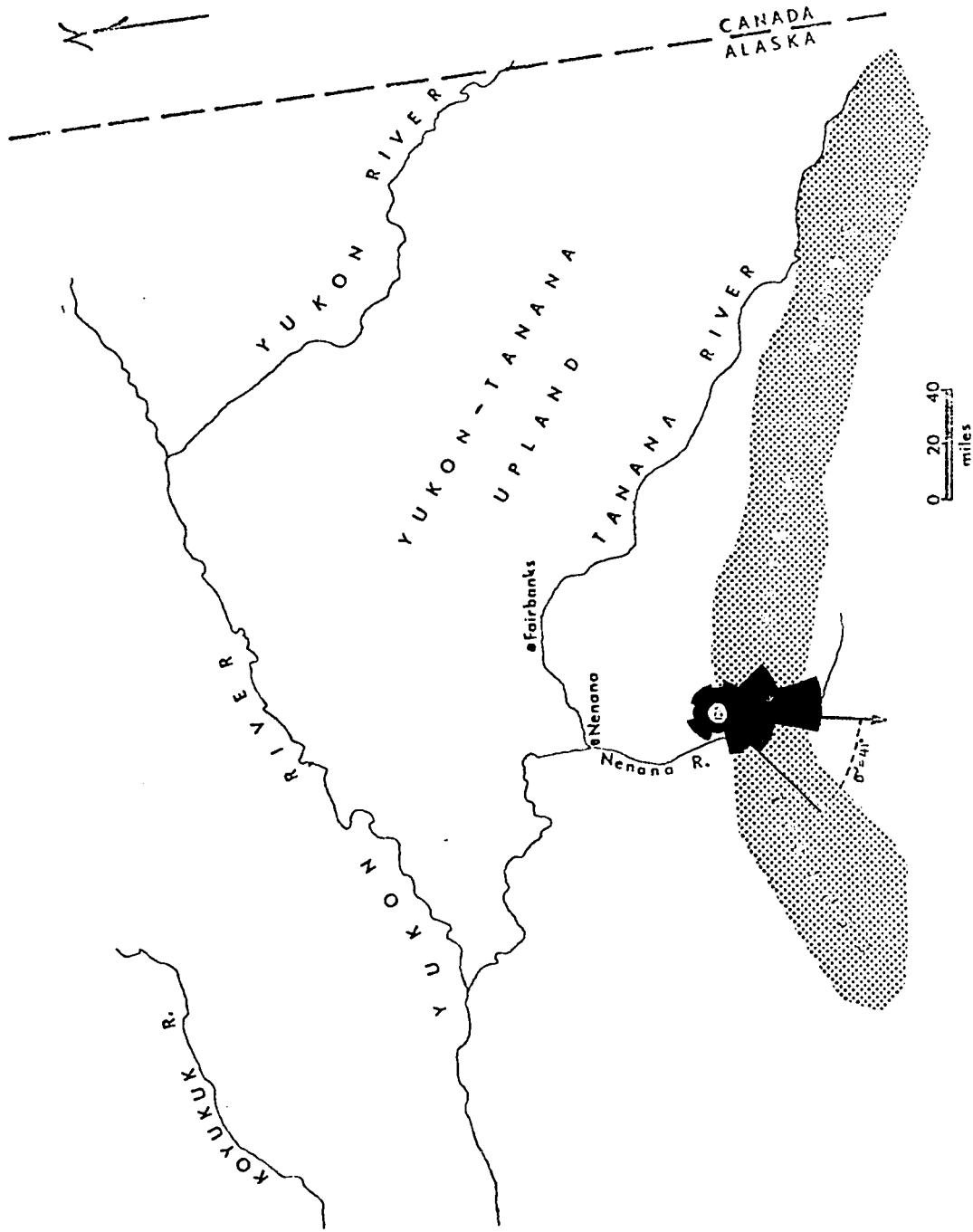


Figure 9. Regional map of central Alaska with a composite rose diagram of all crossed readings from the study area.

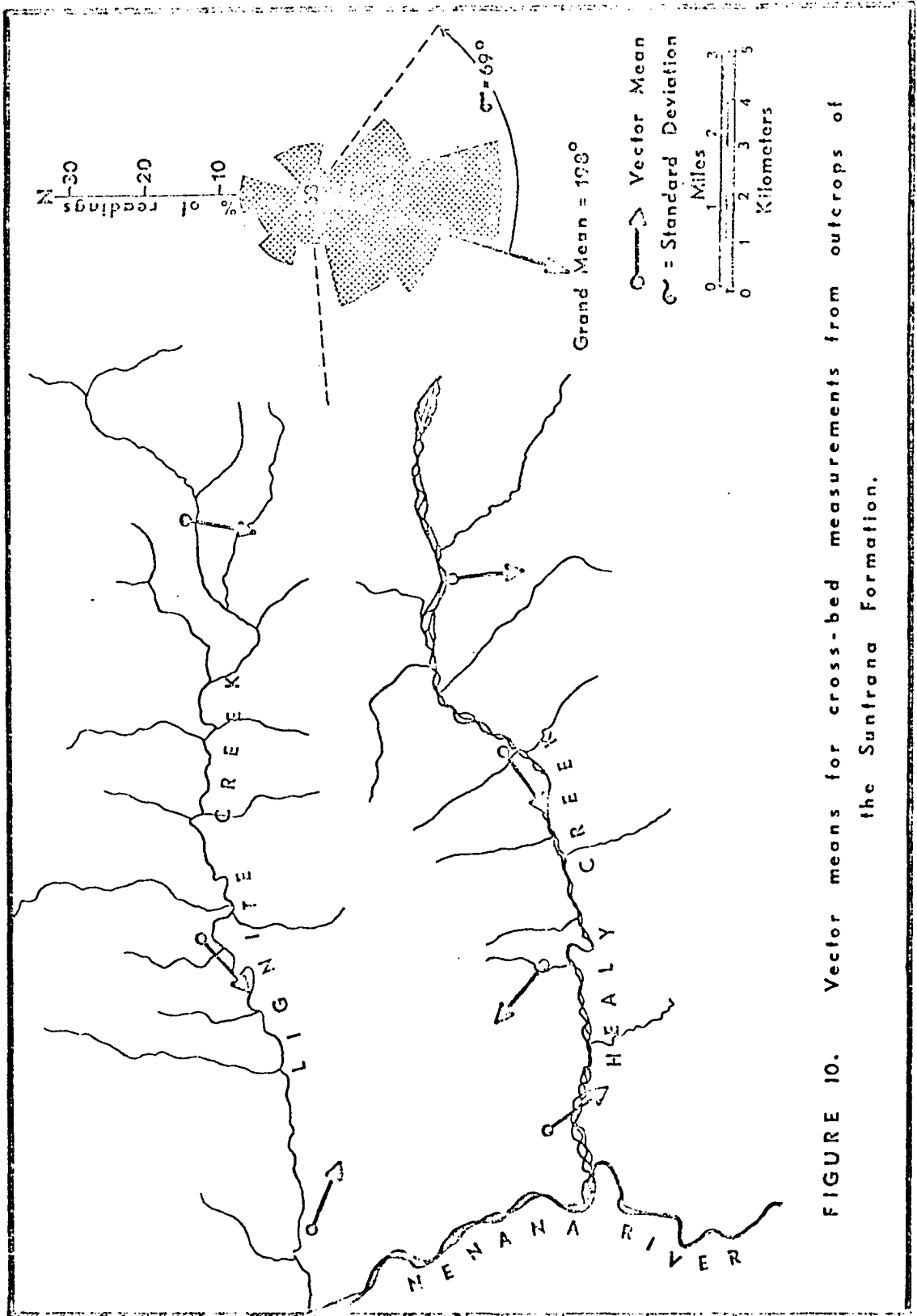


FIGURE 10. Vector means for cross-bed measurements from outcrops of the Suntrana Formation.

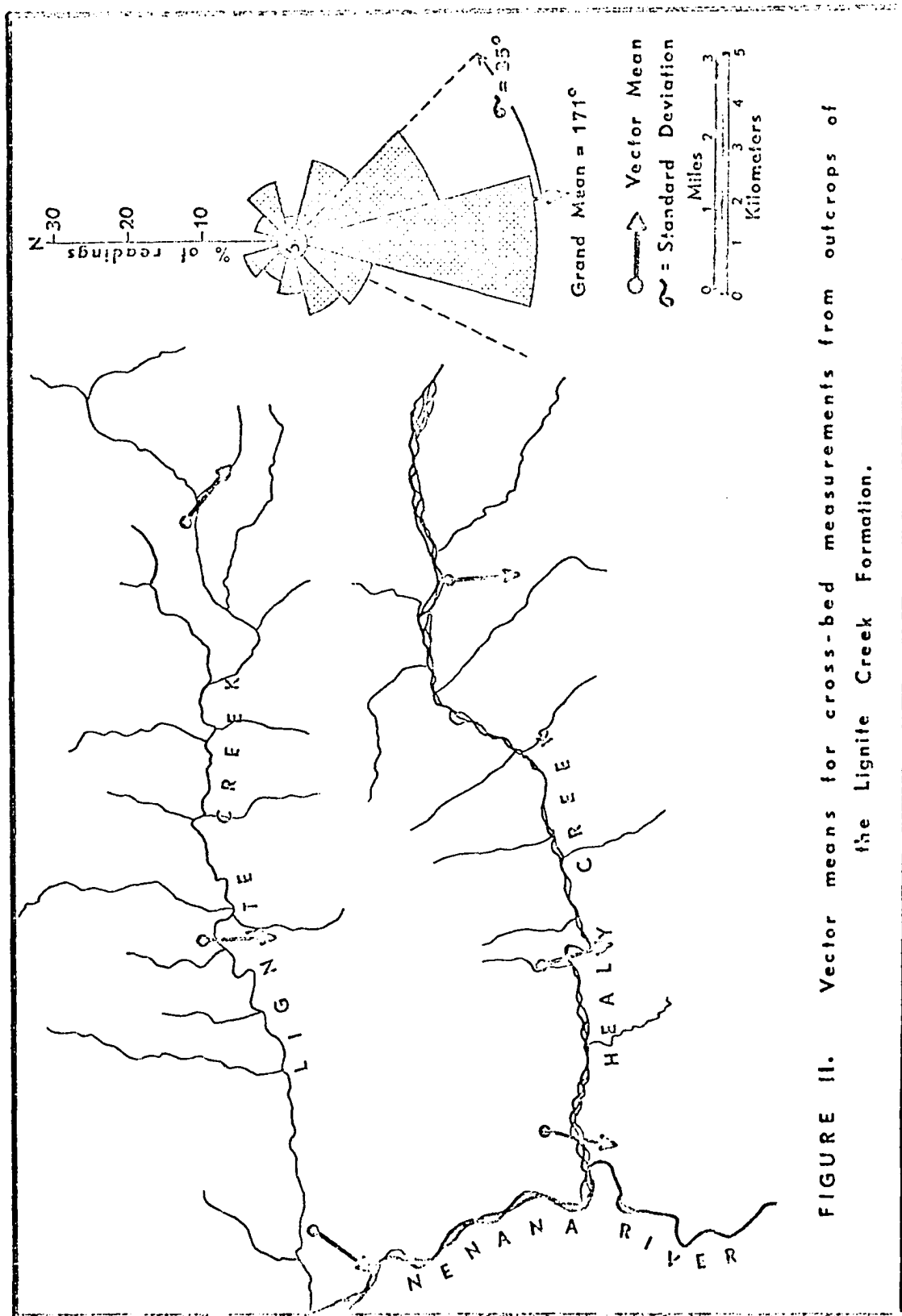


FIGURE II. Vector means for cross-bed measurements from outcrops of the Lignite Creek Formation.

Standard deviations from the grand means are quite different in the two formations. The standard deviation in the Suntrana Formation is much greater (69°) than that in the Lignite Creek Formation (35°). Potter and Pettijohn (1963, p. 88) report the most common range of standard deviations in fluvial-deltaic deposits to be between 63° and 78° whereas marine deposits tend to have higher standard deviations, between 78° and 89° .

Pebble Data

Factor Analysis

Isopach maps were constructed for two of the Q-mode factors. These maps proved valuable in reconstructing and interpreting sedimentation patterns at certain stratigraphic horizons in the Healy Creek and Suntrana formations (Fig. 12, p. 35).

The first factor is the most significant. It indicates a thickening of the pebble "facies" to the southeast along an axis which strikes approximately N. 68° W. (Fig. 13). This factor apparently represents a complex relationship among the resistant rock types such as quartz, chert, argillite, quartzite, and sandstone (table 3, p. 37).

High positive values of factor 7 mainly indicate a paucity of chert (table 3, p. 37). Again a linear north-south trend is evident from the isopach map of the data. Directional data, however, indicate that paleoflow was to the southwest during this depositional episode in the history of the Suntrana Formation (Fig. 14, p. 38).

Petrography

One hundred one pebbles were sectioned for petrographic study. Metamorphic, sedimentary, igneous extrusive and igneous intrusive rock types are represented in the pebble suite. The general rock groups are briefly described in the following paragraph. The pebbles were named from the American Geological In-

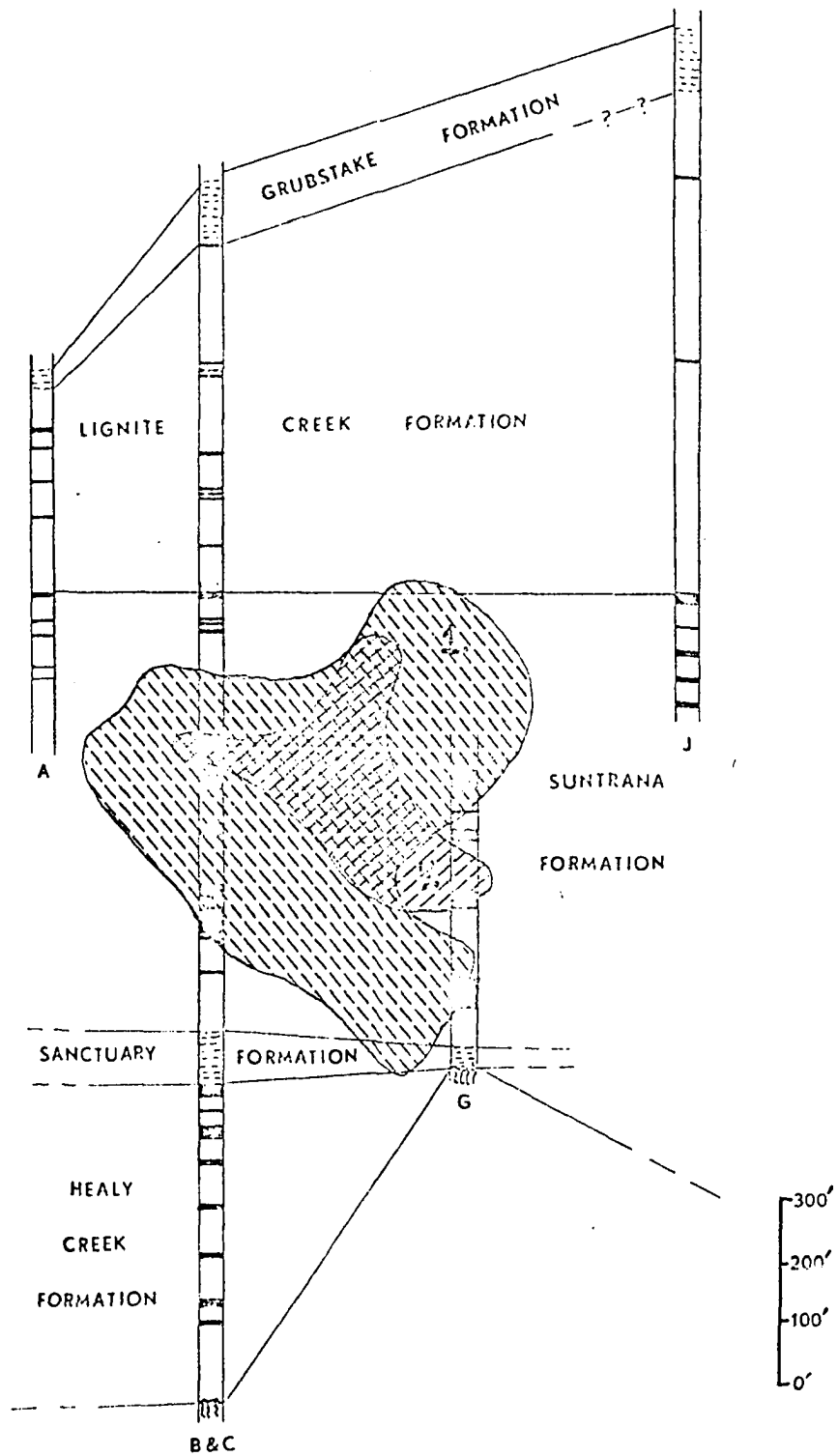


Figure 12. Stratigraphic intervals covered by "isopach" maps of Q-mode factors 1 and 7.

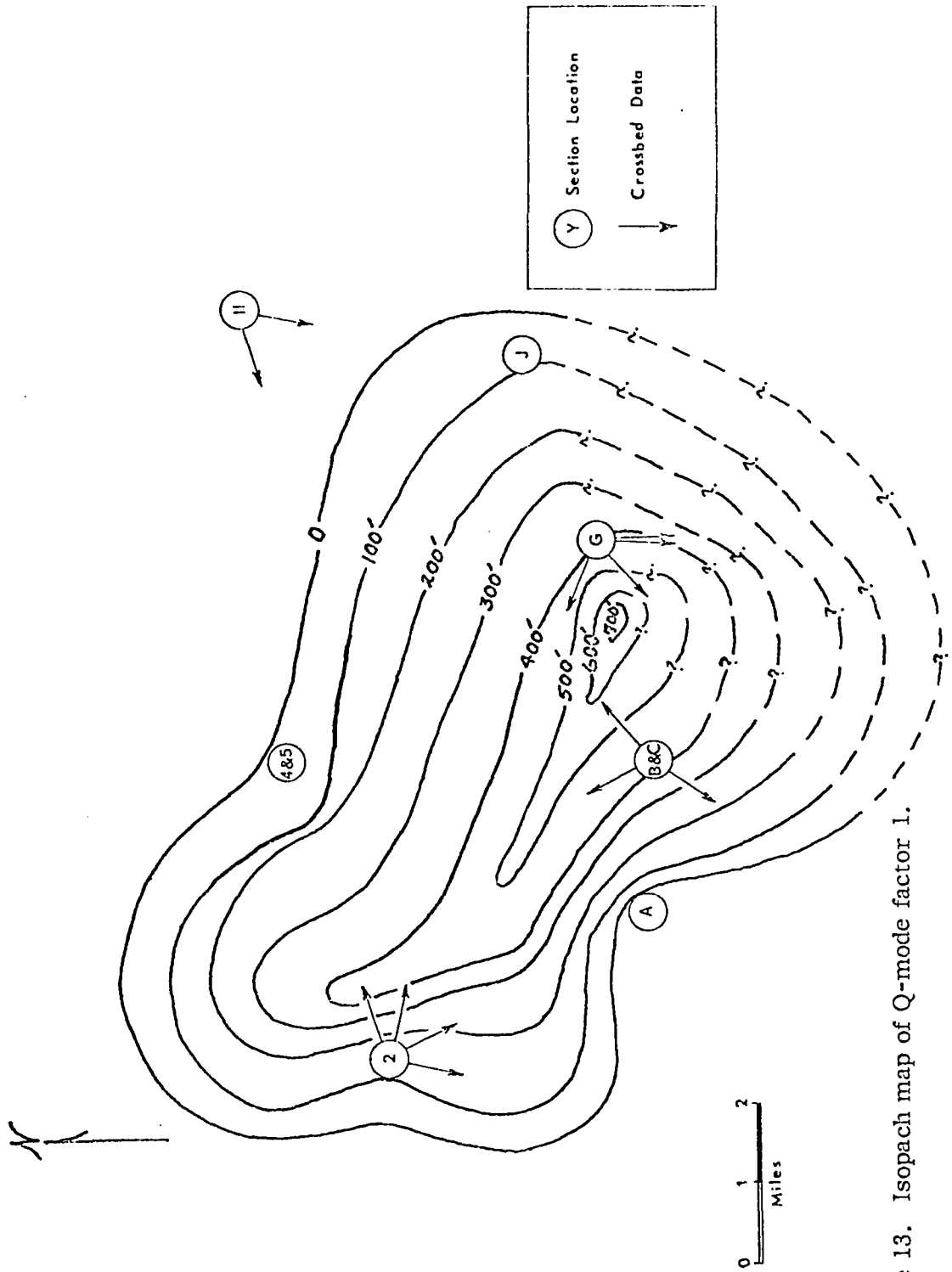


Figure 13. Isopach map of Q-mode factor 1.

TABLE 3
 "End Member" Samples for Q-Mode Factors 1 and 7
 (The positive samples are the most representative members and the
 negative samples are the least representative members of the two factors.)

Mineral	Sample No.	FACTOR 1		FACTOR 7	
		5-37 (+)	SC-D-17 (-)	UV-C-2 (+)	A-D-8 (-)
Quartz		32.0	26.4	42.7	21.2
Chert		17.9	23.7	4.4	26.7
Argillite		10.3	5.5	6.2	10.1
Quartzite		34.8	17.3	32.9	24.8
Sandstone		2.8	5.5	2.7	1.8
Conglomerate		--	2.7	--	--
Breccia		--	--	.9	--
Schist		--	2.7	.9	.9
Others		--	--	--	--
Granite		--	1.8	--	2.8
Rhyolite		--	2.7	--	1.8
Syenite		--	--	--	--
Trachyte		.9	2.7	--	.9
Quartz Monzonite		.9	1.8	--	3.7
Quartz Latite		--	1.8	2.7	--
Latite		--	--	2.7	--
Monzonite		--	--	--	--
Rhyodacite		--	--	--	--
Granodiorite		--	--	.9	--
Andesite		--	--	--	--
Diorite		--	--	--	--
Dacite		--	--	--	2.8
Quartz Diorite		--	--	--	--
Diabase		--	--	--	--
Schist		--	1.8	1.8	.9
Unknowns		--	3.6	.9	.9

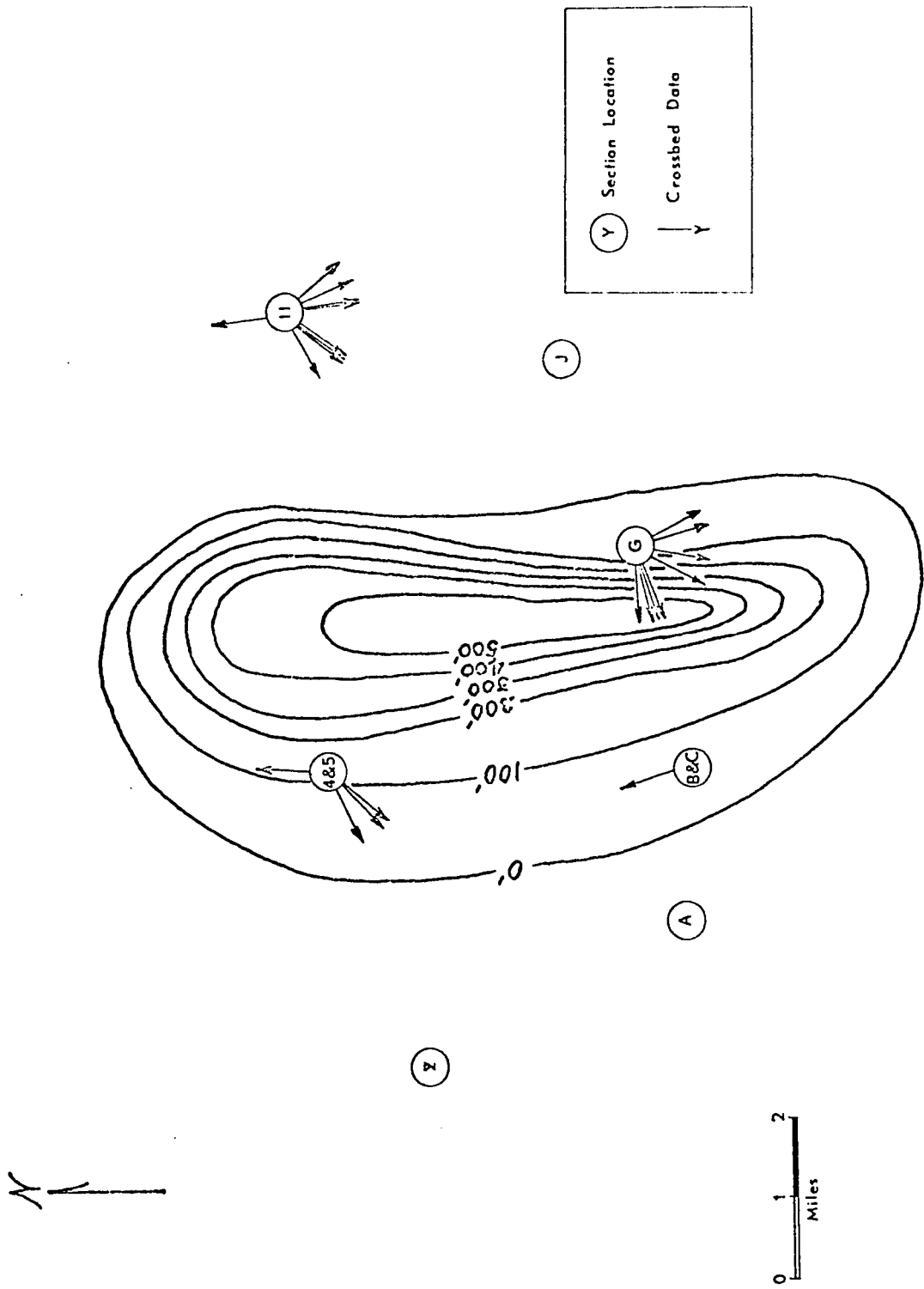


Figure 14. Isopach map of Q-mode factor 7.

stitute rock classification (Peterson, 1961; Fig. 15 , p. 40).

Igneous extrusives:

The rhyolites are generally porphyritic with euhedral to subhedral phenocrysts of quartz and K-feldspar (and sometimes plagioclase) in a fine-grained groundmass of alkalic feldspar and quartz. Phenocrysts displaying micrographic intergrowths are not uncommon and some of the rocks have vesicles filled with zeolites or other secondary minerals.

The quartz latites are also porphyritic with euhedral to subhedral altered phenocrysts of quartz and oligoclase. Occasionally phenocrysts of sodic orthoclase are present. Micrographic intergrowths are common and the often-devitrified groundmass is usually composed of feldspar, some quartz, chlorite, and opaques.

The rhyodacite group is also characterized by porphyritic texture. Plagioclase (oligoclase - andesine) phenocrysts are euhedral to subhedral, altered, and occasionally glomerophyritic. In at least one instance altered hornblende phenocrysts were noted. The mesostasis is generally quartz and plagioclase. One specimen contains abundant glass in the groundmass, and tiny plagioclase laths are not uncommon in these specimens.

Only one dacite specimen was encountered in the thin-sectioned pebbles. This rock is also porphyritic with euhedral to subhedral phenocrysts of quartz and andesine. The plagioclase phenocrysts are generally smaller than those of quartz and usually occur in clusters (glomeroporphyritic). Occasional patches of blue tourmaline are a distinctive and very interesting feature of this rock.

The trachytes are often porphyritic with quartz, K-feldspar, and occasionally plagioclase (oligoclase) and/or mafic phenocrysts in a fine- to medium-grained mesostasis of K-feldspar, some plagioclase, some quartz, and opaques plus alteration products. One specimen is a particularly fine example of trachytic texture. In some specimens, the groundmass consists mainly of devitrified

FIGURE 15

Classification of igneous rocks (after Peterson, 1961).

DESCRIPTIVE CLASSIFICATION OF IGNEOUS ROCKS					
	Alkalic feldspar > 2/3 total feldspar	Alkalic feldspar 1/3 to 2/3 total feldspar	Plagioclase 2/3 to 9/10 total feldspar	Plagioclase > 9/10 total feldspar	
				An < 50	An > 50
	*CI 0 to 20+		CI 10 to 40		CI 40 to 70
Quartz > 10%	Rhyolite	Quartz Latite	Rhyodacite	Dacite	Quartz Basalt
	GRANITE CI 5-15 An 0-15	QUARTZ MONZONITE CI 10-20 An 12-33	GRANODIORITE CI 15-30 An 25-40	QUARTZ DIORITE CI 25-40 An 35-50	QUARTZ GABBRO CI 40-70 An 50-90
	ALASKITE CI < 5 An 0-35		TRONDHJEMITE CI < 10 An 15-30		
	Trachyte	Latite	Andesite		Basalt
Quartz < 10% Feldspathoids > 10%					DIABASE
	SYENITE CI 5-25 An 0-30	MONZONITE CI 20-35 An 25-45	DIORITE CI 25-40 An 35-50		GABBRO CI 40- 70 An 50-100

*Color Index

leucocratic minerals. Sodic orthoclase is present in at least one specimen.

The latites are porphyritic volcanics with altered oligoclase to andesine phenocrysts in a fine- to medium-grained groundmass of plagioclase, K-feldspar, and a little quartz. Biotite phenocrysts are present in one specimen and highly altered unidentifiable xenoliths are present in another.

The andesite group is characterized by porphyritic textures. Phenocrysts are generally andesine and are often epidotized. In one specimen, altered augite occurs as phenocrysts. Mafics altered to chlorite are common and often the groundmass contains small plagioclase laths showing flow structures. A little quartz and K-feldspar are sometimes present and one specimen contains a few small euhedral garnets.

Two volcanic breccias were present in the pebble assemblage. These rocks display characteristic volcanic textures and are highly altered.

Igneous intrusives:

The two granite pebbles contain high percentages of quartz and K-feldspar with some oligoclase. Mafic constituents are less than 5% and the K-feldspar is commonly quite sodic. One specimen is characterized by a cataclastic texture and the other has a texture indicating recrystallization following deformation.

The quartz monzonite generally have hypidiomorphic- to allotriomorphic-granular textures. One specimen, however, has a cataclastic texture. Myrmekitic texture is characteristic of some of the specimens. Plagioclase ranges from oligoclase to andesine and K-feldspar is commonly sodic. Mafics include hornblende and biotite and are generally less than 5% of the rocks. One sample contains garnet.

The granodiorite specimens show metamorphic deformation. Quartz percentages are high and plagioclase is oligoclase to andesine with minor (if present) K-feldspar. Mafics, when present, are altered to chlorite.

One syenitic type rock occurs in the pebble assemblage. This rock has a poikilitic texture in that plagioclase and biotite occur within larger twinned (Carlsbad law) K-feldspar crystals. The plagioclase has reverse zoning and is often rimmed with quartz in micrographic intergrowths.

The monzonite specimen has a hypidiomorphic texture with subhedral crystals of partially altered mafics (sodic? hornblende, pyroxene? and biotite), oligoclase, and generally anhedral K-feldspar and minor quartz constituents. Micrographic texture is occasionally present between plagioclase and K-feldspar.

The diabase specimen has a subophitic (?) texture and contains subhedral augite, labradorite, and biotite. Uralitic hornblende occasionally rims the augite, biotite is often partially altered to chlorite, and plagioclase is usually highly altered to sericite. Titaniferous iron minerals are also a major constituent.

Allotriomorphic- to hypidiomorphic-granular texture characterizes the hornblende-pyroxene gabbro specimen. Slightly sodic (?) amphibole rims the pyroxene (augite?) and labradorite is generally unaltered. Some epidote-clinzoisite is also present.

Sedimentary rocks:

The cherts are extremely fine-grained, commonly carbonaceous, and occasionally metamorphosed. Secondary quartz veins are common and a few of the specimens appear somewhat "brecciated" due to the numerous quartz veins.

The argillite group is texturally similar to the cherts in that they are often cut with secondary quartz veins; however, they contain much more carbonaceous (?) material. Some of these argillites have developed quartz segregation bands and sometimes contain low-grade metamorphic minerals. These are often "cherty" argillites.

Most of the conglomerates are chert pebble conglomer-

ates. Subround to subangular chert and quartzite granules and/or pebbles generally occur in a matrix of finer quartz grains, chert fragments, and chert cement. Cross-cutting quartz veins are not uncommon. One specimen is an orthoquartzite conglomerate and another is essentially a chert graywacke conglomerate. Several of the specimens are "stretched" from metamorphic processes.

The chert-quartz breccias are largely composed of angular to subangular chert and quartz fragments with minor amounts of various other constituents. One specimen has been metamorphosed.

The sandstone group contains representatives of three types of sandstones (Folk, 1968): (1) impure arkose; (2) leucoxene arenite; and (3) orthoquartzite. The impure arkose contains about 50% feldspar, 25% rock fragments, 15% quartz, and 10% other constituents. It is composed of angular particles and the sorting is very poor. Some secondary quartz veins are present and the presence of minor epidote-clinozoisite indicates low grade metamorphism. The leucoxene arenite is poorly sorted and contains angular quartz (10%), feldspar (< 5%), and leucoxene (> 30%) fragments in a cherty matrix. The orthoquartzite are about 90% quartz with some feldspar and other minor constituents. Both specimens contain low-grade metamorphic minerals and slight metamorphism is evident in the textures. Quartz grains are typically strained and sometimes have granulated boundaries; also, some recrystallization has occurred.

Metamorphic rocks:

Most of the representatives of the amphibolite group are ortho-amphibolites. One or two specimens may be para-amphibolites, however. These specimens are generally non-schistose and in some, relict igneous textures are preserved. High percentages of amphibole and plagioclase are common and mineral assemblages indicate that the specimens are low- to medium-grade (greenschist to amphibolite facies) metamorphic rocks.

The mica schists are probably derived from sedimentary

parents. They are schistose with lepidoblastic texture and contain high percentages of quartz, and 10 to 15% mica and chlorite. One of the specimens also contains high percentages of epidote-clinozoisite and feldspar.

The three specimens of contact metamorphic rocks contain pyroxene which developed in contact metamorphic environments. In one specimen, a single skeletal crystal of pyroxene occurs in an orthoquartzite. The other two specimens are remarkably similar to each other and are apparently the result of contact metamorphism of graywacke. The pyroxene in these rocks is very fine-grained and incipient. Other major constituents include plagioclase, some quartz, chert, opaques, chlorite, and actinolite.

Quartz pebbles in this suite are indicative of quartz types derived from metamorphic terranes. Some are sheared, but all have undulose extinction resulting from strain. Most grains have sutured boundaries and composite grains are common. Several of the pebbles are optically continuous--a result of the granular quartz being annealed by metamorphic processes.

Altered rocks:

Rocks in this category are highly altered and are only tentatively identified. These include: (1) a volcanic with filled vesicles and microporphyratic intergranular texture with pigeonite microphenocrysts and extremely altered plagioclase laths; (2) an unidentifiable metavolcanic (?) which is devitrified into radial aggregates; (3) a metavolcanic having relict porphyritic texture and which is highly altered to clay minerals; (4) a highly altered intrusive igneous rock which could possibly have been a diorite; and (5) a sheared altered rock with much secondary clay mineralization.

Sixty-eight of the 101 pebbles selected for thin section study were found to have been correctly identified in hand specimen. Figure 16, p. 45 illustrates the correlation between hand specimen names and rock names derived from thin section study among the various rock classes. Figure 17 on the same page represents

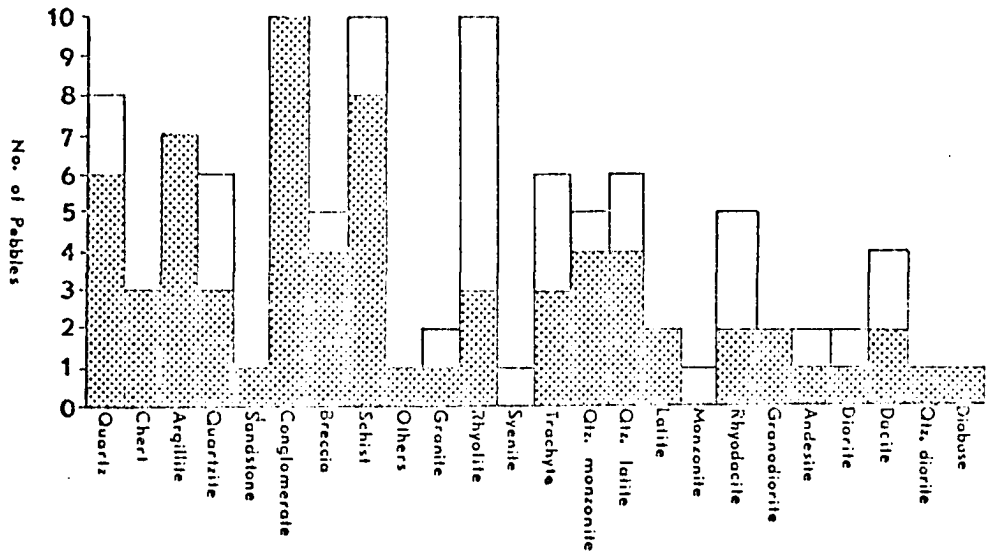


FIGURE 16. Correlation between hand specimen and thin section identifications of 101 pebbles. Unstippled areas indicate poor correlations.

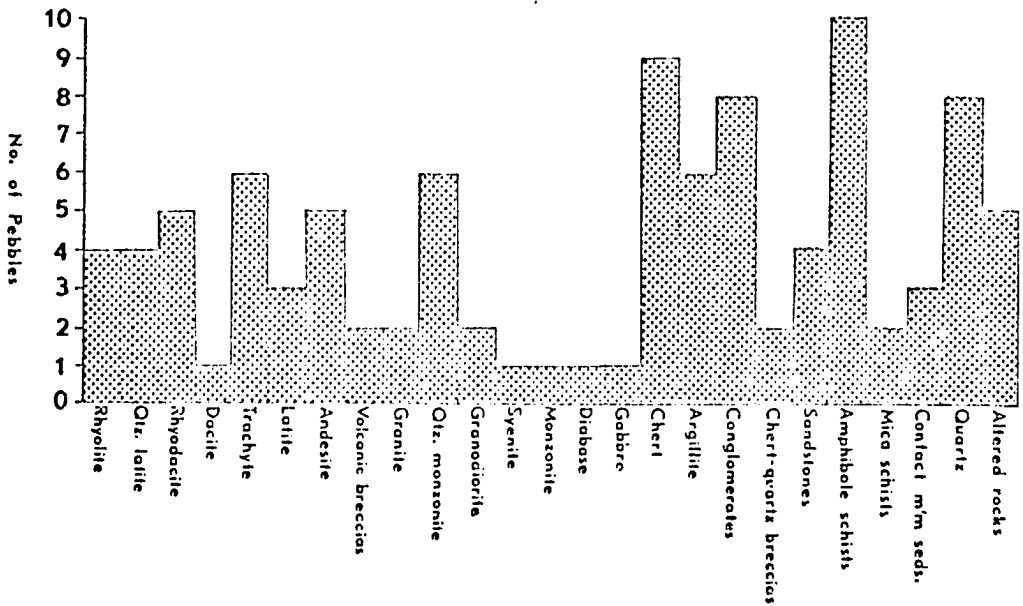


FIGURE 17. Pebble assemblage determined from thin sections.

the actual pebble assemblage studied in thin section.

The descriptive petrographic data indicate a source area in which the basement consists of low- to medium-grade (greenschist to amphibolite facies) crystalline schist intruded by acidic and basic intrusives and mantled by acidic to intermediate volcanics and sediments.

Heavy Mineral Data

Heavy mineral analyses were made of the medium (2 phi to 3 phi) fraction in six sand samples. Each of the three formations studied is represented by one sample from each of the two reference sections (Plates I and II in pocket).

Individual mineral grains in all samples were angular to subangular, with more rounded grains being rare. Figure 18, p. 47 illustrates the frequencies of the various mineral species in the three formations.

It is evident from the diagram that certain assemblages characterize these formations in the specified size range. Significant percentages of chlorite, epidote, garnet (mostly almandite), alterites plus rock fragments, and opaques characterize most of the samples. Biotite and rutile are common to both samples in meaningful amounts in the Healy Creek Formation while concentrations of andalusite, diopside, sphene, and apatite are apparently more sporadic. Minerals occurring in minor and trace amounts include muscovite, sillimanite, kyanite, staurolite, clinozoisite, tremolite, actinolite, green hornblende, blue-green hornblende, hypersthene, augite, zircon, brookite, anatase, blue tourmaline, and brown tourmaline.

The assemblage from the samples in the Suntrana Formation includes significant amounts of andalusite, clinozoisite, zircon, sphene, and brown tourmaline. Minor amounts of sillimanite, kyanite, tremolite, actinolite, green hornblende, hypersthene, diopside, spodumene, rutile, brookite, apatite, and blue tourmaline are also present.

The most characteristic mineral types occurring in both samples of the Lignite Creek Formation are actinolite, green hornblende, blue-green hornblende, brown hornblende, sphene, staurolite, and rutile. Biotite, muscovite, andalusite, kyanite, sillimanite, clinozoisite, tremolite, diopside, and feldspar plus quartz are locally abundant. Trace amounts of enstatite, hypersthene, zircon, apatite, and brown

tourmaline also occur in one or both samples.

CHAPTER IV

INTERPRETATION OF PROVENANCE AND DEPOSITIONAL AREA

Any hypothesis regarding provenance and genesis of sandstones must include consideration of these factors: (1) geology of the source terrane; (2) tectonics of the source land; (3) tectonics of the depositional site; (4) depositional environment; and (5) paleoclimate and its effects on weathering of the material (Folk, 1968, p. 116). The data presented in the previous chapter are discussed in light of these topics.

Geology of the Proposed Source Terrane

Directional data from crossbeds indicate that the major source of the sediments was to the north of the Healy area (Fig. 9 , p. 31). This data appears to justify exclusion of the Alaska Range as a major source terrane, although the rocks in that area are sometimes quite similar to those of the proposed source, mainly the Yukon-Tanana Upland.

The region described in the following section includes the Yukon-Tanana Upland and the Kokrine-Hodzana Highlands (Wahrhaftig, 1965; see fig. 19, p. 50). Common rock types of the area are described in metamorphic, sedimentary, and igneous suites, respectively.

Metamorphic Rocks

The crystalline bedrock of the central and eastern portions of the Yukon-Tanana Upland consists of a thick sequence of variably metamorphosed and complexly folded rocks ranging from lower greenschist facies to upper amphibolite facies in metamorphic grade. Radiometric age dates varying from Ordovician

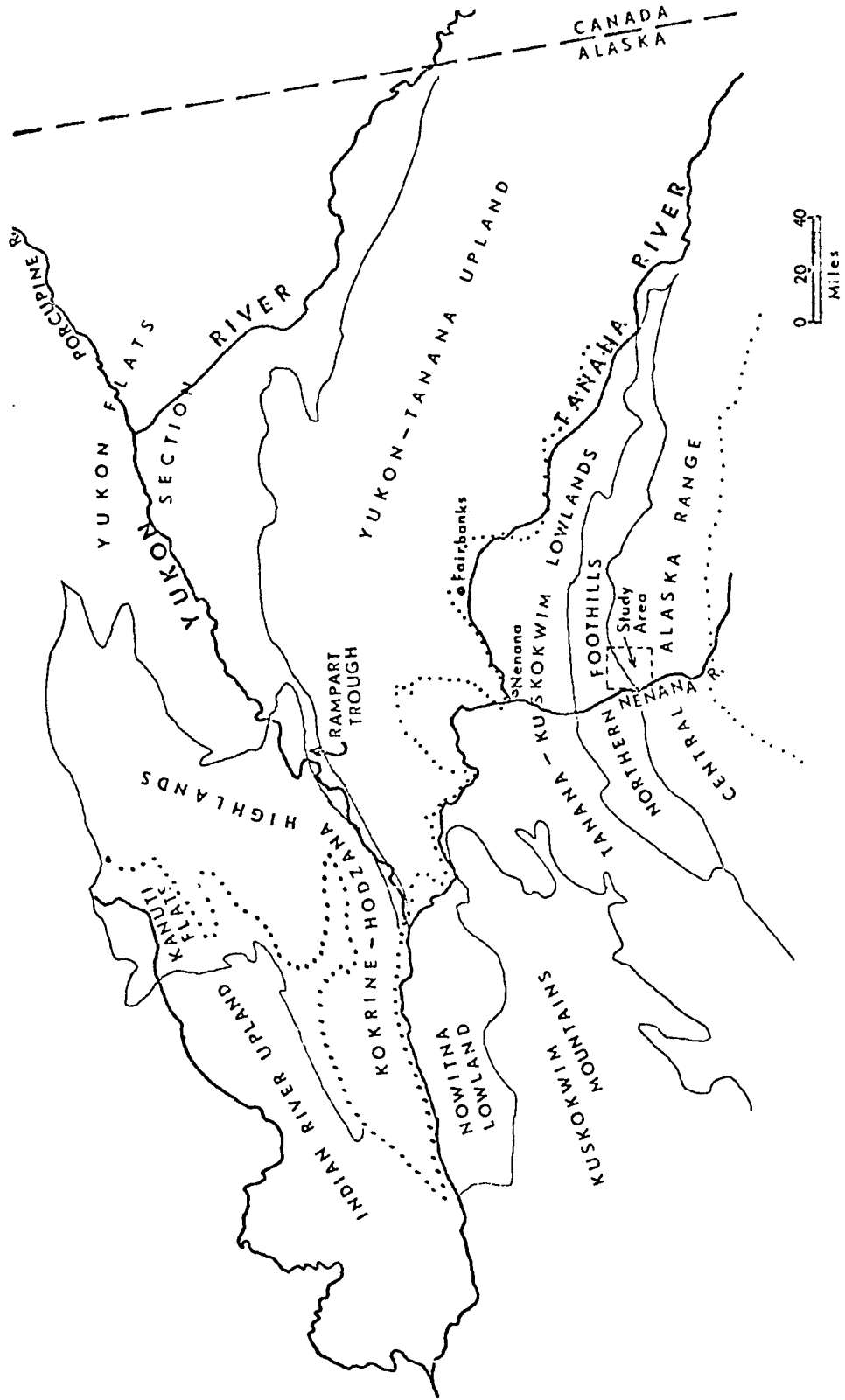


Figure 19. Physiographic provinces of east-central Alaska (after Wahrhaftig, 1965).

through Tertiary indicate periods of igneous activity as well as different episodes of regional metamorphism. Interpretations of age and correlations of crystalline bedrock units are further complicated by their deformation and the presence of retrograded rocks and contact metamorphic aureoles. Phyllite, calc-phyllite, quartz-graphite schist, quartz-mica schist, marble, quartzite, chert, argillite, slate, and metavolcanics are common representatives of the greenschist facies. Amphibolite facies rocks include quartz-biotite gneiss, augen gneiss, hornblende gneiss, granitic gneiss, amphibolite, quartzite, and marble. Many of the amphibolite facies rocks are highly garnetiferous (Foster and Weber, 1970; and Weber, 1971, personal communication). Eakin (1916, p. 26) described the metamorphic rock complex in the Yukon-Koyukuk region as a series of para- and ortho-metamorphics. The para-metamorphic rock types present include schistose quartzites and quartzitic, quartz-mica, graphitic and garnetiferous schists; ortho-metamorphic rocks include amphibolite schists, augen gneisses, and feldspathic and sericitic schists. These rocks may be equivalent to the metamorphic complex of the Yukon-Tanana Upland (Eakin, 1916, p. 31).

Sedimentary Rocks

A thick sedimentary sequence of highly-deformed Cambrian to Mississippian rocks occurs in a belt along the north side of the Yukon-Tanana Upland (Fig. 20, p. 52). These rocks, including some Paleozoic greenstone volcanics, crop out in several bands and basins in the area (Foster and Weber, 1970). The Paleozoic units are probably correlative with similar rock types in the Circle and Eagle areas (Mertie, 1937, pp. 95-97; Williams, 1959, p. 298). Shale, mudstone, chert, sandstone, conglomerate, limestone, argillite, and the basaltic volcanics are the major rock types (Brabb and Churkin, 1969; Mertie, 1937, pp. 75-127).

Sedimentary rocks in the Yukon-Koyukuk region have been dated as belonging to the Devonian period and earlier Paleozoic, the Cretaceous, and Tertiary (Eocene?) periods (Eakin, 1916). A sequence of fine clastics, impure limestones, cherts, and some igneous (greenstone?) materials represent the Lower Paleozoic. Limestones associated with volcanics are characteristic of the Early Cretaceous and Late Cretaceous; Tertiary sediments consist of a sequence of clays and shales

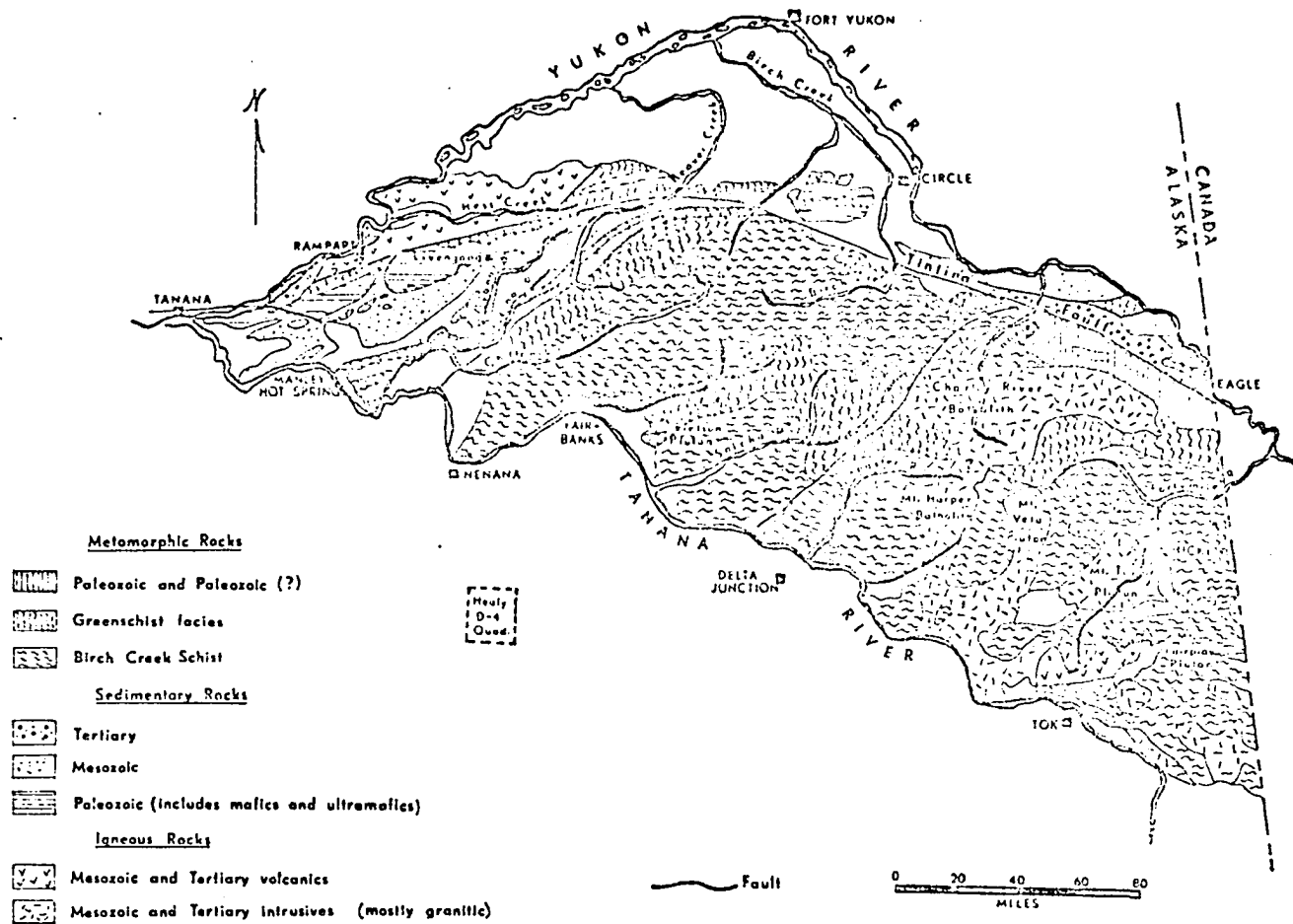


Figure 20. General geologic map of the Yukon-Tanana Upland (after Foster and Weber, 1970).

grading upward into sandstones and conglomerates (Eakin, 1916, p. 66). These younger sedimentary rocks are distributed along a linear belt trending northeastward essentially parallel to the Yukon River.

Igneous Intrusives

Granitic to granodioritic intrusions of Mesozoic age crop out over large areas in the eastern portion of the Yukon-Tanana Upland. The rock types present include granite, quartz monzonite, and granodiorite. Monzonite and syenite occur in lesser amounts. Numerous smaller Mesozoic granitic intrusives are characteristic of the western part of the Upland. Monzonitic and syenitic bodies are again present, but apparently are rare (Weber, 1971, personal communication). Most of the intrusives are quartz monzonites, granodiorites, and granites. Radiometric age dates on some of these intrusives indicate that they are Late Cretaceous in age (Weber, 1971, personal communication). A line of alkaline intrusives borders the southern edge of the Yukon-Tanana Upland (Forbes, 1968, personal communication; Fig. 21, p. 54).

Granitic rocks in the Kokrine-Hodzana Highlands area (Yukon-Koyukuk region) are tentatively assigned Late Paleozoic (?) and Mesozoic to Tertiary ages. The older granitic rocks include granites, monzonites, and diorites, and commonly grade into gneisses as do the younger granites. The latter vary from aplitic or pegmatitic to dioritic compositions with the normal, medium-grained, equigranular granite phases being the most prevalent (Eakin, 1916, p. 50).

Many basic and ultrabasic sills and dikes occur throughout the Yukon-Tanana Upland and in the Kokrine-Hodzana Highlands. These apparently are often associated with the Tintina lineament and other major faults and are generally assigned Paleozoic ages (Williams, 1959, p. 320). These rocks are variously referred to as greenstones, serpentinites, and ultrabasic bodies. Basic rocks often associated with the ultrabasic include diabases, gabbros, and some diorites (Williams, 1959, p. 320).

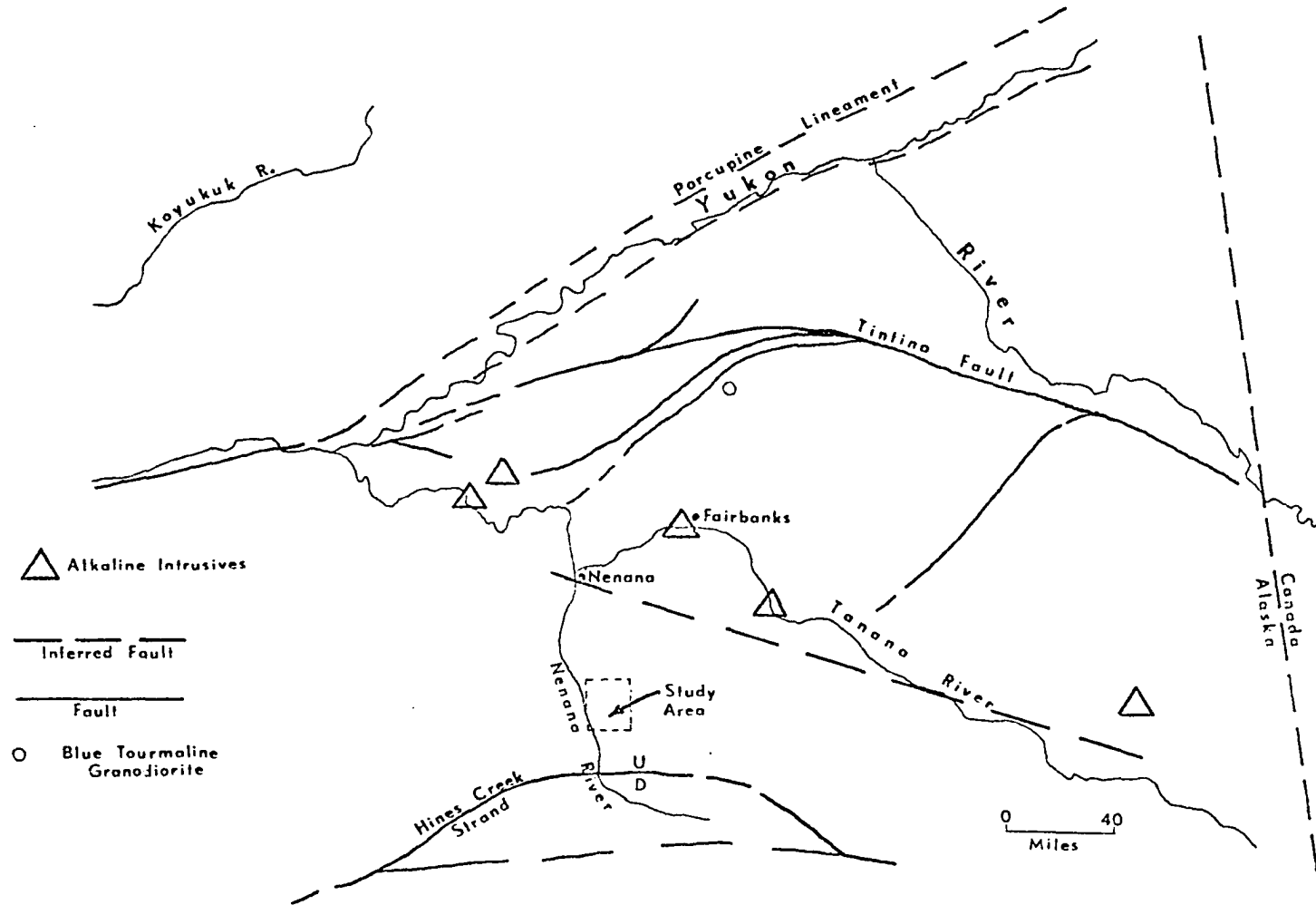


Figure 21. Major faults of east-central Alaska and alignment of alkalic intrusives (after Foster and Weber, 1970; Grantz, 1966; and Forbes, 1968, personal communication).

Igneous Extrusives

Most of the igneous extrusive rocks in the northwestern part of the Yukon-Tanana Upland are Paleozoic in age. These are mostly basalts and related rocks of the Rampart group and the approximately equivalent Circle volcanics of Mississippian (?) age (Mertie, 1937).

Church and Durfee (1961) described altered pyroxene andesites and related pyroclastics of the "Tatalina group" (Prindle, 1913, p. 37) in the White Mountain area. These are of questionable Ordovician age (Church and Durfee, 1961, p. 39).

The Woodchopper volcanics of the Charley River area are assigned a Devonian (?) age and are not considered to be correlative with the Rampart group (Mertie, 1937, p. 127). These volcanics are mostly basalts with thin interbeds of sedimentary rocks. Isolated occurrences of Paleozoic basalts and diabases were mapped by Prindle (1913) near the headwaters of the Charley River.

Tertiary basalts and diabases are fairly common in the Tanacross quadrangle (Foster, 1970) and a few isolated exposures of basalt are known in the immediate vicinity of Fairbanks (Prindle, 1913, p. 74).

Eakin (1916) mapped basalts, andesites, and andesite breccias of Tertiary or younger age near the headwaters of the Kanuti River in the Kokrine-Hodzana Highlands.

Pebble Types versus Geology of the Proposed Source Area

The above descriptions of the bedrock geology of the Yukon-Tanana Upland and the Kokrine-Hodzana Highlands indicate a long, complex history of that region. From Late Precambrian to Middle or Late Paleozoic time, the Upland was a site of deposition of mostly eugeosynclinal sediments (Weber, 1971, personal communication). Most of the record of that period of deposition is preserved in the sedimentary rocks characteristic of the northwestern part of the Upland. These rock types include quartzites, quartz-mica schists, grits, slate, chert, limestone, greenstone, siliceous shale, tuff, chert pebble conglomerate, and graywacke. Diabase, diorite, gabbro, and basaltic volcanics commonly intrude or are interlayered with these sediments (Weber, 1971, personal communication).

Most of these polymictic rock types are well-represented in the pebbles of

the Healy Creek-Lignite Creek area, particularly argillite (or siliceous shale), quartzite, quartz-mica schists, chert, chert pebble conglomerate, and graywacke. Diabase, gabbro, and basic volcanic rocks are also represented in the study area, although the occurrences as pebbles are uncommon. These rock types are less resistant than the previously mentioned types and therefore common occurrences of these basic igneous rocks would not be expected.

Extensive exposures of granitic intrusives, sometimes of batholithic dimensions, and polymetamorphic terrane characterize the eastern part of the Upland. These rock types, predominantly quartz monzonite and granodiorite, are represented in the pebbles of the study area. Quartz monzonites and granites are well-represented in the pebble assemblage, especially in the Lignite Creek Formation. These granitic rocks would be expected to occur in greater abundance than the granodiorites and more basic rocks because they are more resistant to weathering.

Monzonitic and syenitic intrusives are uncommon in the Upland and are rare in the pebble assemblage. These rock types should be destroyed quickly by weathering because of their lack of quartz.

Volcanics are well-represented in the pebble assemblage, but are generally not common in the Yukon-Tanana Upland except in the northwestern and eastern extremities. Volcanics were probably common in the Upland before uplift and subsequent erosion of the sedimentary and extrusive igneous material which undoubtedly once mantled the crystalline rocks.

At least one unusual rock type is present in the pebble assemblage. This rock, a blue tourmaline dacite (p. 92, specimen A-D-3-22 No. 9 in Appendix II) is similar to a blue tourmaline granodiorite described by Church and Durfee (1961, pp. 67-68) from the White Mountains (Fig. 21, p. 54). The pebble may have originated from this area, or at least it seems quite probable that it is genetically related to the granodiorite. Other rock types described by Church and Durfee (1961) such as the quartz monzonites are similar to, and perhaps related to pebbles from the study area. Rocks containing sodic (?) mafics may be derived from or genetically related to the belt of alkaline rocks known to occur along the southern border of the Yukon-Tanana Upland.

Heavy Minerals versus Geology of Proposed Source Area

Heavy mineral species from the sandstones in the study area are indicative of an igneous and metamorphic source (Table 4 , p. 58). Possible source rock types for the minerals closely correlate with the rock types characteristic of the Yukon-Tanana Upland and with the rock types present in the pebble assemblage.

Healy Creek Formation

In the Healy Creek Formation, the heavy minerals occurring in amounts greater than 5% of the total assemblage are biotite, andalusite, chlorite, and garnet (almandite?). These minerals have probably been locally derived from schists, as suggested by Wahrhaftig and others (1969, p. D8).

Kyanite, staurolite, and epidote occur in amounts greater than 1% of the heavy mineral assemblage. Most of these minerals plus the more common ones mentioned above are generally formed during medium-grade metamorphism of pelitic rocks. Diopside most often results from thermal metamorphism although it also occurs in basic igneous rocks. Zircon, sphene, rutile, apatite, and brown tourmaline are common accessories in igneous and metamorphic rocks.

Trace amounts (< 1%) of muscovite, sillimanite, clinozoisite, tremolite, actinolite, green hornblende, blue-green hornblende, hypersthene, augite, brookite, anatase, and blue tourmaline also occur in the Healy Creek Formation. The muscovite, clinozoisite, tremolite, actinolite, and possibly hornblende are also low- to medium-grade metamorphic minerals which may have formed locally in an area of thrust-faulting. Hypersthene and augite are usually derived from intermediate to basic igneous rocks, and brookite and anatase may have either igneous or metamorphic origins. Blue tourmaline is probably indicative of an igneous source. Blue tourmaline of similar appearance is present in a pebble studied in thin section. (See page 39.)

TABLE 4
Sources of Derivation for Heavy Mineral Species
(After Milner, 1962)

Heavy Minerals	Possible Sources of Derivation (Rock Types)																									
	Igneous Rocks	Granites and equivalent rock types	Syenites and equivalent rock types	Diorites and equivalent rock types	Intermediate rocks	Basic rocks	Ultrabasic rocks	Pegmatites	Metamorphic Rocks	Crystalline schists	Mica schists	Gneisses	Metamorphic basic igneous rocks	Metamorphosed ls. and Mg ls.	Hornblende schist	Metamorphic sedimentary rocks	Contact metamorphic rocks	Phyllites	Altered Rocks	Alteration of plagioclase feldspar	Altered gabbros and peridotites	Serpentine	Secondary alteration of Fe-Mg mafics	Alteration of limestones	Decomposition of ilmenite	
Biotite	x								x																	
Muscovite	x								x																	
Andalusite		x														x										
Sillimanite										x																
Kyanite									x	x	x															
Staurolite									x								x									
Clinozoisite									x			x								x						
Tremolite									x	x			x								x	x				
Actinolite									x														x			
Hornblendes		x	x	x					x						x											
Enstatite						x	x									x										
Hypersthene					x	x	x																			
Diopside	x					x				x		x				x										
Augite					x	x																				
Spodumene		x						x			x	x														
Zircon	x	x	x	x	x					x				x												
Sphene		x			x				x	x		x													x	
Rutile	x	x	x							x																x
Brookite	x	x	x							x																
Anatase	x									x																
Apatite	x	x	x																							
Tourmaline		x	x					x		x		x						x								
Chlorite																						x	x			
Epidote										x																
Garnet	x																									

Suntrana Formation

Heavy minerals occurring in concentrations of 5% or greater in the Suntrana Formation include chlorite, andalusite, epidote, garnet (almandite?), alterites plus rock fragments, and opaques. These minerals, as mentioned earlier, are probably derived from a low- to medium-grade metamorphic source.

Minerals occurring in concentrations greater than 1% but less than 5% are biotite, staurolite, clinozoisite, zircon, sphene, and brown tourmaline. The biotite, staurolite, clinozoisite, and perhaps sphene are generally low- to medium-grade metamorphic products of pelitic rocks and/or intermediate to basic igneous rocks or graywackes. Zircon is commonly derived from a granitic igneous source and brown tourmaline occurs in granitic rocks as a late phase mineral or in metamorphic rocks as the product of metasomatism (Deer, Howie, and Zussman, 1967).

Trace minerals (< 1%) in the Suntrana Formation are sillimanite, kyanite, tremolite, actinolite, green hornblende, hypersthene, diopside, augite, spodumene, rutile, brookite, apatite, and blue tourmaline. The origins of these minerals excepting spodumene have been discussed above but will be briefly reiterated. Sillimanite may have originated in areas of thrust-faulting; tremolite, actinolite, green hornblende, and kyanite are products of low- to medium-grade regional metamorphism of various rock types; and hypersthene and augite are generally derived from intermediate to basic igneous rocks. Diopside may result from thermal metamorphism, and spodumene is most commonly associated with granitic pegmatite. Tourmaline, apatite, and sometimes rutile are generally associated with granitic igneous sources, and brookite may be from either an igneous or a metamorphic source.

Lignite Creek Formation

Abundant (> 5%) heavy minerals in the Lignite Creek Formation include epidote, green hornblende, blue-green hornblende, brown hornblende, and alterites plus rock fragments. The epidotes are principally derived from regional metamorphism of basic igneous rocks (Deer, Howie, and Zussman, 1967, p. 67). Hornblendes in abundance are especially indicative of metamorphic or volcanic rocks. Brown hornblende is particularly diagnostic of basaltic rocks.

Biotite, muscovite, chlorite, andalusite, sillimanite, kyanite, staurolite, clinozoisite, garnet, tremolite, actinolite, diopside, sphene, rutile, and alterites plus rock fragments occur in concentrations $> 1\%$ but less than 5% of the total percentages in the Lignite Creek Formation samples. These minerals with the exception of sphene and rutile are diagnostic of a metamorphic source. Sphene and rutile are common in both metamorphic and igneous rocks.

Enstatite, hypersthene, and zircon occur in trace amounts ($< 1\%$) in the Lignite Creek Formation. Zircon is generally indicative of a granitic igneous source and enstatite and hypersthene are derived from an intermediate to basic igneous rock source.

Heavy minerals from the Healy Creek, Suntrana, and Lignite Creek formations are indicative of a complex igneous and low- to medium-grade metamorphic source terrane. Trace amounts of high-grade metamorphic minerals are possibly derived from thrust-faulted areas.

Tectonics of the Source Land

The tectonics of central Alaska are extremely complex and no attempt at a thorough analysis of structural features is made here. A few of the more important features of the Mesozoic and Cenozoic tectonics are described and discussed in an attempt to shed some light on the structural history of the coal basins.

Since Early Mesozoic time, the structural habit of East-Central Alaska has been dominated by movement along major fault zones resulting in fault block tectonics. Among these major features, the Tintina fault zone, the Hines Creek strand of the Denali fault, and inferred structural features of the Tanana Valley pertain to the structural interpretation of the Healy Creek-Lignite Creek area (Fig. 21, p. 54).

The Alaskan segment of the Tintina fault zone strikes northwest and borders the northern part of the Yukon-Tanana Upland. This strike-slip fault may splay out into several faults near the western border of the Upland. Studies indicate that continued westerly rotation of the south block of the Tintina has resulted in the superimposition of a dominantly northeasterly structural trend on the original northwesterly trend (Foster and Weber, 1970). The main lateral displacement along the fault

may have occurred during Late Cretaceous (Grantz, 1966, p. 36). Movement of uncertain type with a strong dip-slip component has occurred on faults paralleling and adjacent to the Tintina; the age of these movements may be as late as Pliocene (?) or younger (Grantz, 1966, p. 36).

The Hines Creek strand of the Denali fault lies approximately ten miles due south of the Healy area and strikes east-northeast to east. Stratigraphic relationships within the Cantwell Formation (Paleocene) (Wolfe and Wahrhaftig, 1968, p. 41) indicate that much displacement already existed by Cantwell time along the Hines Creek strand, where stratigraphic displacement is up to the north. Movement continued into early Tertiary time west of the Nenana River Valley, and smaller post mid-Pliocene vertical movements, also stratigraphically up to the north, have continued into the recent. Direct evidence of pre-Paleocene lateral slip has not been found and only the vertical displacements can be proven (Grantz, 1966, pp. 16-17).

The presence of a fault zone north of the Tanana Valley is largely based on geophysical evidence (Brosgé, *et al.*, 1970) and alignment of alkaline intrusives (Forbes, 1968, personal communication) (Fig. 21, p. 54). North-south structures and east-west faults are also based on geophysical evidence (Brosgé, *et al.*, 1970).

Periods of intrusive activity may be related to the fault block movements. Intrusive activity during the Mesozoic [Jurassic (?) and Late Cretaceous (?)] resulted in stocks, batholiths and other intrusive bodies of major proportion in the eastern part of the Yukon-Tanana Upland (Gates and Gryc, 1963, p. 273; Mertie, 1937, p. 226). Granitic bodies of smaller proportions were injected in the western part of the Upland at about the same time. Marked increases in amounts of detrital potassium feldspar in rocks of post middle Early Cretaceous (Brabb, 1969) suggest that earlier Mesozoic intrusives in the Yukon-Tanana Upland were unroofed by Late Mesozoic time (Churkin, 1970, p. 80). Intrusive activity occurred in the extreme west of the Upland during middle to late Tertiary time (Mertie, 1937, pp. 225-226).

The evidence for major vertical movements along older strike-slip faults such as the Tintina and the Hines Creek strand of the Denali fault during Late Mesozoic and Tertiary time is strong. Therefore it is probable that Tertiary tectonics in east-central Alaska were characteristically of horst and graben type. Many of the Recent sedimentary basins such as the Tanana Valley probably result from these Cenozoic fault block movements.

According to a chart compiled by Hubert (1961) (Table 5, p. 62), the quantities and types of non-opaque heavy mineral species similar to those present

TABLE 5
Heavy Minerals in Sandstones
(After Hubert, 1961)

Rock Type	Orthoquartzite (first and "second" cycle)	Miogeosynclinal graywackes and derived micaceous quartzose sandstones	Coastal Plain graywackes and derived micaceous quartzose sandstones
Source Rocks	"Peneplaned" crystallines and older orthoquartzites	Low to medium rank metamorphic rocks; sediments	Metamorphic rocks; pegmatites; sediments (igneous rocks)
Weight Percent	0.01-1.0 (mean about 0.02)	0.1-1.0 (mean about 0.2)	0.1-1.0 (mean about 0.4)
Number of non-opaque species	Poor to very poor 2-5	Poor to moderate 5-10	Rich 10-15
Number of non-opaque varieties	Many (25) for tourmaline and zircon	Many (25) for tourmaline and zircon	Many (25) for tourmaline and zircon
Tectonism	Quiescence for first cycle. Uplift for "second" cycle	Lateral folding of flanks of miogeosynclines	Uplift of continent
Principal non-opaque species	Rounded; zircon, tourmaline, rutile, (garnet, staurolite much more rare)	Mixed angular and rounded zircon, tourmaline, rutile, muscovite, apatite, staurolite, garnet and a few more	Mixed angular and rounded zircon and tourmaline; kyanite, garnet, staurolite, hornblende, apatite, etc.
Authigenic species	Anatase, rutile, tourmaline	pyrite, barite	pyrite, barite
Physiography	Shorelines and shallow seas (fluvial rare)	Deltas, shorelines, shallow seas (fluvial rare)	Deltas, shorelines, shallow seas, fluvial
ZTR Maturity Index	High 75-100 (mean about 97)	Low to moderate 20-85	Low to moderate 20-85

TABLE 5, Cont.
Heavy Minerals in Sandstones
(After Hubert, 1961)

Rock Type	Eugeosynclinal feldspathic gray-wackes	Post-geosynclinal arkoses (Live) and glacial deposits	Shield arkoses (Dead) and derived feldspathic quartose sandstones
Source Rocks	Metamorphic rocks; volcanics	Igneous and metamorphic rocks; pegmatites	Batholiths (and metamorphic rocks)
Weight Percent	0.1-4.0 (mean ?)	1.0-10.0 (mean about 1.7)	1.0-7.0 (mean ?)
Number of non-opaque species	Poor to moderate 5-8	Very rich 15-20	Poor to moderate 5-8
Number of non-opaque varieties	Very few	Very few	Very few
Tectonism	Collapse trough plus volcanism	Fault troughs on older geosynclines	Rapid uplift
Principal non-opaque species	hornblende, augite, hypersthene, epidote, idiomorphic apatite and biotite and a few more (largely metamorphic types)	zircon, tourmaline, garnet, clinozoisite-epidote, staurolite, muscovite, biotite, sillimanite, apatite, etc.	zircon, tourmaline, garnet, clinozoisite-epidote, staurolite, muscovite, biotite, and a few more
Authigenic species	chlorite, pyrite	often hydro-thermal barite, pyrite, anatase	anatase
Physiography	Deep water marine	Fluvial (marine more rare)	Fluvial (marine more rare)
ZTR Maturity Index	Very low 5-40	Very low 5-40	Low to moderate 20-85

Dark line indicates the model which best suits the sandstones of the study area.

TABLE 5, Cont.
 Heavy Minerals in Sandstones
 (After Hubert, 1961)

Rock Type	Volcanic arkose	
Source Rocks	Volcanics (some sediments)	
Weight percent	?	
Number of non-opaque species	Poor to moderate 5-10	
Number of non-opaque varieties	Very few	
Tectonics	Extrusion of volcanic flows	
Principal non-opaque species	augite, hornblende, zeolites, hypersthene, epidote, idiomorphic apatite and biotite and a few more	
Authigenic species	zeolites, chlorite	
Physiography	Fluvial and marine	
ZTR Maturity Index	Very low 5-40	

in the sandstones of the coal-bearing group indicate an igneous and metamorphic source terrane. The model described in the chart represents an older geosynclinal belt which has been more recently block-faulted. This model seems to accurately describe the Yukon-Tanana Upland and adjacent areas, since the Mesozoic and Cenozoic tectonics of the Upland are characterized by fault-block movements superimposed upon Paleozoic geosynclinal features.

Tectonics of the Depositional Site

It is extremely difficult to reconstruct the tectonics of the Healy Creek and Lignite Creek coal basins exclusive of the other coal basins in the Nenana coal field because the tectonics of all the basins are inter-related. Published data on the thicknesses of the various Tertiary formations are quite sparse in areas outside of the Healy Creek and Lignite Creek basins. On the basis of Wahrhaftig's (1951) stratigraphic sections and Wahrhaftig and others (1969) thickness information, however, a few generalizations can be made: (1) the thickest parts of the various formations trend approximately east-west parallel to the present structural trends; (2) the basin axis was slightly east and south of the Healy Creek and Lignite Creek coal basins; and (3) the sedimentary wedges generally tend to thicken to the south or southeast from the northernmost edge of the Nenana coal field (Rex Creek coal basin).

The cyclic nature of the coal-bearing formations may result from a variety of factors, including tectonic controls. These tectonic controls may specifically be fault movements. If such is the case, spasmodic down-warping of the basin floor due to active faulting would at least partially explain the cyclic tendencies of the sedimentary sequences. Deposition of some of the more widespread sedimentary units may well have been controlled by this mechanism, i. e., the Suntrana formation. The Healy Creek and Lignite Creek formations, which contain thin, localized coals and more discontinuous sedimentation units than the Suntrana Formation, may represent a change to dominantly sedimentary controls of the sediment accumulation.

Environment of Deposition

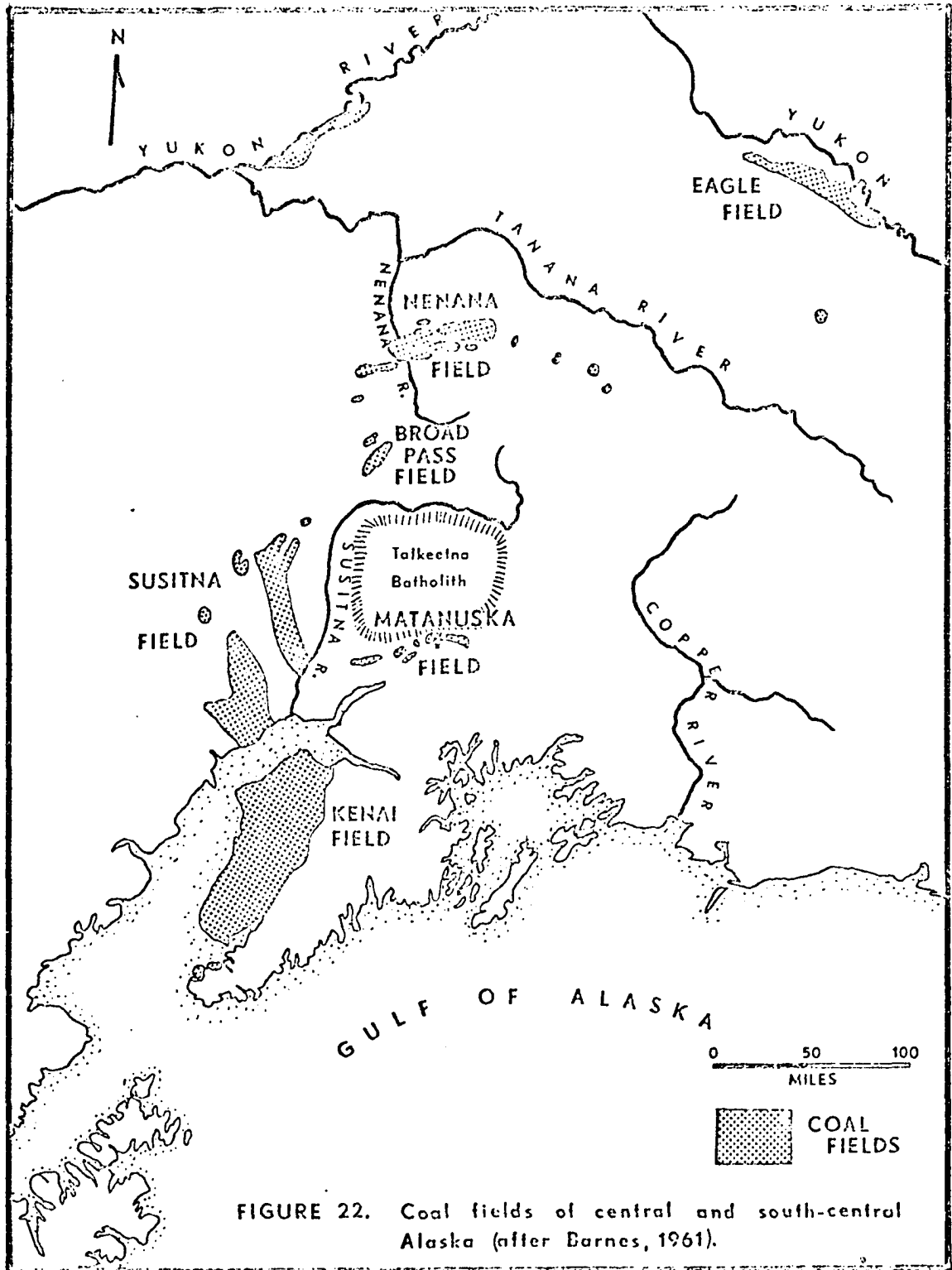
Evidence indicating a fluvial-lacustrine environment of deposition for the sediments in the coal-bearing group is convincing. Plant fossils are not uncommon and are often well-preserved. Coals, usually indicative of a terrestrial environment, are a major part of the stratigraphic section in the study area. Sedimentary structures, including some channels and abundant crossbeds, also indicate a fluvial environment. A strong southerly orientation of corrected crossbed data coupled with moderate to low (69° to 35°) standard deviations from the grand means of the same data also support a fluvial environment interpretation. Crossbed directions in marine sandstones generally have higher standard deviations and tend to be bimodal (Tanner, 1955, p. 2482). The numbers and types of heavy mineral species preserved in the sandstones are also indicative of a fluvial environment according to the chart compiled by Hubert (1961). (See page 63.)

A more specific environment of deposition is difficult to ascertain from the available data because specific environment studies were not made; however, a few speculations on the subject seem to be appropriate at this point.

The basins may have resulted from ponding caused by blockage of stream drainages due to periodic uplifts of the ancestral Alaska Range, perhaps in the area of the Talkeetna batholith (Fig. 22, p. 67). Sudden uplift to the south and subsequent ponding resulted in the deposition of the Sanctuary Formation (Wahrhaftig, *et al.*, 1969, p. D15); similar tectonic movements may have been responsible for formation of the coal-forming bogs. Some of the thinner, more discontinuous coals such as those in the Lignite Creek Formation may have also resulted from some sedimentary controls.

If sedimentary controls are indeed partially responsible for the cyclic tendencies in some of the coal-bearing sediments, then some of these possible controls must be mentioned. These coals possibly developed in bogs resulting from changes in stream channels. The changes may have resulted from: (1) aggradation in the stream channels and subsequent change in the stream gradient; (2) diversion of drainages to new low places resulting from stream aggradation or meandering; and (3) differential compaction of the sediments.

The strong southerly orientation of the directional data, particularly in the Lignite Creek Formation, suggests a paleoslope with a fairly high gradient. Perhaps alluvial fans were major geomorphic features of the region at that time. The



coal-bearing sandstones may very well have been related to such landforms.

Paleoclimate

According to Wolfe (1966), the paleofloras of the Cook Inlet region are similar to the paleofloras of the study area. Wolfe further interprets these floras as being indicative of a warm temperate to temperate climate (1966, pp. B3-B10). Coal formation is more favorable in temperate to cool climates because decay rate is slower there than it is in tropical climates (Weller, 1960).

Heavy mineral fragments studied are almost entirely angular to subangular on the roundness scale and many moderately unstable minerals are preserved. These observations indicate that mechanical abrasion was probably more important than chemical weathering of the material; also, rapid deposition of the sediments is probably responsible in part for the state of preservation of the minerals.

CHAPTER V
GENESIS OF THE SANDSTONES AND SEDIMENTARY HISTORY

A sedimentary model for genesis of the sandstones is proposed in this chapter. A brief summary, conclusions, and areas of future research are also included.

Healy Creek Formation

Wahrhaftig (in Wahrhaftig, et al., 1969, p. D9) states that the predominant direction of streamflow during the late Oligocene in the Healy Creek Formation was to the north and that the sediments were locally derived from a metamorphic terrane. The few crossbed measurements taken by the writer indicate a local direction of flow to the southwest in the Healy Creek Formation. These data, however, are insufficient to refute Wahrhaftig's interpretation.

Descriptions of the Healy Creek Formation (Wahrhaftig, et al., 1969, pp. D8-D9) indicate textural immaturity in the sediments. Heavy minerals are not abundant and consist almost entirely of low-grade metamorphic and stable igneous accessory minerals (Table 2, p. 28). The mineral grains are angular to sub-angular and garnet (almandite?) is quite common. Many if not most of the heavy minerals are probably derived from the adjacent metamorphic terrane as Wahrhaftig has suggested. The low-grade metamorphic minerals are probably primary. Higher grade metamorphic minerals and igneous accessory minerals may have originally been incorporated into the unmetamorphosed sediments which later became crystalline schist from which the Healy Creek Formation was derived. The low percentage of heavy minerals in the sandstones and the abundance of quartz and chert pebbles in the pebble suites (p. 19) attest to the quartz-rich nature of the source rocks of the formation.

Patchy distribution and variations in thickness of the Healy Creek Formation all along the northern edge of the Alaska Range may be indicative of a series of

structural basins of varying depths which were part of a single large structural trend. The greatest measured thickness of the formation is 1150 feet at the eastern end of the Lignite Creek basin. A thickness of 800 feet is recorded in the eastern end of the Healy Creek coal basin, and about 1000 feet of the formation is present in the Mystic Creek coal basin. About 2000 feet of coal-bearing strata from the Jarvis Creek coal basin have been correlated with the Healy Creek Formation (Wahrhaftig, et al., 1969, p. D8).

Rapid subsidence of structural basins seems to be indicated by the sediments of the Healy Creek Formation. Wahrhaftig (in Wahrhaftig, et al., 1969, p. D9) suggested considerable topographic relief in the depositional basins. Such basins were possibly tilted fault-block basins and the Healy Creek Formation may have been deposited as alluvial fans which filled these basins. Sedimentary controls and some spasmodic vertical movements along the faults would help to explain the cyclic nature of the lenticular sediments in the formation.

The Sanctuary Formation accumulated in a large, shallow lake formed by stream blockages caused by sudden depression of the basin. This basin continued to subside during the deposition of the overlying formations (Wahrhaftig, et al., 1969, p. D15).

Suntrana Formation

Following deposition of the lacustrine Sanctuary Formation, cyclic sedimentation was resumed during accumulation of the Suntrana Formation. The submature to mature sandstones in the Suntrana Formation are quite different from the less mature sandstones of the Healy Creek Formation (Wahrhaftig, et al., 1969, pp. D16 and D8). The more mature nature of the sandstones in the Suntrana Formation may be due to winnowing action of the streams and a more distant source area for the sediments.

Heavy mineral suites in the formation are somewhat similar to those of the Healy Creek Formation (Fig. 18, p. 47) in that relatively few, mostly low-grade metamorphic mineral species and stable mineral species make up the major parts of the assemblages. As in the Healy Creek Formation, the minerals are angular to subangular in the Suntrana Formation.

The pebble assemblages of the Suntrana Formation are more complex than those of the Healy Creek Formation. Granitic igneous rock types are not uncommon and a greater variety of rock types having sedimentary origins are present. Most of the rock types are fairly resistant to abrasion due to the presence of abundant quartz and fairly uniform, often fine-grained textures.

Crossbed data indicate a source to the north-northeast of the study area (Fig. 10, p. 32). The standard deviation from the grand mean (69°) of the crossbed readings measured in this formation suggests a low gradient with perhaps some channel meandering.

Isopach maps of the Q-mode factors 1 and 7 (Figs. 13 and 14, pp. 36, 38) probably are related to structural components within the depositional basin. The isopach map of factor 1 probably reflects the general configuration of the sedimentary basin in the study area during middle Miocene. The depositional strike of the basin delineated by this mapped factor is approximately N. 68° W. This strike is parallel or subparallel to the strikes of regional structural trends including the northeastern part of the Tintina fault zone, the inferred structures in the Tanana Valley, and the Hines Creek strand of the Denali fault. Crossbed measurements taken at the stratigraphic interval where factor 1 occurs (Fig. 12, p. 35) are in accord with this interpretation.

Factor 7 probably represents a north-south structural component active in the depositional basin during accumulation of the middle and upper Suntrana Formation (Fig. 14, p. 38). Evidence supporting this interpretation is apparent in northward extensions of the Suntrana Formation in the area of the Rex Creek coal basin (Fig. 23, p. 72). The north-south alignment of basaltic dikes south of the study area may also be related to this structural component.

The Suntrana Formation attains a maximum thickness of 1290 feet in the eastern part of the Healy Creek coal basin and is about 1000 feet thick in the Wood River coal basin north and west of these locations; the formation pinches out along a line shown in Fig. 24, p. 73. These data, though sparse, seem to indicate thickening of the formation along the main axis of subsidence or downwarping.

The major contributing source of the sediments in the Suntrana Formation may lie beneath the Quaternary alluvial fill in the structural trough of the Tanana Valley. According to Churkin (1970), the bedrock beneath the present Tanana Valley was exposed in a structural high during the Tertiary period (Fig. 25, p. 74). The Yukon-Tanana Upland is also a possible source for the sediments.

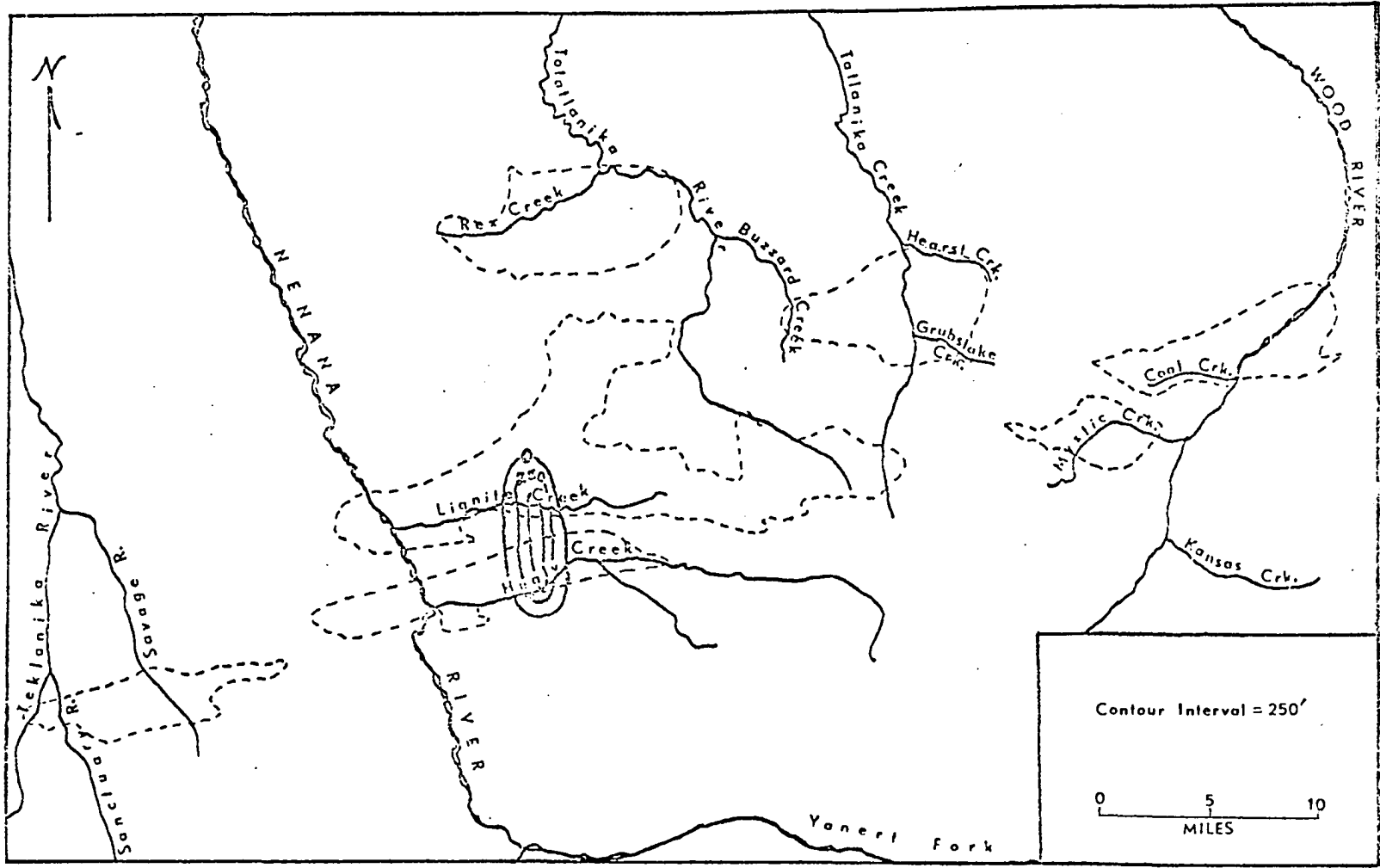
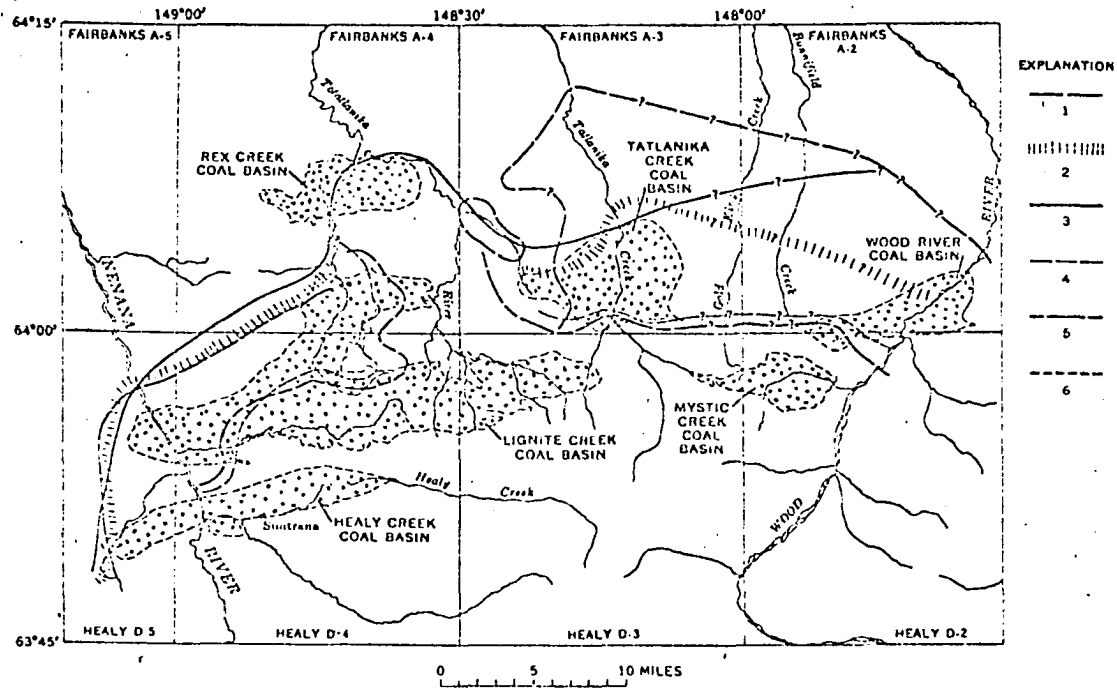


Figure 23. "Isopach" map of factor 7 compared to regional distribution of coal basins in the Nenana coal field. Note correlation of north-south factor trend with northern extension of coal field.



—Map of the Nenana coal field and environs, Central Alaska Range, showing the major coal basins of the coal field and northern limits of several of the formations. 1, northern limit of deposition of the Grubstake Formation; 2, approximate zone of interfingering of coal-bearing and noncoal-bearing facies of the Lignite Creek Formation; 3, northern limit of deposition of the Suntrana Formation; 4, northern limit of deposition of the Sanctuary Formation; 5, northern limit of deposition of the Healy Creek Formation; 6, boundary of coal basin.

Figure 24. Nenana coal field basins showing northern limits of the coal-bearing formations (after Wahrhaftig, et al., 1969).

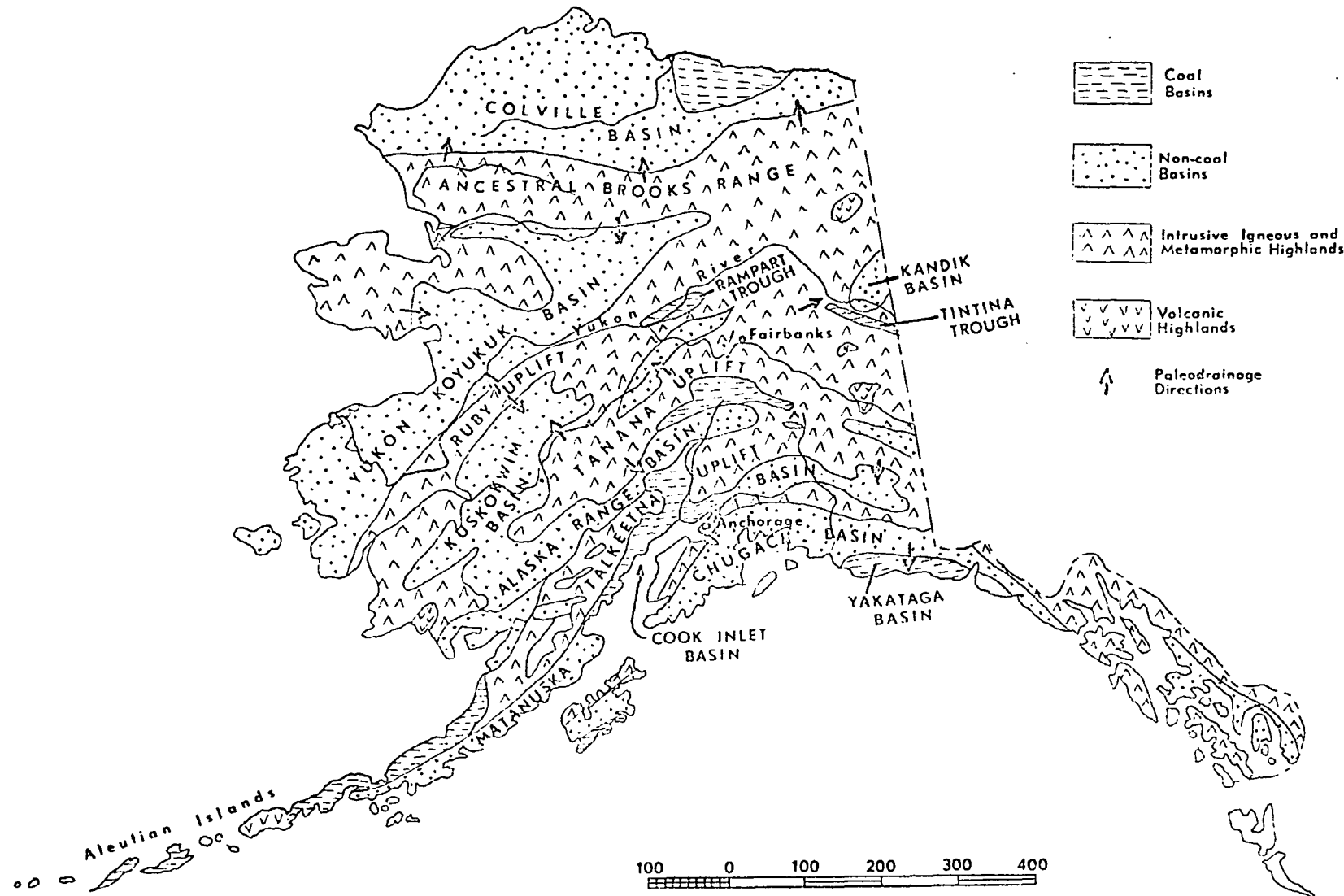


Figure 25. Highlands and basins of Mesozoic and Early Cenozoic time (after Churkin, 1970).

The cyclic nature of the sediments in the Suntrana Formation was probably controlled by spasmodic tectonic activity due to faulting and/or perhaps folding. Some sedimentary controls may have been partially responsible for development of the cyclic phenomenon, but the writer believes that such controls were probably minor because of the regional distribution of some of the individual coal seams.

Lignite Creek Formation

Cyclic sedimentation in the Lignite Creek Formation is much less pronounced than in the Suntrana Formation and the coal seams are generally much thinner and fewer in number. The sandstones contain about ten percent heavy minerals (Wahrhaftig, *et al.*, 1969, p. D20), are generally clean, well-sorted, and sub-arkosic. The relative textural maturity probably indicates exposure of the sands to winnowing action during stream transport from the "distant" source. The relative mineralogical immaturity is probably due to (1) change in major source area from the sources of the underlying formations, and (2) rapid transport and burial of the sediments. The heavy mineral assemblages, pebble assemblages, and crossbed directional data are compatible with these conclusions.

There is a definite change in the heavy mineral assemblage from those of the underlying formations. Higher percentages of most of the heavy minerals represented in the Healy Creek and Suntrana formations are present, and the addition of more unstable minerals, especially hornblende varieties, is obvious (Fig. 18 p. 47). Slightly greater quantities of heavy minerals definitely indicative of a complex metamorphic source terrane are also present. The heavy minerals are angular to subangular and therefore probably indicate a primary sedimentary cycle and rapid burial.

A definite increase in the complexity of the pebble types from those of the underlying formations is also characteristic of the Lignite Creek Formation (Table 6, p. 76). A much greater variety of igneous and metamorphic rock types are represented in the suite and several unstable rock types such as gabbro, monzonite, and syenite (?) are present, although they are fairly rare. Most of these rocks could not be keyed to specific areas, but nonetheless were found to be similar to some rocks of the Yukon-Tanana Upland. The problems involved in these comparisons

TABLE 6
 Resumé of Prominent Characteristics of the "Tertiary Coal-Bearing Group" Strata

Formation	Crossbed Direction	Pebble Characteristics	Heavy Mineral Characteristics	Cyclicality	Coal Characteristics
Grubstake Formation	*to north	*Quartz and chert from Cantwell Formation	?	*poorly developed (?)	*very thin (1" to 1'), bony
Lignite Creek Formation	persistently to south	Assemblage complex; diverse igneous, metamorphic, and sedimentary types	Low- to medium-grade metamorphic minerals more prominent; metastable amphiboles definitely prominent	*moderately	*generally thin,
Suntrana Formation	to south-southwest	Assemblage moderately complex; mostly granitic igneous types, low-grade metamorphics, and resistant sedimentary types	Mostly low- to medium-grade metamorphic types; some stable igneous types (generally granitic accessories)	*moderately well-developed	*sometimes thin but commonly fairly thick; laterally persistent over wide areas
Sanctuary Formation	none	none	?	*poorly developed	*present but not described, uncommon
Healy Creek Formation	*diversity of directions, predominant direction to north	Assemblage simple; almost entirely quartz, chert, argillite, and quartzite	Mostly low- to medium-grade metamorphic types, some stable igneous types (generally granitic accessories)	*moderately to poorly developed	*lenticular; sediment components often "mixed"

*Wahrhaftig et al., 1969.

are manifold, especially since the bedrock geology of east-central Alaska is so complex and, commonly, not mapped in detail. At least one rock, however, is perhaps successfully keyed to a general area near Livengood (Fig. 21, p. 54).

A low standard deviation (35°) from the grand mean in the crossbed data from the Lignite Creek Formation suggests a paleoslope with a fairly high gradient (Table 7, p. 78). The streams depositing the sediments were perhaps similar to many of the braided streams of central Alaska.

Available thickness data (Wahrhaftig *et al.*, 1969, p. D21) indicate that probably the same structural controls present within the basin during deposition of the underlying coal-bearing formations were also active during the accumulation of the Lignite Creek Formation (Table 7, p. 78). Therefore, the changing character of the sandstones deposited throughout the history of the basin largely resulted from changes in source areas.

The major source of the sediments of the Lignite Creek Formation was probably the northwestern part of the rejuvenated Yukon-Tanana Upland and the adjacent region to the south which presently constitutes the floor of the Tanana Valley structural trough (Table 7, p. 78).

Sedimentary History and Brief Tectonic Synthesis

Deposition of the Tertiary coal-bearing sediments began in the middle or late Oligocene and continued through late Miocene and perhaps into early Pliocene. Downwarping (or faulting) of the Birch Creek Schist along the northern edge of the present Alaska Range in middle or late Oligocene time provided the structural setting for the deposition of the Healy Creek Formation. Sediments locally derived from the Birch Creek Schist were deposited, often rapidly, as periodic structural movements (faulting?) continued into early Miocene time. Subsidence rate approximately equalled the rate of accumulation of sediments within the basin(s) (Wahrhaftig *et al.*, 1969, p. D15). The axis of the subsiding basin during the deposition of the Healy Creek Formation apparently was along the southeastern border of the Lignite Creek coal basin. Paleodrainage patterns were diverse at that time, but general direction of streamflow was to the north (Wahrhaftig *et al.*, 1969, p. D9).

In early to middle Miocene time, an increase in the rate of downwarping (or

TABLE 7
 Resumé of Interpretations for the "Tertiary Coal-Bearing Group" Strata

Formation	Tectonics of Depositional Site	Paleoclimate	Gradient of Paleoslope	Source Area	Tectonics of Source Area	Transport Directions
Grubstake Formation	*Rapid subsidence of two small basins	**Temperate to warm-temperate climates	?	*Central Alaska Range	Moderate uplift in central Alaska Range	*to north
Lignite Creek Formation	*Continued subsidence and enlargement of the previously-defined basin		moderately steep	Northwestern Yukon-Tanana Upland	Rejuvenation of Yukon-Tanana Upland; fault block movements	to south
Suntrana Formation	*Continued subsidence of basin formed during deposition of the Sanctuary Formation		moderate to low	Yukon-Tanana Upland and what is now the Tanana Valley	Uplift of Tanana Valley area and Yukon-Tanana Upland	to south-southwest
Sanctuary Formation	*Sudden down-warping (faulting?) of large area		?	?	Mild uplift of ancestral Alaska Range?	north (?)
Healy Creek Formation	Series of structurally related basins formed by block-faulting(?)		*moderately steep?	Surrounding metamorphic terrane	Mild uplift of ancestral central Alaska Range?	*generally northward

*Wahrhaftig et al., 1969.

**Wolfe, J. A., 1966.

downfaulting) of a large area caused ponding which resulted in a freshwater lake. The lacustrine sediments representing this episode in the history of the area constitute the Sanctuary Formation. The axis of the depressed basin was apparently coincident with the structural axis present during deposition of the Healy Creek Formation. Subsidence along this axis continued throughout the depositional history of the overlying formations (Wahrhaftig *et al.*, 1969, p. D15).

Periodic movements along older established structures during middle Miocene time are recorded in the laterally persistent cyclic sequences of the Suntrana Formation. Uplift in the Tanana Valley area and in the Yukon-Tanana Upland about this same time resulted in highlands which provided sources for the sediments being supplied to the basin(s). Some of the sediments may also have been derived from local structurally and topographically high areas. The axis of the subsiding basin(s) lay along the southern edge or slightly to the south of the Nenana coal field (Wahrhaftig *et al.*, 1969, p. D17). Paleoflow during this time was to the south-southwest (Tables 6 and 7, pp. 76, 78).

Rejuvenation of the Yukon-Tanana Upland in middle Miocene time provided a renewed source of sediments. This resulted in a sudden change in character of the sediments between the Suntrana Formation and the overlying, more arkosic Lignite Creek Formation. Local tectonic activity within the depositional basins became more irregular and perhaps less intense during deposition of the Lignite Creek Formation (middle Miocene). South-flowing streams transported the sediments from the source to the depositional site (Table 7, p. 78).

As uplift of the Alaska Range was renewed in late Miocene time, two fairly small basins developed in which the lacustrine Grubstake Formation was deposited. The larger basin is now represented by exposures on Tatlanika Creek, Wood River, Healy Creek, and Lignite Creek. The other much smaller basin is represented by exposures on Buzzard Creek (Fig. 4, p. 10). The axes of the two basins generally coincide with the trend of the postulated basin axes of the underlying formations, but introduction of a north-south structural high in the area of the heatwaters of Tatlanika Creek (Fig. 4, p. 10) during deposition of the Grubstake Formation appears to have separated the two basins. Paleoflow during the late Miocene (Grubstake time) was reversed, shifting from south to north (Wahrhaftig *et al.*, 1969). Violent uplift of the Range during Pliocene time (Wahrhaftig, 1970, personal communication) is represented by the sediments of the Nenana Gravel.

Conclusions

The following conclusions are deduced from the data presented:

(1) Petrographic studies of pebbles and heavy minerals from the Healy Creek-Lignite Creek area indicate complex low- to medium-grade metamorphic and granitic igneous terranes as sources for the Tertiary coal-bearing sediments.

(2) The source area(s) for the sediments are characterized by block-faulting of older geosynclinal suites.

(3) The source area(s) of the sandstones of the Suntrana and Lignite Creek formations are north of the study area. The major contributing source areas for these formations include the Yukon-Tanana Upland and the highland just south of the Upland that is now the Tanana Valley.

(4) Possible source rock types for the heavy minerals correlate with rock types present in the pebble assemblages. These rock types, in turn, closely correlate with rock types characteristic of the Yukon-Tanana Upland.

(5) Numbers and types of heavy mineral species from the coal-bearing formations are typical of a fluvial environment according to the model compiled by Hubert (1961).

(6) Standard deviations from the grand means of the crossbed data from the Suntrana and Lignite Creek formations are typical of fluvial environments.

(7) Heavy minerals from six samples indicate that heavy mineral assemblages of the Healy Creek and Suntrana formations are similar, and these differ from the heavy mineral assemblage of the Lignite Creek Formation.

(8) Cyclicity in the Suntrana Formation may have been largely controlled by tectonic movements while sedimentary controls may have played more important roles in the development of the less regular and more discontinuous cyclic sequences in the Healy Creek and Lignite Creek formations.

(9) A decrease in the standard deviations from the grand means in the crossbed data through time is evident. The standard deviation from the grand mean in the Lignite Creek Formation is much lower than the standard deviation from the grand mean in the underlying Suntrana Formation. This fact suggests an increase in paleoslope and a related increase in stream gradients. Streams depositing the Suntrana sediments may have been meandering streams, while those depositing Lignite Creek sediments may have been braided streams.

(10) Isopach maps of factor analysis data seem to delineate north-south and

west-northwest structural components present in the depositional basin during the accumulation of the Suntrana Formation.

Suggested Areas of Future Research

(1) The areal distribution of coal fields (Fig. 22, p. 67) from east-central Alaska to the Kenai Peninsula suggests that these basins are related to a large structure trending northeast-southwest which once cut across the present arcuate axis of the Alaska Range (Fig. 25, p. 74). If these basins are indeed related in this manner, a most unusual cross-cutting feature is present in the structural fabric of central and south-central Alaska. Regional provenance, paleocurrent, paleobotanical, and palynological studies would be very interesting and, when integrated, would probably yield very exciting theories on the structural history of the Alaska Range. Also, studies to precisely determine dates of important geologic events would be extremely helpful in determining the kinematic structural history of central Alaska.

(2) Thorough studies of the primary sedimentary structures such as cross-bedding types and channel features in the Healy Creek-Lignite Creek coal basins and other coal basins in central Alaska would help to establish the sedimentary regimes of the streams that deposited the Tertiary sediments. These studies would be useful in interpreting the depositional environments in the basins. Similar studies on present streams matched with studies of the paleoflow regimes would help in a thorough interpretation of the structures and environment.

(3) Studies on secondary sedimentary features including soft-sediment deformational structures, concretions, and the like would be helpful in revealing post-depositional deformation and diagenesis.

(4) Regional grain size analyses and further heavy mineral studies would yield data that would be well suited to factor analysis work.

(5) Detailed paleotopographic maps constructed on some of the laterally persistent units, especially those in the Suntrana Formation, would greatly aid in a detailed structural analysis of the sedimentary basins.

(6) Studies on lateral changes in pebble assemblages and/or heavy mineral assemblages on a regional basis might define source area(s) more specifically. This type of study would also aid in defining the nature of the sedimentary processes that

produced the coal-bearing sediments.

(7) Trace element studies on blue tourmalines and other fairly uncommon or diagnostic minerals might help define genetic relationships among similar minerals in source area rocks and/or heavy mineral assemblages.

(8) Radiometric dates on pebbles and/or minerals compared to similar rocks or minerals from a possible source area would also help establish or repudiate postulated genetic relationships among rock types.

REFERENCES CITED

REFERENCES CITED

- Allen, J. R. L., 1963, The classification of cross-stratified units, with notes on their origin: *Sedimentology*, Vol. 2, pp. 93-114.
- Barnes, F. F., 1961, Coal fields of the United States: U. S. Geological Survey Bull. 1242-B; 2 plates.
- Black, C. A., 1965, Removal of free iron oxides in *Methods of Soil Analysis*, Part 1, No. 9; in the series AGRONOMY: American Society of Agronomy, Inc.; Madison, Wisconsin, pp. 574-577.
- Brabb, E. E., 1969, Six new Paleozoic and Mesozoic formations in east-central Alaska: U. S. Geological Survey Bull. 1274-1, pp. 11-126.
- _____, and Churkin, M., Jr., 1969, Geologic map of the Charley River quadrangle, east-central Alaska: U. S. Geological Survey Misc. Geol. Inv. Map I-573.
- Brooks, A. H., 1911, The Mount McKinley region, Alaska, with descriptions of the igneous rocks and of the Bonnifield and Kantishna districts, by L. M. Prindle: U. S. Geological Survey Prof. Paper 70, 234 p.
- Brosge', W. P., Brabb, E. E., and King, E. R., 1970, Geologic interpretation of reconnaissance aeromagnetic survey of northeastern Alaska: U. S. Geological Survey Bull. 1271-F, 14 p.
- Cameron, E. M., 1967, A computer program for factor analysis of geochemical and other data: Geological Survey of Canada, Dept. of Energy, Mines, and Resources; pp. 4-35 of paper 67-34.
- Capps, S. R., 1912, The Bonnifield region, Alaska: U. S. Geological Survey Bull. 501, 64 p.
- _____, 1919, The Kantishna region, Alaska: U. S. Geological Survey Bull. 687, 118 p.
- _____, 1940, Geology of the Alaska Railroad region: U. S. Geological Survey Bull. 907, 201 p.
- Chayes, Felix, 1952, Notes on the staining of potash feldspar with sodium cobaltinitrite in thin section: *Am. Mineralogist*, v. 37, pp. 337-340.
- Church, R. E., and Durfee, M. C., 1961, Geology of the Fossil Creek area, White Mountains, Alaska: unpub. master's thesis, Univ. of Alaska, 96 p.
- Churkin, Michael, Jr., 1970, Paleozoic and Precambrian rocks of Alaska and their role in its structural evolution: U. S. Geological Survey Open File Report 448, 156 p.

- Collier, A. J., 1903, Coal resources of the Yukon: U. S. Geological Survey Bull. 218, 71 p.
- Deer, W. A., Howie, R. A., and Zussman, Jr., 1967, An Introduction to the Rock-forming Minerals: New York, N. Y.; John Wiley & Sons; 528 p.
- Eakin, H. M., 1916, The Yukon-Koyukuk region, Alaska: U. S. Geological Survey Bull. 631, 88 p., 1 plate.
- Folk, R. L., 1968, Petrology of Sedimentary Rocks: Austin, Texas; Hemphill's, Univ. of Texas; 170 p.
- Foster, Helen L., 1970, Reconnaissance geologic map of the Tanacross quadrangle, Alaska: U. S. Geological Survey Misc. Geol. Inv. Map I-593.
- _____, and Weber, F. R., 1970, The Yukon-Tanana Upland: unpub. abstract, 6 p.
- Gates, G. O., and Gryc, George, 1963, Structure and tectonic history of Alaska in Childs, O. E., and Beebe, B. W., Backbone of the Americas: Am. Assoc. Petroleum Geologists Memoir 2; p. 264-277.
- Grantz, Arthur, 1966, Strike-slip faults in Alaska: U. S. Geological Survey Open File Report 267, 82 p.
- Hubert, John F., 1961, Heavy minerals in sandstones: unpub. chart, Univ. of Missouri, Rolla, Missouri.
- Klovan, J. E., 1968, Selection of target areas by factor analysis: "Western Miner," Feb., 1968 issue, pp. 44-54.
- _____, 1968, Q-mode factor analysis program in FORTRAN IV for small computers in Computer programs for multivariate analysis in geology: State Geological Survey, Univ. of Kansas, Lawrence, Kansas; pp. 39-51.
- Laniz, R. V., Stevens, R. E., and Norman, M. B., 1963, Staining of plagioclase feldspar and other minerals with F. D. and C. red #2: U. S. Geological Survey Prof. Paper 501 B, pp. B152-153.
- Martin, G. C., 1919, The Nenana coal field, Alaska: U. S. Geological Survey Bull. 664, 54 p.
- Mertie, J. B., 1937, The Yukon-Tanana region, Alaska: U. S. Geological Survey Bull. 872, 276 p., 1 plate.
- Milner, H. B., 1962, Sedimentary Petrography: London; George Allen and Unwin, Ltd., 4th ed., vol. 2, 715 p.
- Peterson, Donald W., 1961, American Geological Institute data sheet 23: "Geotimes," vol. V, No. 6, March 1961, pp. 30-34.
- Potter, P. E., and Pettijohn, F. J., 1963, Paleocurrents and Basin Analysis: Berlin;

Springer-Verlag, 296 p.

- Prindle, L. M., 1907, The Bonnifield and Kantishna regions in Brooks, A.H., and others, Report on progress of investigations of mineral resources of Alaska in 1906: U. S. Geological Survey Bull. 314, pp. 205-226.
- _____, 1913, Geologic reconnaissance of the Circle quadrangle, Alaska: U. S. Geological Survey Bull. 538, 82 p.
- Pryor, W. A., 1958, Dip direction indicator: Jour. Sed. Petrology, Vol. 28, p. 230.
- Royce, C. A., Jr., 1970, Heavy mineral analysis and evaluation of directional data in An Introduction to Sediment Analysis: Arizona State Univ., pp. 93-96 and pp. 137-149.
- Rummel, R. J., 1970, Applied Factor Analysis: Evanston, Illinois; Northwestern Univ. Press; 617 p.
- Tanner, W. F., 1955, Paleogeographic reconstruction from cross-bedding studies: Am. Assoc. Petroleum Geologists Bull, Vol. 39, pp. 2471-2483.
- Wahrhaftig, Clyde, 1965, Physiographic divisions of Alaska: U. S. Geological Survey Prof. Paper 482; 52 p., 6 plates.
- _____, 1968, Schists of the central Alaska Range: U. S. Geological Survey Bull. 1254-E, 22 p.
- _____, 1970, Geologic map of the Healy D-4 quadrangle, Alaska: U. S. Geological Survey Map GQ-806.
- _____, Hickcox, C. A., and Freedman, Jacob, 1951, Coal deposits on Healy and Lignite Creeks, Nenana coal field, Alaska, in Barnes, F. F. and others, Coal investigations in south-central Alaska, 1944-46: U. S. Geological Survey Bull. 963-E, pp. 141-165.
- _____, Wolfe, J. A., Leopold, E. B., and Lanphere, M. A., 1969, The coal-bearing group in the Nenana coal field, Alaska: U. S. Geological Survey Bull. 1274-D, 30 p.
- Weller, J. Marvin, 1960, Stratigraphic Principles and Practice: New York, New York; Harper & Row, Publishers, 725 p.
- Williams, J. R., 1959, Geologic reconnaissance of the Yukon Flats district, Alaska: U. S. Geological Survey Bull. 1111-H, 41 p.
- Wolfe, J. A., 1966, Tertiary plants from the Cook Inlet region, Alaska: U. S. Geological Survey Prof. Paper 398-B, p. B-32.
- _____, and Wahrhaftig, Clyde, 1968, The Cantwell Formation of the central Alaska Range in Cohee, G. V., Bates, R. G., Wright, W. B., 1970, Changes in stratigraphic nomenclature by the U. S. Geological Survey, 1968: U. S. Geological Survey Bull. 1294-A, pp. 41-46.

APPENDICES

APPENDIX I
DIRECTIONAL DATA

The procedures used to evaluate directional data (crossbed measurements) in this report are taken directly from Royse (1970, pp. 137-146); therefore general discussion of the procedures are omitted here. The frequencies of corrected crossbed measurements occurring in the various circular class intervals, however, are included for possible future use.

Table 8, p. 89 gives the number of corrected readings in each of the circular classes at the various localities for each formation. Vector means at each locality for the Suntrana and Lignite Creek formations were calculated from this data (Figs. 10 and 11, pp. 32-33). The vector mean for the Healy Creek Formation was not included in the text because of the meager number of readings. Addition of the total readings in each class for each formation from all localities formed the basis for construction of the rose diagrams and calculation of the standard deviations of the grand means. The grand mean for all readings in each formation was calculated from the tabulated vector means from all the localities (Table 9, p. 90).

TABLE 8
Frequency Distribution of Corrected Crossbed Readings

Formations	Localities	Class on Circular Diagram											
		I	II	III	IV	V	VI	VII	VIII	IX	X	XI	XII
		Mid-Point Azimuth of Each Class											
		0°	30°	60°	90°	120°	150°	180°	210°	240°	270°	300°	330°
Suntrana Formation	A	1	-	1	1	1	-	1	2	-	-	1	-
	B	2	-	1	-	-	1	3	1	-	-	1	4
	G	-	-	-	-	-	1	3	2	4	2	3	-
	J	-	-	-	-	-	2	2	1	-	-	-	-
	2	-	-	1	2	-	1	1	-	-	-	-	-
	5	1	-	-	-	-	-	2	2	3	1	-	-
11	1	-	-	-	-	3	4	3	2	-	-	-	
Lignite Creek Formation	A	-	-	1	-	1	3	2	3	3	-	1	-
	B	-	-	-	1	1	2	4	-	-	1	-	-
	J	-	-	1	-	1	3	7	2	1	-	-	1
	2	-	-	-	-	-	1	-	1	-	-	1	-
	5	-	-	1	-	1	2	4	-	-	2	-	1
11	-	2	1	-	2	1	3	-	1	-	-	1	
Healy Creek Formation	C	-	-	-	-	-	-	-	3	-	-	-	-
Suntrana Formation (all readings)		5	-	3	3	1	8	16	11	9	3	5	4
Lignite Creek Formation (all readings)		-	2	4	1	6	12	20	6	5	3	2	3

TABLE 9
 Tabulation of Vector Means for Calculation of the Grand Mean

Class on Circular Diagram	I	II	III	IV	V	VI	VII	VIII	IX	X	XI	XII
Mid-Point Azimuth of Each Class	0°	30°	60°	90°	120°	150°	180°	210°	240°	270°	300°	330°
Lignite Creek Formation	-	-	-	-	1	1	3	1	-	-	-	-
Suntrana Formation	-	-	-	-	1	1	2	-	2	-	1	-
Healy Creek Formation	-	-	-	-	-	-	-	1	-	-	-	-
All Formations	-	-	-	-	2	2	5	2	2	-	1	-

APPENDIX II
PETROGRAPHY OF PEBBLES

Rock names from petrographic analysis of 101 thin sections of pebbles are based on visual estimates of mineral percentages. Feldspar stains aided considerable in the naming process, particularly in fine-grained volcanic rocks. In the following brief descriptions, certain conventions were used. (1) A mineral name followed by the term "bearing" such as "biotite-bearing" indicates a trace (less than 1%) of that mineral in the rock. The term is only used as a qualifying adjective for the rock name. (2) In a series of qualifying minerals placed before the rock name, the minerals are ranked according to their estimated percentages. The mineral having the highest percentage is thus placed closest to the rock name. (3) "Major" constituents are those which constitute at least 10% of the rock. (4) "Minor" constituents are those which constitute at least 1% but less than 10% of the rock. Common igneous accessory minerals, iron oxides, and opaques are usually omitted from the descriptions, unless they occur in unusual quantities. Minerals essential to the rock name are often not included in the ensuing description unless they are unusual. The classification scheme used in deriving names for the igneous rocks is included in the text on page 40. The classification scheme used for sandstones is after Folk (1968).

BRIEF PETROGRAPHIC DESCRIPTIONS

Sample Numbers

1. A-D-3-1 Quartzose rock containing minor feldspar. Quartz grains contain "dirty" inclusions, show strain, and have sutured boundaries.
2. A-D-3-1 Subidioblastic low- to medium-grade chlorite, epidote, hornblende ortho-amphibolite.
3. A-D-3-3 Argillaceous chert with some secondary quartz veins.
4. A-D-3-3 Cherty argillite crosscut by secondary quartz veins.
5. A-D-3-5 Epidote-bearing, slightly chloritic impure arkose.
6. A-D-3-6 Slightly carbonaceous chert conglomerate crosscut with some secondary quartz veins.
7. A-D-3-8 Epidote-bearing quartz vein (?) rock containing albite and some apatite and K-feldspar.
8. A-D-3-14 Hypidiomorphic-seriate to granular, chlorite- and apatite-bearing muscovite, biotite quartz monzonite with some myrmekitic texture.
9. A-D-3-22 Porphyritic-aphanitic apatite and zircon-bearing blue tourmaline dacite contains euhedral to subhedral quartz and plagioclase phenocrysts in a fine-grained, equigranular groundmass. Plagioclase phenocrysts tend to occur in clusters.
10. A-D-3-22 Apatite, epidote, actinolitic ortho-amphibolite (metamorphosed dacite?) with relict microporphyritic texture.
11. SR-A-1-1 Chlorite-bearing, slightly micaceous quartz rock. Quartz grains show undulatory (strain) extinction and muscovite flakes have parallel orientation.
12. SR-A-1-1 Chlorite-bearing quartz rock. Quartz grains show undulatory extinction and sutured or granulated boundaries.
13. SR-A-1-1 Optically continuous composite quartz rock. Smaller quartz grains constituting the rock have been annealed together.
14. SR-A-1-1 Quartz rock containing large composite quartz grains as well as smaller single grains. Most show undulatory extinction and have sutured grain boundaries.
15. SR-A-1-1 Chlorite- and biotite-bearing quartz rock. This rock has been

- strongly sheared by synkinematic metamorphic deformation. Strained composite grains and s-planes are characteristic.
16. Sc-D-2-9 Sheared altered rock containing much secondary clay, and some biotite, chlorite, and quartz.
 17. Sc-D-2-11 Porphyritic rhyolite with phenocrysts displaying micrographic texture. Quartz and K-feldspar constitute the mesostasis and vesicles are filled with zeolites (?).
 18. Sc-D-2-11 Epidote- and biotite-bearing meta-rhyolite with filled vesicles (quartz) and quartz "lenses" which probably result from mobilization of quartz during metamorphism.
 19. Sc-D-2-11 Chlorite-bearing syenite (?) with minor biotite. Subhedral plagioclase and biotite crystals occur poikilitically within one large, twinned K-feldspar crystal. Plagioclase crystals have reverse zoning and characteristically have micrographic texture. Quartz is minor.
 20. Sc-D-2-11 Porphyritic trachyte with euhedral to subhedral phenocrysts of quartz and feldspar; the latter tend to occur in clusters. The mesostasis is fine-grained and shows some devitrification.
 21. Sc-D-2-17 Chlorite-bearing, feldspar, quartz, leucoxene arenite with a chert matrix. Fine-grained rock with angular, poorly-sorted grains.
 22. Sc-D-4-13 Porphyritic epidote, garnet-bearing andesite with some quartz and chlorite. Plagioclase phenocrysts are euhedral to anhedral and the plagioclase microlites in the groundmass suggest flow structure.
 23. Sc-D-4-15 A porphyritic chlorite-bearing quartz latite with euhedral quartz phenocrysts up to 7 mm. in diameter and a few plagioclase phenocrysts. Graphic intergrowth of plagioclase and K-feldspar is common in the groundmass, especially bordering quartz phenocrysts.
 24. Sc-D-4-15 Allotriomorphic- to hypidiomorphic-granular fine-grained quartz monzonite. Antiperthite (albite host) constitutes about 35% of the rock.
 25. Sc-D-4-18 Porphyritic rhyodacite (?) crystal tuff with angular fragments of quartz and feldspar in a very fine-grained matrix of feldspar and quartz.
 26. Sc-D-4-18 Hornfelsed plagioclase arkose of the pyroxene hornfels facies. Contains some chert, quartz, chlorite, apatite, and quite a bit of plagioclase and incipient pyroxene.
 27. Sc-D-4-18 Porphyritic rhyodacite with euhedral to subhedral plagioclase

- phenocrysts and subhedral to anhedral quartz phenocrysts. Groundmass is mostly quartz and glass.
28. Sc-D-5-6 Chert conglomerate containing minor chlorite and sericite of which the latter is aligned along a vague s-plane. Secondary quartz veins in the chert pebbles are parallel to, and therefore related to the s-plane.
 29. Sc-D-5-6 Chert pebble conglomerate contains anhedral recrystallized and detrital quartz, with some chlorite and sericite. Pebbles are subround to somewhat angular and several different kinds of chert are present. Secondary quartz veins appeared in the pebbles before they were incorporated into the conglomerate.
 30. Sc-D-5-6 Slightly metamorphosed orthoquartzite conglomerate contains minor chlorite and sericite. Quartz is recrystallized. The conglomerate texture is more easily discernible with the naked eye.
 31. Sc-D-5-25 Microporphyritic altered pyroxene-bearing volcanic with micropenocrysts of pigeonite and plagioclase in a matrix of highly altered plagioclase laths plus pyroxene in intergranular texture.
 32. Sc-D-5-25 Non-schistose lower medium-grade sphene, epidote ortho-amphibolite. Grains of amphibole and epidote are subhedral to euhedral, while plagioclase is subhedral to anhedral. Sphene is abundant.
 33. Sc-D-11-25 Non-schistose ortho-amphibolite contains mainly chlorite, andalusite (?) (or mullite), sphene plus ilmenite and highly altered feldspar. Biotite, quartz, and amphibole are present in minor amounts.
 34. Sc-D-11-25 Low- to medium-grade non-schistose ortho-amphibolite contains actinolite, K-feldspar, plagioclase, and sphene (plus ilmenite and leucoxene) as major constituents.
 35. Sc-D-11-25 Greenschist facies (low-grade) sphene-bearing chlorite, quartz, actinolite, sericite, ortho-amphibolite (?) or metamorphosed graywacke. Strongly schistose, nematoblastic texture, with two obvious s-planes.
 36. Sc-D-11-25 Greenschist facies (low-grade) ortho-amphibolite contains mostly plagioclase and actinolite with minor epidote. Non-schistose; subhedral plagioclase grains are larger than subhedral actinolite grains. Quartz occurs as porphyroblasts.
 37. Sc-D-11-25 Subophitic sericitized diabase contains mainly subhedral crystals of plagioclase (labradorite), augite rimmed with hornblende, some biotite, and minor chlorite.

38. Sc-D-14-14 Allotriomorphic-granular quartz monzonite with minor garnet, hornblende, muscovite, and chlorite.
39. Sc-D-14-20 Non-schistose, greenschist facies actinolite ortho-amphibolite. Actinolite constitutes 85-90% of the rock while plagioclase and biotite are minor constituents.
40. Sc-D-14-22 Porphyritic altered andesite with subhedral pyroxene (augite?) phenocrysts in a mesostasis of altered plagioclase microlites. Chlorite is present, as is minor hornblende and traces of epidote. Opaques are a prominent constituent.
41. Sc-D-14-22 Very low-grade meta-argillite, mostly consisting of non-schistose sericite, other clay minerals, quartz, and chert fragments.
42. Sc-D-14-24 Non-schistose greenschist facies meta-volcanic (andesite or dacite?) characterized by relict porphyritic texture; relict plagioclase phenocrysts and microlites highly altered to clay minerals and sericite. Actinolite (50%) and chlorite (10%) are largely restricted to the groundmass.
43. Sc-D-19-2 Chert crosscut by many secondary quartz veins, some of these containing altered plagioclase and argillaceous material. Chlorite is a minor constituent.
44. Sc-D-19-2 Slightly argillaceous chert occasionally crosscut by secondary quartz veins. Traces of biotite and chlorite are present.
45. Sc-D-19-3 Meta-argillite contains detrital quartz grains of uniform size and evenly-distributed argillaceous (or carbonaceous?) material. Aligned muscovite delineates an s-plane.
46. Sc-D-19-4 Slightly metamorphosed orthoquartzite contains minor amounts of accessory minerals, sericite, and feldspar. Quartz and feldspar grains are equigranular and idioblastic.
47. Sc-D-19-3 Meta-argillite contains segregation banding of equigranular, recrystallized quartz versus carbonaceous (?) material and opaques. Minor chlorite and amphibole generally occur with quartz and are not concentrated locally.
48. Sc-D-19-3 Meta-argillite contains very fine-grained quartz with bands of carbonaceous (?) material. Minor chlorite generally occurs within the secondary quartz veins.
49. Sc-D-19-4 Chert contains localized patches of opaques (carbonaceous material?) which also occur as fracture fillings. Clay minerals and sericite are distributed throughout the rock.
50. Sc-D-19-4 Meta-volcanic with relict porphyritic-aphanitic texture. Relict phenocrysts of plagioclase and quartz occur in a devitrified groundmass. One well-defined s-plane is present.

51. Sc-D-19-6 Volcanic breccia consists mostly of very fine-grained altered material (glass, feldspar, etc.), minor plagioclase microphenocrysts, minor chlorite in radiating aggregates, and minor quartz.
52. Sc-D-19-12 Porphyritic rhyolite with euhedral to subhedral phenocrysts of quartz, albite, and altered K-feldspar in a groundmass of similar composition. Muscovite-sericite and trace amounts of epidote are also present.
53. UV-C-2-15 Porphyritic quartz latite with phenocrysts of mostly K-feldspar with some plagioclase. K-feldspar phenocrysts are generally euhedral to subhedral and often occur in clusters. Minor chlorite is present and secondary quartz veins crosscut the rock.
54. UV-C-2-15 Porphyritic quartz latite with phenocrysts of altered plagioclase and highly altered biotite (?). Chlorite, K-feldspar, clinzoisite, and apatite occur in minor amounts.
55. UV-C-2-15 Porphyritic quartz latite with euhedral to subhedral phenocrysts of quartz, altered plagioclase and K-feldspar in a groundmass of devitrified feldspar and quartz. Some micrographic intergrowths occur in the phenocrysts. Sericite-muscovite and traces of clinzoisite are also present.
56. UV-C-2-19 Hypidiomorphic-granular, slightly metamorphosed granodiorite contains much biotite altering to chlorite and highly sericitized and otherwise altered feldspars. Clinzoisite and epidote occur in minor amounts.
57. UV-C-13-2 Chert contains a few crosscutting secondary quartz veins with minor opaques in these veins.
58. UV-C-13-3 Argillite is fine-grained, essentially equigranular and contains some carbonaceous (?) material. Many crosscutting quartz veins are present.
59. UV-C-13-4 Slightly metamorphosed orthoquartzite contains minor amounts of feldspar, muscovite-sericite, clinzoisite, and chlorite. Most quartz grains show strain and have granulated boundaries. Some recrystallization has occurred.
60. UV-C-13-4 Metamorphosed sheared chert contains carbonaceous (?) material, some chlorite, and some apatite. Quartz is recrystallized parallel to the s-plane; crosscutting quartz veins cut the s-plane.
61. UV-C-13-4 Contact metamorphosed orthoquartzite of the pyroxene-hornfels facies contains a single euhedral skeletal pyroxene (hypersthene ?) grain. Minor sericite is also present.
62. G-2-11 Porphyritic rhyodacite contains clustered euhedral to subhedral plagioclase phenocrysts in a groundmass of plagioclase micro-

- lites, perhaps some K-feldspar, and minor quartz. Some flow structure is noted. Chlorite and muscovite-sericite are present in minor amounts.
63. G-2-11 Porphyritic trachyte with subhedral phenocrysts of feldspar in a fine-grained mesostasis containing some microlites. Quartz, chlorite, epidote, and sericite occur in minor amounts.
 64. G-2-11 Porphyritic trachyte with phenocrysts of subhedral K-feldspar and altered mafics in a mesostasis of K-feldspar, alteration minerals, and minor quartz.
 65. G-2-11 Altered porphyritic rhyodacite (?) has euhedral to subhedral highly epidotized plagioclase phenocrysts in a mesostasis containing plagioclase laths, quartz, and minor sericite-muscovite, and chlorite.
 66. G-2-14 Hypidiomorphic monzonite contains subhedral crystals of altered mafics and plagioclase while K-feldspar and minor quartz are anhedral. Minor amounts of chlorite, biotite, apatite, sodic (?) hornblende, and pyroxene (?) are present.
 67. 2-5-6 Chert conglomerate consists of angular quartz and chert pebbles in a chert matrix. Muscovite-sericite occurs in minor amounts.
 68. 2-5-6 Chert graywacke conglomerate contains a volcanic pebble and chert pebbles in a matrix of feldspathic graywacke composition. The rock is "stretched" due to metamorphism.
 69. 2-5-6 Chert pebble conglomerate contains different types of pebbles in a matrix of chert, opaques, and quartz grains. Two pebbles have "silicified oolitic" textures.
 70. 5-6-11 Optically continuous composite quartz pebble with undulatory extinction.
 71. 5-14-13 Porphyritic andesite with epidotized andesine phenocrysts and highly altered mafics in a mesostasis of plagioclase microlites, possibly K-feldspar, and some quartz.
 72. 5-14-13 Porphyritic latite with highly sericitized plagioclase phenocrysts in a fine-grained felted mesostasis of feldspar microlites, quartz, and alteration minerals with some vague flow structure. Highly altered xenoliths are also present.
 73. 5-14-13 Porphyritic andesite with epidotized feldspar phenocrysts (?) in a matrix of minor quartz, K-feldspar, plagioclase, and alteration minerals plus some actinolite.
 74. 5-14-18 Hornfelsed plagioclase arkose of the contact metamorphic pyroxene-hornfels facies. Abundant pyroxene is incipient and actinolite is also present.

75. 5-17-6 Chert pebble conglomerate is composed almost entirely of chert but contains minor opaques and quartz and traces of epidote, chlorite, and sericite.
76. 5-17-6 Chert pebble conglomerate with a matrix of smaller angular to subround chert and quartz grains. Secondary quartz veins cross-cut the rock.
77. 5-17-7 Volcanic breccia is very rich in iron and highly altered to clay. Phenocrysts and rock fragments sometimes surrounded by flow texture. Only identified minerals are apatite, albite, green biotite, and chlorite.
78. 5-17-7 Chert and quartz breccia contains grains of many sizes, many quartz grains show strain, some have granulated boundaries, and some are composite. Minor sericite and traces of plagioclase are present.
79. 5-17-7 Epidote-mica schist has a "crushed" texture due to cataclasis. Two or three s-planes are present which are emphasized by the subparallel alignment of epidote-clinozoisite, and the micas. Quartz, epidote-clinozoisite, and feldspar are the major constituents.
80. 5-17-8 Quartz-mica schist has a granoblastic-lepidoblastic texture with one or two s-planes and a couple of quartz veins cutting the s-planes. Quartz is the only major constituent; muscovite-sericite, chlorite, and opaques occur in minor amounts.
81. 5-17-11 Porphyritic rhyolite has euhedral to subhedral phenocrysts of plagioclase, orthoclase, and quartz in a mesostasis of alkalic feldspar and quartz. Micrographic texture is very common. Biotite, epidote, chlorite, and sericite are minor constituents.
82. 5-17-11 Porphyritic trachyte contains very few euhedral to subhedral quartz phenocrysts and many devitrified spherulites. The fine-grained groundmass is mostly K-feldspar with some plagioclase and minor quartz.
83. 5-17-1 Allotriomorphic-seriate granite has been deformed and leucocratic constituents have recrystallized. Plagioclase, biotite, and chlorite are minor constituents. Sodic (?) orthoclase is present.
84. 5-17-10 Granite with cataclastic texture contains xenoblastic porphyroblasts of sodic (?) orthoclase and plagioclase. Muscovite, chlorite, and epidote are minor constituents.
85. 5-17-14 Metamorphosed quartz monzonite has cataclastic, xenoblastic texture. Micrographic texture and some glass (?) appear in the plagioclase. Sodic (?) orthoclase is present and micas are a minor constituent.
86. 5-20-16 Porphyritic latite with euhedral to subhedral biotite and feldspar

- phenocrysts. The equigranular groundmass is fine-grained. Sericite, clinozoisite, and sphene are minor constituents.
87. 5-31-15 Porphyritic rhyodacite contains altered phenocrysts of plagioclase, amphibole and biotite (?) in a fine-grained mesostasis of quartz, feldspar, chlorite, sericite, and other alteration minerals.
 88. 5-31-19 Deformed granodiorite is characterized by a cataclastic texture. K-feldspar, opaques, chlorite, and apatite are minor constituents.
 89. 11-10a-7 Chert-quartz breccia has mostly angular to subround chert with quartz pebbles and fragments and minor amounts of plagioclase, chalcedony, microcline, sericite, and chlorite.
 90. 11-10a-7 Chert breccia contains abundant recrystallized quartz and minor muscovite. "Brecciation" is due to metamorphic processes.
 91. 11-10a-21 Highly altered diorite (?) contains altered feldspar, biotite, chlorite, sericite, and ilmenite in a subophitic texture.
 92. 11-16a-13 Trachyte contains mostly K-feldspar laths which exhibit flow texture. About 10% of chlorite is present.
 93. 11-16a-13 Porphyritic trachyte contains a few euhedral plagioclase and K-feldspar (?) phenocrysts in a medium-grained matrix of opaques, quartz, K-feldspar, plagioclase, and chlorite.
 94. 11-16a-23 Allotriomorphic- to hypidiomorphic-granular hornblende-pyroxene gabbro. Labradorite, chlorite, pyroxene, and opaques are major constituents while epidote, amphibole, and K-feldspar are minor.
 95. 11-16a-25 Greenschist facies ortho-amphibolite is non-schistose and contains major percentages of ilmenite and leucoxene, incipient epidote, and actinolite. Clinozoisite, chlorite, plagioclase, quartz, and apatite occur in minor amounts.
 96. A-D-3-10 Quartz monzonite has a cataclastic texture and few mafics, which are altered. Pennine chlorite and muscovite occur in minor amounts.
 97. A-D-3-14 Hypidiomorphic-granular quartz monzonite contains minor amounts of chlorite, epidote, and muscovite-sericite.
 98. A-D-3-3 Metamorphosed chert or siltstone has quartz segregation bands parallel to s-planes. Carbonaceous (?) material occurs in major amounts and muscovite-sericite and biotite are minor.
 99. A-D-3-20 Altered porphyritic andesite contains feldspar and epidotized phenocrysts in a mesostasis characterized by feldspar

microlites. Quartz, chlorite, and allanite occur in minor amounts.

100. A-D-3-21 Low- to medium-grade ortho-amphibolite with non-schistose (hornfelsic) texture. Minor amounts of chlorite, quartz, leucoxene, and plagioclase are present.
101. 5-20-16 Altered porphyritic latite contains euhedral to subhedral plagioclase phenocrysts in a mesostasis of mostly K-feldspar, epidote, chlorite, and other alteration products plus minor quartz.

APPENDIX III FACTOR ANALYSIS

Factor analysis is a tool used to simplify complex matrices of data by attempting to extract a minimum number of new variables which yield a known fraction of the information content of the original variables. These new variables are linear combinations of the original ones (Klovan, 1968). Two related factor analysis procedures, R-mode and Q-mode, were utilized in this study.

R-Mode Factor Analysis

The R-mode correlation matrix of the 49 pebble samples (table 10, pp. 104-108) consists of variables (columns) which refer to rock types, and cases (rows) which, in this case, also refer to rock types. In such a matrix all pairs of variables are inspected for their relationships between all the pairs of variables. These relationships are expressed in coefficients of correlation which express the degree of relationship between the row and column variables of the correlation matrix. Coefficient values approaching zero indicate increasingly tenuous relationships. Negative values indicate inverse relationships (Rummel, 1970). The eigenvalues of the unrotated factor matrix express the importance of each of the factors. These eigenvalues are proportional to the amount of variance accounted for by the factors they represent and they equal the sum of the column of squared loadings for each factor.

The first ten factors of the unrotated factor matrix were rotated mathematically in order to maximize variance of the squared factor loadings (table 11, p. 109). (For details on the theory of n-dimensional space and ramifications of why rotation is desirable, the reader is invited to study the article by Klovan, 1968, and pertinent sections in the book by Rummel, 1970.) These factors were chosen for rotation on the basis of the eigenvalues listed above the columns in the unrotated factor matrix. Eigenvalues greater than 1 formed the basis for selection of factors to be rotated

(table 12 , p. 113). The total number of factors chosen for rotation account for 75.5% of the total variance among all the variables.

The print-out of R-mode factor scores (table 13, p. 115) shows the degree of involvement of each pebble sample in each of the ten rotated factors. A high positive value of , say, factor 6 in a certain sample indicates that much of the variance within that sample is accounted for by that particular factor.

Q-Mode Factor Analysis

The data manipulations in Q-mode factor analysis are essentially the same as those used in R-mode factor analysis, but the data involved are different. Whereas R-mode analysis involves relationships of variables within samples, Q-mode analysis involves comparative relationships among entire samples. Thus the resulting clusters of like samples can be mapped areally.

The Q-mode factor analysis correlation matrix inspects relationships between all possible pairs of pebble samples. These comparisons are based on the relationship of each pebble sample to the ten variables or factors derived during R-mode factor analysis. Rotation of the resulting matrix yields the Q-mode varimax factor matrix (table 14 p. 117). This matrix is a set of ten completely new factors consisting of particular sample associations which are derived from interaction of the ten previous R-mode factors among all the pebble samples.

Table 15, page 119 is a list of groups of samples having greater than or equal to 75% total variance accounted for by each factor. These "end member" samples illustrate the make-up of the particular factors they represent. Table 16 on page 120 is a list of the single samples which are most representative of each Q-mode factor.

In the following tables, these abbreviations are used for the rock names: QUAR = quartz; CHER = chert; ARG = argillite; QZT = quartzite; SAND = sandstone; CONG = conglomerate; BREC = breccia; SC-1 = quartz-mica schist; OTHR = other; GRAN = granite; RHYL = rhyolite; SYEN = syenite; TRAC = trachyte; QM = quartz monzonite; QL = quartz latite; LAT = latite; MONZ = monzonite; RHYD = rhyodacite; GROD = granodiorite; AND = andesite; DIOR = diorite; DACT = dacite; QD = quartz diorite; DIAB = diabase; SC-2 = para- and ortho-amphibolites; and UNKN = unknown.

The isopach map of Q-mode factor 2 was not included in the thesis text because lack of lateral sample control made interpretation impossible. The available contoured data are therefore included here (figure 26, page 121).

TABLE 10
R-Mode Correlation Matrix of 49 Samples

	Quar	Cher	Arg	Qzt	Sand	Cong
Quar	1.000	-0.232	-0.220	-0.321	-0.359	-0.197
Cher	-0.232	1.000	0.181	-0.653	-0.092	-0.021
Arg	-0.220	0.181	1.000	-0.160	-0.271	-0.216
Qzt	-0.321	-0.653	-0.160	1.000	0.177	0.175
Sand	-0.359	-0.092	-0.271	0.177	1.000	0.156
Cong	-0.197	-0.021	-0.216	0.175	0.156	1.000
Brec	-0.099	-0.069	-0.143	0.012	-0.135	-0.115
Sc-1	-0.300	-0.094	-0.198	0.155	0.134	0.201
Othr	-0.196	-0.130	0.212	-0.040	-0.175	-0.154
Gran	-0.717	0.148	-0.004	0.073	0.345	0.017
Rhyl	-0.485	0.073	0.100	-0.003	0.072	0.106
Syen	-0.124	0.242	0.246	-0.085	-0.138	-0.007
Trac	-0.195	-0.051	0.250	-0.139	0.003	0.025
QM	-0.484	0.188	-0.036	0.021	0.274	-0.020
QL	-0.170	0.113	-0.136	-0.105	0.264	0.014
Lat	0.134	-0.270	-0.122	0.085	0.033	-0.179
Monz	-0.091	0.071	0.151	-0.221	-0.077	0.110
Rhyd	-0.194	0.092	0.045	-0.139	0.061	0.031
Grod	-0.062	-0.170	-0.005	0.180	-0.166	-0.025
And	-0.236	0.232	0.015	-0.249	0.033	-0.192
Dior	-0.352	0.002	-0.053	0.199	0.091	-0.152
Dact	-0.262	0.267	0.020	-0.125	0.053	-0.074
QD	-0.240	-0.037	0.098	-0.033	0.231	-0.154
Diab	-0.077	0.118	0.103	-0.168	-0.138	-0.116
Sc-2	-0.360	0.009	-0.150	0.140	-0.045	0.127
Unkn	-0.504	0.114	-0.123	0.025	0.329	0.198

TABLE 10, Cont.
R-Mode Correlation Matrix of 49 Samples

	Brec	SC-1	Othr	Gran	Rhyl	Syen
Quar	-0.099	-0.300	-0.196	-0.717	-0.485	-0.124
Cher	-0.069	-0.094	-0.130	0.148	0.073	0.242
Arg	-0.143	-0.198	0.212	-0.004	0.100	0.246
Qzt	0.012	0.155	-0.040	0.073	-0.003	-0.085
Sand	-0.135	0.134	-0.175	0.345	0.072	-0.138
Cong	-0.115	0.201	-0.154	0.017	0.106	-0.007
Brec	1.000	0.270	0.209	0.105	0.167	-0.074
SC-1	0.270	1.000	-0.021	0.273	0.326	-0.105
Othr	0.209	-0.021	1.000	0.359	0.371	-0.056
Gran	0.105	0.273	0.359	1.000	0.401	0.055
Rhyl	0.167	0.326	0.371	0.401	1.000	0.016
Syen	-0.074	-0.105	-0.056	0.055	0.016	1.000
Trac	0.079	0.141	0.188	0.127	0.230	-0.083
QM	0.088	0.167	0.030	0.462	0.298	0.150
QL	-0.116	0.025	-0.114	0.111	0.017	-0.077
Lat	0.053	-0.062	-0.042	-0.041	-0.079	-0.044
Monz	-0.006	0.099	0.358	-0.007	0.570	-0.035
Rhyd	-0.098	-0.021	-0.029	0.273	-0.025	-0.041
Grod	-0.069	-0.052	-0.016	0.014	-0.042	-0.048
And	0.187	-0.132	0.252	0.317	-0.005	-0.045
Dior	0.359	0.242	0.066	0.278	0.089	-0.059
Dact	-0.000	-0.018	0.007	0.209	-0.037	-0.041
QD	0.033	0.216	0.055	0.363	0.284	-0.027
Diab	-0.074	-0.105	0.194	0.273	-0.060	-0.021
SC-2	0.099	0.069	0.344	0.299	0.188	-0.015
Unkn	0.080	0.153	0.010	0.508	0.139	0.022

TABLE 10, Cont.
R-Mode Correlation Matrix of 49 Samples

	Trac	QM	QL	Lat	Monz	Rhyd
Quar	-0.195	-0.484	-0.170	0.134	-0.091	-0.194
Cher	-0.051	0.188	0.113	-0.270	0.071	0.092
Arg	0.250	-0.036	-0.136	-0.122	0.151	0.045
Qzt	-0.139	0.021	-0.105	0.085	-0.221	-0.139
Sand	0.003	0.274	0.264	0.033	-0.077	0.061
Cong	0.025	-0.020	0.014	-0.179	0.110	0.031
Brec	0.079	0.088	-0.116	0.053	-0.006	-0.098
SC-1	0.141	0.167	0.025	-0.062	0.099	-0.021
Othr	0.188	0.030	-0.114	-0.042	0.358	-0.029
Gran	0.127	0.462	0.111	-0.041	-0.007	0.273
Rhyl	0.230	0.298	0.017	-0.079	0.570	-0.025
Syen	-0.083	0.150	-0.077	-0.044	-0.035	-0.041
Trac	1.000	0.092	-0.044	-0.097	0.098	0.446
QM	0.092	1.000	0.129	-0.104	-0.044	0.042
QL	-0.044	0.129	1.000	0.258	0.047	0.275
Lat	-0.097	-0.104	0.258	1.000	-0.073	-0.087
Monz	0.098	-0.044	0.047	-0.073	1.000	-0.069
Rhyd	0.446	0.042	0.275	-0.087	-0.069	1.000
Grod	-0.075	0.262	0.359	0.241	-0.081	0.085
And	-0.054	0.252	0.502	-0.094	0.126	0.442
Dior	-0.127	-0.044	-0.092	0.042	0.028	-0.070
Dact	-0.070	0.410	0.133	-0.086	0.150	0.022
QD	0.186	0.044	0.113	-0.058	-0.046	0.197
Diab	-0.083	0.421	0.302	-0.044	-0.035	0.181
SC-2	0.218	0.033	0.023	0.020	-0.092	0.205
Unkn	0.161	0.045	0.157	0.017	0.118	0.171

TABLE 10, Cont.
R-Mode Correlation Matrix of 49 Samples

	Grod	And	Dior	Dact	QD	Diab
Quar	-0.062	-0.236	-0.352	-0.262	-0.240	-0.077
Cher	-0.170	0.232	0.002	0.267	-0.037	0.118
Arg	-0.005	0.015	-0.053	0.020	0.098	0.103
Qzt	0.180	-0.249	0.199	-0.125	-0.033	-0.168
Sand	-0.166	0.033	0.091	0.053	0.231	-0.138
Cong	-0.025	-0.192	-0.152	-0.074	-0.154	-0.116
Brec	-0.069	0.187	0.359	-0.000	0.033	-0.074
SC-1	-0.052	-0.132	0.242	-0.018	0.216	-0.105
Othr	-0.016	0.252	0.066	0.007	0.055	0.194
Gran	0.014	0.317	0.278	0.209	0.363	0.273
Rhyl	-0.042	-0.005	0.089	-0.037	0.284	-0.060
Syen	-0.048	-0.045	-0.059	-0.041	-0.027	-0.021
Trac	-0.075	-0.054	-0.127	-0.070	0.186	-0.083
QM	0.262	0.252	-0.044	0.410	0.044	0.421
QL	0.359	0.502	-0.092	0.133	0.113	0.302
Lat	0.241	-0.094	0.042	-0.086	-0.058	-0.044
Monz	-0.081	0.126	0.028	0.150	-0.046	-0.035
Rhyd	0.085	0.442	-0.070	0.022	0.197	0.181
Grod	1.000	0.181	-0.039	0.120	-0.064	0.416
And	0.181	1.000	0.153	0.448	0.186	0.581
Dior	-0.039	0.153	1.000	0.041	0.205	-0.059
Dact	0.120	0.448	0.041	1.000	-0.054	0.431
QD	-0.064	0.186	0.205	-0.054	1.000	-0.027
Diab	0.416	0.581	-0.059	0.431	-0.027	1.000
SC-2	0.175	0.029	0.136	-0.038	-0.015	-0.105
Unkn	-0.159	0.250	0.459	0.223	0.192	-0.113

TABLE 10, Cont.
R-Mode Correlation Matrix of 49 Samples

	SC-2	Unkn
Quar	-0.360	-0.504
Cher	0.009	0.114
Arg	-0.150	-0.123
Qzt	0.140	0.025
Sand	-0.045	0.329
Cong	0.127	0.198
Brec	0.099	0.080
SC-1	0.069	0.153
Othr	0.344	0.010
Gran	0.299	0.508
Rhyl	0.188	0.139
Syen	-0.015	0.022
Trac	0.218	0.161
QM	0.033	0.045
QL	0.023	0.157
Lat	0.020	0.017
Monz	-0.092	0.118
Rhyd	0.205	0.171
Grod	0.175	-0.159
And	0.029	0.250
Dior	0.136	0.459
Dact	-0.038	0.223
QD	-0.015	0.192
Diab	-0.105	-0.113
SC-2	1.000	0.222
Unkn	0.222	1.000

TABLE 11
Unrotated Factor Matrix (R-Mode)

Factor	1	2	3	4	5	6	7
Eigenvalue	4.15	2.85	2.32	1.89	1.69	1.63	1.47
Percent	16.0	10.9	8.9	7.3	6.5	6.3	5.6
Cumulative Percent	16.0	26.9	35.9	43.2	49.6	55.9	61.6
Quar	0.837	0.230	0.000	- 0.098	0.036	0.240	- 0.231
Cher	- 0.246	0.445	0.364	0.510	- 0.219	0.044	0.050
Arg	- 0.055	0.261	0.553	- 0.092	0.122	- 0.110	0.376
Qtz	0.002	- 0.554	- 0.469	- 0.267	- 0.011	- 0.308	0.252
Sand	- 0.339	- 0.289	- 0.407	0.446	0.038	0.010	- 0.132
Cong	- 0.058	- 0.317	- 0.098	0.354	0.172	- 0.439	- 0.289
Brec	- 0.198	- 0.228	0.090	- 0.382	- 0.352	0.329	- 0.026
Sc-1	- 0.331	- 0.475	- 0.034	0.005	- 0.105	- 0.075	- 0.226
Othr	- 0.344	- 0.015	0.419	- 0.615	0.047	- 0.006	- 0.052
Gran	- 0.834	- 0.117	- 0.044	0.008	- 0.021	- 0.018	0.193
Rhyl	- 0.529	- 0.294	0.423	- 0.171	0.006	- 0.274	- 0.319
Syen	- 0.018	0.133	0.243	0.216	- 0.145	- 0.252	0.468
Trac	- 0.272	- 0.124	0.355	- 0.028	0.633	0.063	0.041
Qm	- 0.561	0.216	- 0.162	0.033	- 0.190	- 0.473	0.108
Ql	- 0.325	0.362	- 0.461	0.063	0.245	0.102	- 0.349
Lat	0.127	- 0.043	- 0.384	- 0.327	0.050	0.175	- 0.085
Monz	- 0.213	- 0.000	0.498	- 0.132	- 0.085	- 0.129	- 0.656
Rhyd	- 0.370	0.234	- 0.057	0.135	0.660	0.261	0.089
Grod	- 0.110	0.317	- 0.458	- 0.459	0.161	- 0.315	0.042
And	- 0.560	0.581	- 0.138	- 0.116	- 0.043	0.333	- 0.117
Dior	- 0.357	- 0.340	- 0.078	- 0.137	- 0.450	0.442	0.186
Dact	- 0.403	0.447	- 0.118	0.079	- 0.363	- 0.107	- 0.100
Qd	- 0.394	- 0.153	0.054	0.062	0.176	0.348	0.104
Diab	- 0.332	0.692	- 0.206	- 0.258	- 0.073	- 0.165	0.005
Sc-2	- 0.346	- 0.250	- 0.014	- 0.250	0.300	- 0.045	0.205
Unkn	- 0.581	- 0.269	- 0.089	0.302	- 0.071	0.309	- 0.014

TABLE II, Cont.
Unrotated Factor Matrix (R-Mode)

Factor	8	9	10	11	12	13	14
Eigenvalue	1.32	1.22	1.10	0.94	0.87	0.74	0.63
Percent	5.1	4.7	4.2	3.6	3.3	2.9	2.4
Cumulative Percent	66.6	71.3	75.5	79.2	82.5	85.4	87.8
Quar	- 0.012	- 0.147	- 0.044	- 0.104	0.066	- 0.062	0.195
Cher	0.219	0.058	0.299	0.049	0.061	0.286	- 0.112
Arg	- 0.300	0.229	0.157	0.302	- 0.191	0.070	- 0.122
Qtz	- 0.057	0.041	0.305	0.188	0.011	- 0.110	- 0.150
Sand	- 0.310	0.048	0.184	- 0.342	- 0.059	- 0.062	- 0.200
Cong	0.389	- 0.004	0.057	0.238	0.142	- 0.161	0.122
Brec	0.166	- 0.350	- 0.331	0.032	- 0.108	- 0.312	- 0.257
Sc-1	- 0.120	- 0.355	- 0.340	0.288	0.020	0.077	0.256
Othr	0.101	0.077	0.252	- 0.318	0.165	- 0.095	0.084
Gran	- 0.055	0.007	0.044	- 0.231	0.117	- 0.001	0.238
Rhyl	- 0.212	0.102	- 0.181	- 0.054	0.109	0.058	- 0.104
Syen	- 0.011	0.337	- 0.335	0.049	0.129	- 0.475	0.132
Trac	- 0.020	- 0.258	- 0.069	0.027	- 0.459	- 0.055	0.013
Qm	- 0.177	- 0.286	- 0.182	- 0.221	- 0.170	- 0.059	- 0.088
Ql	- 0.095	0.292	- 0.233	0.090	0.107	- 0.037	- 0.219
Lat	- 0.151	0.483	- 0.350	- 0.188	- 0.351	- 0.044	0.217
Monz	- 0.039	0.297	0.134	0.147	- 0.065	- 0.073	- 0.017
Rhyd	0.133	- 0.151	0.011	0.156	0.008	- 0.161	- 0.008
Gron	0.027	0.112	- 0.210	0.273	0.008	0.215	- 0.028
And	0.094	- 0.030	0.146	0.078	0.166	- 0.225	- 0.133
Dior	0.079	0.130	0.051	0.304	0.002	0.146	- 0.034
Dact	0.114	- 0.105	0.248	0.028	- 0.391	0.106	0.134
Qd	- 0.560	- 0.072	- 0.036	0.080	0.311	0.140	0.146
Diab	- 0.039	- 0.186	0.127	0.066	0.111	- 0.043	0.242
Sc-2	0.589	0.112	- 0.138	0.066	0.104	0.267	- 0.049
Unkn	0.242	0.293	0.141	0.083	- 0.203	- 0.078	0.197

TABLE II, Cont.
Unrotated Factor Matrix (R-Mode)

Factor	15	16	17	18	19	20	21
Eigenvalue	0.57	0.50	0.49	0.43	0.31	0.27	0.17
Percent	2.2	1.9	1.9	1.6	1.2	1.0	0.7
Cumulative Percent	90.0	91.9	93.8	95.5	96.7	97.7	98.4
Quar	0.123	0.029	- 0.080	0.102	- 0.015	0.017	0.070
Cher	- 0.128	0.015	- 0.013	- 0.083	0.008	- 0.007	- 0.153
Arg	- 0.267	- 0.128	0.071	- 0.000	- 0.084	0.065	0.148
Qtz	0.072	0.034	0.127	- 0.137	0.122	- 0.070	- 0.095
Sand	- 0.066	0.036	- 0.013	0.170	- 0.255	0.048	0.072
Cong	- 0.189	- 0.269	- 0.189	- 0.071	- 0.155	- 0.062	- 0.037
Brec	- 0.077	- 0.215	- 0.081	- 0.070	- 0.026	0.084	0.050
Sc-1	- 0.126	0.119	0.362	0.097	- 0.053	0.065	0.030
Othr	- 0.137	- 0.056	0.110	0.134	- 0.065	0.043	- 0.159
Gran	- 0.167	0.078	- 0.052	- 0.102	0.089	0.172	- 0.011
Rhyl	0.113	0.059	- 0.132	- 0.170	0.126	- 0.102	0.125
Syen	0.220	0.032	0.098	0.122	- 0.071	- 0.032	- 0.007
Trac	0.030	- 0.039	- 0.067	0.204	0.052	- 0.137	- 0.109
Qm	0.086	0.079	- 0.146	0.053	0.002	- 0.036	- 0.024
Ql	- 0.103	- 0.089	0.218	0.145	0.146	- 0.087	- 0.026
Lat	- 0.147	- 0.028	- 0.022	- 0.232	- 0.105	- 0.074	- 0.035
Monz	0.170	0.159	- 0.020	0.014	- 0.091	0.049	- 0.026
Rhyd	0.066	0.295	- 0.003	- 0.257	- 0.109	0.069	0.007
Grod	0.126	- 0.026	- 0.216	0.151	- 0.060	0.248	- 0.044
And	0.047	- 0.037	0.059	- 0.031	- 0.022	0.002	0.008
Dior	- 0.015	0.223	- 0.167	0.124	- 0.153	- 0.174	- 0.051
Dact	0.270	- 0.186	0.215	- 0.130	- 0.086	- 0.008	- 0.007
Qd	0.244	- 0.325	- 0.068	- 0.055	- 0.067	0.046	- 0.054
Diab	- 0.196	0.052	- 0.108	0.061	0.017	- 0.220	0.108
Sc-2	0.166	- 0.064	0.140	0.047	- 0.105	- 0.090	0.153
Unkn	0.047	- 0.073	- 0.124	0.147	0.241	0.098	0.082

TABLE II, Cont.
Unrotated Factor Matrix (R-Mode)

Factor	22	23	24	26	26
Eigenvalue	0.17	0.10	0.10	0.05	0.00
Percent	0.7	0.4	0.4	0.2	0.0
Cumulative Percent	99.0	99.4	99.8	100.0	100.0
Quar	- 0.011	0.067	- 0.026	- 0.024	0.011
Cher	0.033	- 0.076	0.041	0.030	0.006
Arg	- 0.065	0.030	- 0.029	- 0.005	0.003
Qtz	0.020	- 0.070	- 0.002	0.015	0.007
Sand	0.091	- 0.038	0.061	0.014	0.002
Cong	- 0.039	0.051	- 0.009	- 0.023	0.001
Brec	0.093	- 0.022	- 0.044	0.041	0.001
Sc-1	- 0.060	- 0.026	0.048	- 0.001	0.001
Othr	- 0.037	0.076	0.065	0.064	0.001
Gran	0.117	0.023	- 0.117	- 0.095	0.002
Rhyl	0.059	0.081	0.130	- 0.017	0.002
Syen	0.070	0.004	0.020	- 0.005	0.000
Trac	0.074	- 0.036	0.015	- 0.060	0.001
Qm	- 0.237	0.044	- 0.078	0.025	0.001
Ql	0.044	0.106	- 0.089	0.013	0.001
Lat	- 0.061	- 0.038	0.025	- 0.006	0.001
Monz	0.006	- 0.112	- 0.131	0.012	0.000
Rhyd	- 0.000	0.062	0.002	0.075	0.001
Grod	0.060	- 0.008	0.062	- 0.003	0.000
And	- 0.144	- 0.075	0.092	- 0.119	0.001
Dior	0.006	0.097	- 0.021	- 0.025	0.000
Dact	0.099	0.091	0.015	- 0.001	0.001
Qd	- 0.031	- 0.037	- 0.040	0.035	0.000
Diab	0.105	- 0.096	0.001	0.060	0.000
Sc-2	- 0.032	- 0.050	- 0.058	- 0.006	0.001
Unkn	- 0.083	- 0.020	0.045	0.068	0.002

TABLE 12
 Varimax Rotated Matrix Accounting for 75.5 Percent of Total Problem Variance

Factor	1	2	3	4	5
Sum of Squares	2.767	2.670	1.909	1.716	1.913
0.899 Quar	0.694	-0.133	0.068	0.156	-0.142
0.843 Cher	-0.141	0.164	0.858	-0.131	-0.024
0.721 Arg	0.059	0.030	0.075	-0.779	0.133
0.854 Qtz	-0.214	-0.155	-0.812	0.045	-0.184
0.715 Sand	-0.483	-0.030	-0.150	0.342	0.010
0.699 Cong	-0.118	-0.205	-0.004	0.464	0.018
0.737 Brec	-0.057	-0.001	0.026	0.168	-0.010
0.661 Sc-1	-0.111	-0.221	-0.051	0.400	0.084
0.756 Othr	-0.080	0.231	-0.260	-0.321	0.196
0.754 Gran	-0.626	0.263	-0.066	-0.107	0.241
0.839 Rhyl	-0.166	-0.134	0.016	-0.059	0.125
0.653 Syen	-0.084	-0.193	0.376	-0.535	-0.187
0.694 Trac	0.025	-0.150	0.002	-0.072	0.775
0.807 Qm	-0.050	0.431	0.044	-0.025	-0.020
0.793 Ql	-0.133	0.338	0.180	0.251	0.169
0.692 Lat	-0.009	-0.150	-0.137	-0.016	-0.146
0.873 Monz	-0.023	0.049	0.153	0.039	-0.092
0.766 Rhyd	-0.156	0.225	0.122	0.046	0.788
0.718 Grod	0.217	0.366	-0.255	-0.065	0.026
0.840 And	-0.260	0.785	0.201	0.018	0.215
0.726 Dior	-0.632	0.001	-0.099	-0.023	-0.205
0.621 Dact	-0.176	0.690	0.159	0.069	-0.198
0.668 Qd	-0.296	-0.063	-0.059	-0.134	0.369
0.782 Diab	0.161	0.835	-0.003	-0.117	0.044
0.757 Sc-2	-0.323	-0.076	-0.117	-0.012	0.364
0.774 Unkn	-0.844	0.020	0.125	0.164	0.084

TABLE 12, Cont.
 Varimax Rotated Matrix Accounting for 75.5 Percent of Total Problem Variance

Factor	6	7	8	9	10
Sum of Squares	1.681	1.945	1.397	1.577	2.066
0.899 Quar	0.060	0.156	-0.123	0.044	0.553
0.843 Cher	-0.048	0.022	0.076	-0.140	-0.121
0.721 Arg	-0.132	-0.190	-0.115	-0.142	0.009
0.854 Qtz	-0.078	0.164	0.144	0.010	-0.189
0.715 Sand	-0.351	0.083	-0.398	0.041	-0.226
0.699 Cong	-0.427	-0.127	0.400	-0.176	-0.194
0.737 Brec	0.826	-0.057	0.054	-0.033	-0.121
0.661 Sc-1	0.319	-0.158	-0.125	-0.042	-0.534
0.756 Othr	0.306	-0.580	0.210	-0.087	0.077
0.754 Gran	0.101	-0.102	-0.027	-0.007	-0.446
0.839 Rhyl	0.102	-0.729	-0.041	0.029	-0.479
0.653 Syen	-0.118	0.156	0.175	0.066	-0.269
0.694 Trac	0.028	-0.171	0.004	-0.142	-0.123
0.807 Qm	-0.021	0.040	-0.019	-0.018	-0.783
0.793 Ql	-0.242	-0.039	-0.110	0.681	-0.046
0.692 Lat	0.104	0.019	-0.025	0.776	0.124
0.873 Monz	-0.082	-0.908	-0.020	-0.015	0.074
0.766 Rhyd	-0.130	0.155	0.026	0.081	0.064
0.718 Grod	-0.041	0.089	0.290	0.561	-0.240
0.840 And	0.139	-0.064	-0.082	0.163	0.111
0.726 Dior	0.514	0.026	-0.068	0.004	0.067
0.621 Dact	-0.055	-0.049	0.014	-0.148	-0.129
0.668 Qd	0.135	0.030	-0.604	0.081	-0.171
0.782 Diab	-0.013	0.027	0.015	0.108	-0.175
0.757 Sc-2	0.177	-0.023	0.671	0.112	-0.073
0.774 Unkn	-0.009	-0.077	0.044	0.007	0.052

TABLE 13
List of R-Mode Factor Scores

Factor	1	2	3	4	5	6	7	8	9	10
SC-F-1	-0.876	0.226	0.023	1.276	-0.512	-1.686	0.457	-0.836	0.001	-1.663
A-C-2	-0.438	-0.556	-0.649	1.292	-0.484	1.586	0.036	-0.209	-0.487	-1.318
A-C-8	-0.098	-0.355	-0.829	1.803	-0.267	-1.032	0.218	0.462	-0.635	0.807
A-C-11	0.717	-0.333	-0.877	0.566	-0.612	0.496	0.196	-1.234	0.649	-0.984
A-C-14	0.242	0.105	-1.603	-0.242	0.565	0.165	0.204	0.923	-0.440	0.835
SC-C-14	0.827	-0.279	-1.207	0.072	0.359	-0.624	0.095	0.332	-0.689	-0.133
SC-C-6	0.378	-0.238	-0.595	0.059	-0.412	-1.276	0.175	0.230	-0.822	0.674
SC-C-1	0.896	-0.108	1.280	-0.069	-0.374	0.196	0.520	-0.205	-0.340	0.987
UV-C-6	0.438	0.052	-1.416	-0.385	-0.630	-0.533	0.295	-0.619	-0.473	-0.159
UV-C-2	0.523	-0.492	-1.196	0.334	-0.444	0.110	0.114	0.244	5.222	0.531
UV-C-13	-0.010	-0.262	-1.684	-0.307	-0.469	-0.860	0.083	-0.037	-0.691	0.428
2-13	0.549	-0.017	-1.117	0.183	-0.515	-0.604	0.354	-0.928	-0.427	0.505
2-8	0.636	0.101	-0.251	-1.140	-0.419	-0.360	0.505	-0.545	-0.576	0.280
5-20	0.933	-0.743	0.928	-0.028	-0.241	0.846	-0.041	-0.644	1.796	0.438
5-24	1.044	-0.231	-0.625	0.494	-0.343	1.137	0.143	-0.540	-0.287	0.327
5-31	1.184	0.383	-1.173	-0.460	0.116	-0.532	0.485	-0.087	1.190	0.051
5-34	0.702	-0.231	0.429	0.916	-0.311	-0.100	0.281	-0.071	0.031	0.428
5-37	0.417	-0.056	-0.930	-0.635	-0.218	-0.575	0.594	-0.495	-0.639	0.390
5-39	0.685	-0.198	1.217	-1.038	-0.276	-0.375	0.264	-0.155	-0.558	0.849
11-10A	-0.935	0.642	-0.706	-0.044	-0.864	3.746	0.247	-0.047	-0.560	0.709
SR-A-11	1.141	-0.130	1.387	0.568	-0.182	0.526	0.549	0.054	-0.167	1.233
SR-A-1	1.432	-0.165	0.722	0.048	-0.118	0.425	0.281	-0.711	-0.271	1.143
4-3	1.171	-0.120	0.896	0.621	-0.262	0.062	0.375	-0.272	-0.339	1.213
4-2	0.965	-0.070	0.765	0.313	-0.414	0.250	0.570	-0.187	-0.314	1.052
A-D-3	-2.616	1.884	1.915	1.848	-1.300	0.676	-1.203	0.351	-0.087	1.288
A-D-8	-0.071	1.484	0.264	-0.284	-0.868	-0.348	0.280	-0.072	-1.441	-1.172
A-D-12	0.283	-0.646	0.378	0.173	0.773	1.368	-0.186	1.066	-0.304	0.058
A-D-14	0.454	0.165	-0.244	-0.651	-0.286	-0.584	0.080	1.506	0.631	-1.145

TABLE 13, Cont.
List of R-Mode Factor Scores

Factor	1	2	3	4	5	6	7	8	9	10
A-D-16	-0.381	-0.351	0.424	1.177	-0.235	-1.022	0.146	1.281	-0.073	-0.258
SC-D-11	-0.514	0.550	-0.824	-1.797	1.479	1.488	-1.321	1.924	-0.576	0.854
SC-D-14	1.101	5.725	-0.022	-0.804	0.304	-0.092	0.188	0.105	0.741	-1.198
SC-D-17	-0.210	-0.748	0.993	1.667	1.086	-0.771	-0.375	0.198	0.485	-1.058
SC-D-19	-0.573	-1.320	2.577	-3.670	-1.279	-0.811	1.071	1.202	0.452	-1.848
SC-D-7	-1.659	-0.023	-0.783	0.016	-0.868	-0.087	0.617	-0.661	-0.476	0.320
SC-D-5	-0.195	-0.370	-1.180	0.811	0.817	0.681	0.461	2.753	0.524	-1.945
SC-D-4	-1.461	1.176	1.358	0.222	2.922	-0.825	0.382	-1.943	1.568	0.884
SC-D-2	0.902	-0.271	-0.188	-1.085	0.157	-0.593	-5.745	-0.389	-0.228	0.024
G-2	0.432	-0.540	0.982	0.968	-0.532	-0.851	-2.283	0.101	0.288	-0.122
G-7	-0.012	-0.289	0.634	-0.202	1.043	0.741	0.198	1.643	-0.222	0.267
G-11	-1.783	-0.130	-1.187	-0.161	-0.307	-0.442	-0.414	1.165	0.430	0.477
2-5	-1.260	0.233	-0.270	0.381	-0.801	-1.676	-0.024	-0.317	-1.083	-0.592
5-2	-0.296	-0.227	0.069	-0.362	-0.206	-0.723	0.200	-0.671	0.206	0.237
5-6	-2.427	-0.484	0.015	-1.663	-1.049	0.571	0.459	0.073	0.671	1.298
5-9	-1.674	-0.329	0.365	0.282	-0.618	-0.349	-0.160	0.238	0.418	0.405
5-14	-0.480	-0.433	0.107	0.322	4.275	-0.889	0.891	0.671	-0.894	0.633
5-17	0.932	-0.373	1.100	1.396	-0.034	1.896	-0.015	-0.175	-0.637	-2.780
11-2	0.677	-0.375	0.852	-0.989	1.052	0.349	0.337	-0.721	-0.761	-0.036
11-16A	-1.567	-0.961	-1.004	-1.082	1.494	1.348	-0.386	-3.641	-0.061	-1.635
11-5A	-0.125	-0.272	0.884	-0.344	0.309	-0.048	-0.199	-0.111	0.253	-1.581

TABLE 14
Q-Mode Varimax Factor Matrix on Ten R-Mode Factors

	1	2	3	4	5	6	7	8	9	\bar{I}_0
1 SC-F-1	1.0000	-0.0925	-0.8378	0.2838	0.1416	-0.0006	-0.2187	0.0579	-0.1363	-0.0005
2 A-C-2	1.0013	-0.1988	-0.0587	-0.0159	0.0471	0.8624	-0.1516	0.2277	-0.1544	-0.2199
3 A-C-8	1.0008	0.3167	-0.1476	0.7067	-0.0138	-0.0063	-0.1251	0.5373	-0.0394	-0.2556
4 A-C-11	1.0016	0.1591	-0.4954	-0.2540	0.2727	0.6337	0.4072	0.1180	-0.0423	-0.0330
5 A-C-14	1.0000	0.6178	0.6596	0.1664	0.0134	-0.0522	0.0802	0.2885	-0.1697	0.0253
6 SC-C-14	1.0003	0.7372	0.1685	0.2541	0.5485	0.0188	-0.0824	0.1220	-0.0031	-0.1136
7 SC-C-6	1.0004	0.7595	-0.1186	0.4689	0.0194	-0.2686	-0.2343	0.0317	0.1088	-0.1241
8 SC-C-1	0.9993	-0.0686	0.0344	-0.0472	-0.0378	-0.0858	-0.0726	-0.1768	-0.0338	0.0057
9 UV-C-6	0.9997	0.9020	-0.2966	-0.0976	0.0700	0.2058	-0.0065	0.0037	-0.0249	0.1073
10 UV-C-2	1.0014	-0.0979	-0.0885	0.1011	-0.1005	-0.0153	0.9731	0.0187	-0.0100	0.0248
11 UV-C-13	0.9994	0.9268	-0.2461	0.1664	-0.1217	-0.0190	-0.0791	0.1158	0.0460	-0.1146
12 2-13	1.0000	0.8938	-0.3409	-0.1448	-0.0026	0.0309	0.0489	0.1904	-0.0076	0.0205
13 2-8	1.0005	0.7292	-0.0975	-0.3691	0.0048	-0.1231	-0.1360	-0.3988	-0.0679	0.1772
14 5-20	1.0002	-0.3525	-0.0799	-0.2648	0.0057	0.1100	0.7257	-0.1384	0.1142	-0.1449
15 5-24	1.0006	0.3019	0.1463	-0.2332	0.1639	0.6846	0.1864	0.3356	-0.0185	-0.0419
16 5-31	1.0008	0.4963	-0.0523	-0.0110	0.3192	-0.1268	0.7129	-0.0409	-0.1212	0.3211
17 5-34	1.0001	-0.0780	-0.2409	0.4233	0.2024	0.1659	0.1551	0.2429	-0.0114	-0.1358
18 5-37	1.0000	0.9416	-0.1207	-0.1705	0.0295	-0.1160	-0.1046	-0.0460	-0.1825	0.0038
19 5-39	1.0004	0.1343	0.0585	-0.1759	-0.0682	-0.3758	-0.2091	-0.4848	0.1145	-0.0132
20 11-10-A	1.0010	-0.0874	0.4198	-0.3245	-0.4784	0.6119	-0.0551	0.2142	-0.1941	0.1355
21 SR-A-11	0.9991	-0.2046	0.1482	0.0983	0.0422	0.0089	0.0446	0.0429	-0.0661	-0.0217
22 SR-A-1	0.9994	0.1289	0.0571	-0.2487	0.1492	0.0233	0.1037	0.0827	0.0735	-0.0147
23 4-3	0.9995	0.0302	-0.0062	0.1164	0.0936	-0.0294	0.0131	0.1634	0.0338	-0.0371
24 4-2	0.9995	0.0718	0.0390	0.0634	-0.0142	0.0491	0.0136	0.0413	-0.0864	0.0119
25 A-D-3	1.0008	-0.5319	-0.0808	0.2295	-0.6178	0.0047	-0.2697	0.3245	0.1679	0.2453
26 A-D-8	1.0011	0.1082	-0.2685	0.0392	0.0529	0.1943	-0.6794	-0.2422	-0.0669	0.5859
27 A-D-12	0.9997	-0.3874	0.7912	0.0226	0.1951	0.2745	-0.0509	-0.0047	-0.0539	-0.2982

TABLE 14, Cont.
Q-Mode Varimax Factor Matrix on Ten R-Mode Factors

	1	2	3	4	5	6	7	8	9	10	
28 A-D-14	1.0008	0.0375	-0.4080	0.1510	0.4488	0.2724	0.0059	0.2311	-0.6345	-0.0019	0.2801
29 A-D-16	1.0008	-0.2389	-0.0818	-0.1251	0.9148	0.0567	-0.1102	-0.1610	-0.0338	-0.0445	-0.2002
30 SC-D-11	1.0005	0.0322	-0.2875	0.8972	-0.1736	-0.1345	-0.1347	-0.0898	-0.0081	0.1522	0.1186
31 SC-D-14	1.0013	-0.0665	-0.1059	-0.0208	-0.0896	0.1600	-0.1026	-0.0040	0.0347	-0.0775	0.9663
32 SC-D-17	1.0006	-0.6100	-0.1542	-0.2797	0.3416	0.4687	-0.1470	-0.0190	0.1723	0.0479	-0.3690
33 SC-D-19	1.0013	-0.1498	-0.0421	-0.0527	-0.0641	-0.1132	-0.1555	-0.0707	-0.9570	-0.0806	-0.0765
34 SC-D-7	1.0002	0.3015	-0.2613	-0.3358	-0.0594	-0.7083	0.1074	-0.2611	0.1793	-0.3028	-0.1396
35 SC-D-5	1.0004	-0.1820	-0.5479	0.3956	0.4658	0.3073	0.2958	0.1243	-0.0960	-0.2913	-0.0459
36 SC-D-4	1.0009	-0.4083	-0.0330	-0.2077	-0.3656	0.0099	-0.6756	0.1123	0.3759	-0.2100	0.0409
37 SC-D-2	1.0019	0.0195	-0.1750	0.1250	-0.1673	0.1020	-0.0759	-0.0234	0.0309	0.9537	-0.0058
38 G-2	1.0011	-0.3092	0.0836	-0.2193	0.3072	0.1215	-0.0223	0.0145	0.0394	0.8464	-0.1500
39 G-7	1.0003	-0.3722	0.0639	0.8224	0.2051	0.1150	-0.1453	-0.1018	-0.1602	-0.2180	-0.1464
40 G-11	1.0001	0.1475	-0.6157	0.2056	0.3776	-0.5974	-0.1638	0.0916	0.0831	0.0318	-0.1200
41 2-5	0.9994	0.2358	-0.3397	-0.5819	0.3169	-0.2033	-0.1374	-0.5712	0.0104	0.0477	-0.0211
42 5-2	1.0001	0.2979	0.0466	-0.6517	-0.2245	-0.3008	-0.5067	0.0994	-0.1674	-0.0059	-0.2211
43 5-6	1.0013	0.0182	-0.1297	0.1004	-0.1916	-0.8945	-0.1441	0.0952	-0.2417	-0.1529	-0.1604
44 5-9	1.0004	-0.3086	-0.2278	-0.2289	0.3030	-0.7721	-0.1826	-0.0368	0.0132	0.0301	-0.2778
45 5-14	1.0011	-0.0937	-0.1134	0.3457	-0.0223	0.3944	-0.5991	-0.2068	0.3066	-0.3489	-0.2940
46 5-17	1.0009	-0.4880	0.0170	-0.0850	-0.0742	0.4823	0.6772	-0.2102	-0.0960	-0.0626	-0.0338
47 11-2	1.0005	-0.0314	0.3610	0.1825	-0.6539	0.4018	-0.2308	-0.2908	-0.2461	-0.1253	-0.1810
48 11-16-A	1.0011	-0.0301	-0.3891	-0.2468	-0.8138	0.0364	0.1170	-0.0606	0.1463	-0.0710	-0.2836
49 11-5-A	1.0010	-0.5618	-0.3328	-0.2616	-0.2074	0.3955	0.0437	-0.1268	-0.5300	0.0451	-0.0771
Variance	17.127	17.126	17.126	11.885	10.313	9.938	8.919	7.648	7.132	4.840	5.117
Cum. Variance	17.127	34.253	34.253	46.138	56.451	66.389	75.308	82.956	90.088	94.928	100.045

TABLE 15
 Groups of Samples Having > 75% Total Variance
 Accounted for by Each Q-Mode Factor

Factors	Samples
1	5-37 (+) UV-C-13 (+) UV-C-6 (+) 2-13 (+)
2	4-2 (+) 4-3 (+) SC-C-1 (+) SR-A-11 (+) SR-A-1 (+)
3	SC-D-11 (+)
4	A-D-16 (+)
5	5-6 (-)
6	none
7	UV-C-2 (+)
8	SC-D-19 (-)
9	SC-D-2 (+)
10	SC-D-14 (+)

TABLE 16
The 10 Single Samples Which Are Most Representative of Each Q-Mode Factor

Variables	Factors				
	Sample No. 5-37 (+)	4-2 (+)	3 SC-D-11 (+)	4 A-D-16 (+)	5 5-6 (-)
Quartz	32.0	52.8	22.0	26.2	20
Chert	17.9	25.9	19.4	26.2	25
Argillite	10.3	3.8	14.1	4.8	15
Quartzite	34.8	17.3	19.4	28.1	24
Sandstone	2.8	--	.9	1.9	3
Conglomerate	--	--	--	3.9	--
Breccia	--	--	1.8	--	--
Schist	--	--	--	1.0	--
Others	--	--	5.3	--	--
Granite	--	--	3.5	1.9	3
Rhyolite	--	--	2.6	1.0	1
Syenite	--	--	--	--	--
Trachyte	.9	--	1.8	--	--
Quartz Monzonite	.9	--	.9	1.0	--
Quartz Latite	--	--	--	1.0	--
Latite	--	--	--	--	1
Monzonite	--	--	--	--	--
Rhyodacite	--	--	--	--	--
Granodiorite	--	--	--	--	--
Andesite	--	--	.9	--	--
Diorite	--	--	--	--	2
Dacite	--	--	--	--	--
Quartz Diorite	--	--	--	--	--
Diabase	--	--	--	--	--
Schist	--	--	5.3	1.9	2
Unknown	--	--	1.8	1.9	4

TABLE 16, Cont.
The 10 Single Samples Which Are Most Representative of Each Q-Mode Factor

Variables	Factors					
	Sample No.	6	7	8	9	10
		A-C-2 (+)	UV-C-2 (+)	SC-D-19 (-)	SC-D-2 (+)	SC-D-14 (+)
Quartz		25.1	42.7	23.4	29.4	27.3
Chert		16.7	4.4	31.5	17.6	25.5
Argillite		3.7	6.2	15.3	15.7	11.4
Quartzite		32.6	32.9	18.0	14.7	13.2
Sandstone		2.8	2.7	--	1.0	--
Conglomerate		.9	--	.9	1.0	--
Breccia		.9	.9	--	--	--
Schist		5.6	.9	--	1.0	--
Others		.9	--	--	3.9	1.8
Granite		3.7	--	2.7	2.0	5.3
Rhyolite		1.9	--	1.8	8.8	.9
Syenite		--	--	.9	--	--
Trachyte		--	--	--	2.0	--
Quartz Monzonite		.9	--	2.7	1.0	5.3
Quartz Latite		--	2.7	--	--	1.8
Latite		--	2.7	--	--	--
Monzonite		--	--	--	2.0	--
Rhyodacite		--	--	--	--	.9
Granodiorite		--	.9	--	--	.9
Andesite		--	--	--	--	2.6
Diorite		.9	--	--	--	--
Dacite		--	--	--	--	1.8
Quartz Diorite		--	--	--	--	--
Diabase		--	--	--	--	.9
Schist		.9	1.8	.9	--	--
Unknown		1.9	.9	1.8	--	--

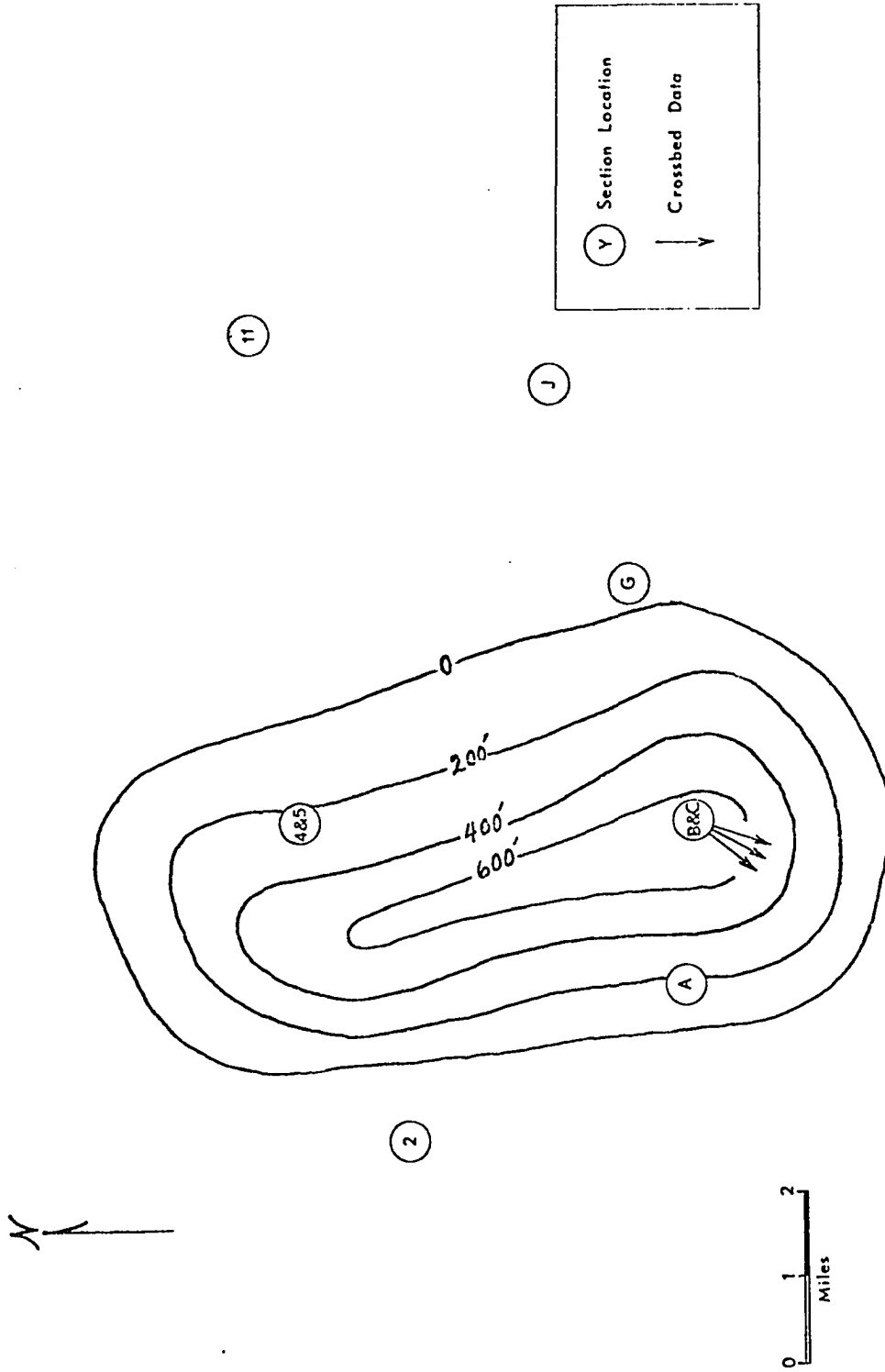
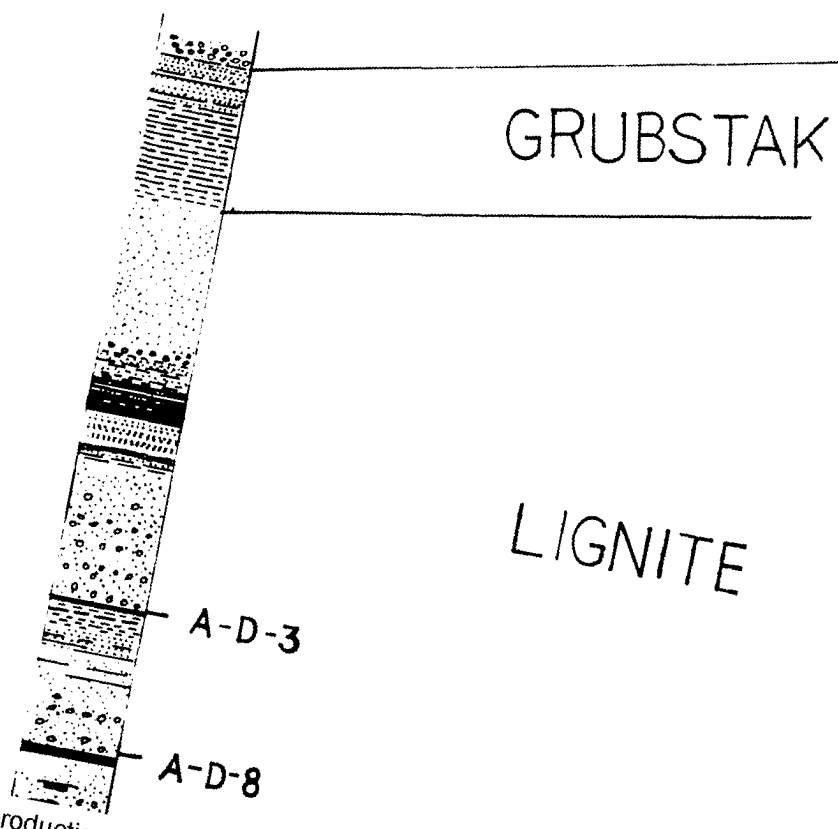


Figure 26. Isopach map of Q-mode factor 2. Stratigraphic interval covered is the Healy Creek Formation.



Reproduced with permission of the copyright owner. Further reproduction prohibited without permission.

GRUBSTAKE

LIGNITE

-D-3

-D-8

SC-F-1

SC-D-11

SC-D-14

SC-D-17

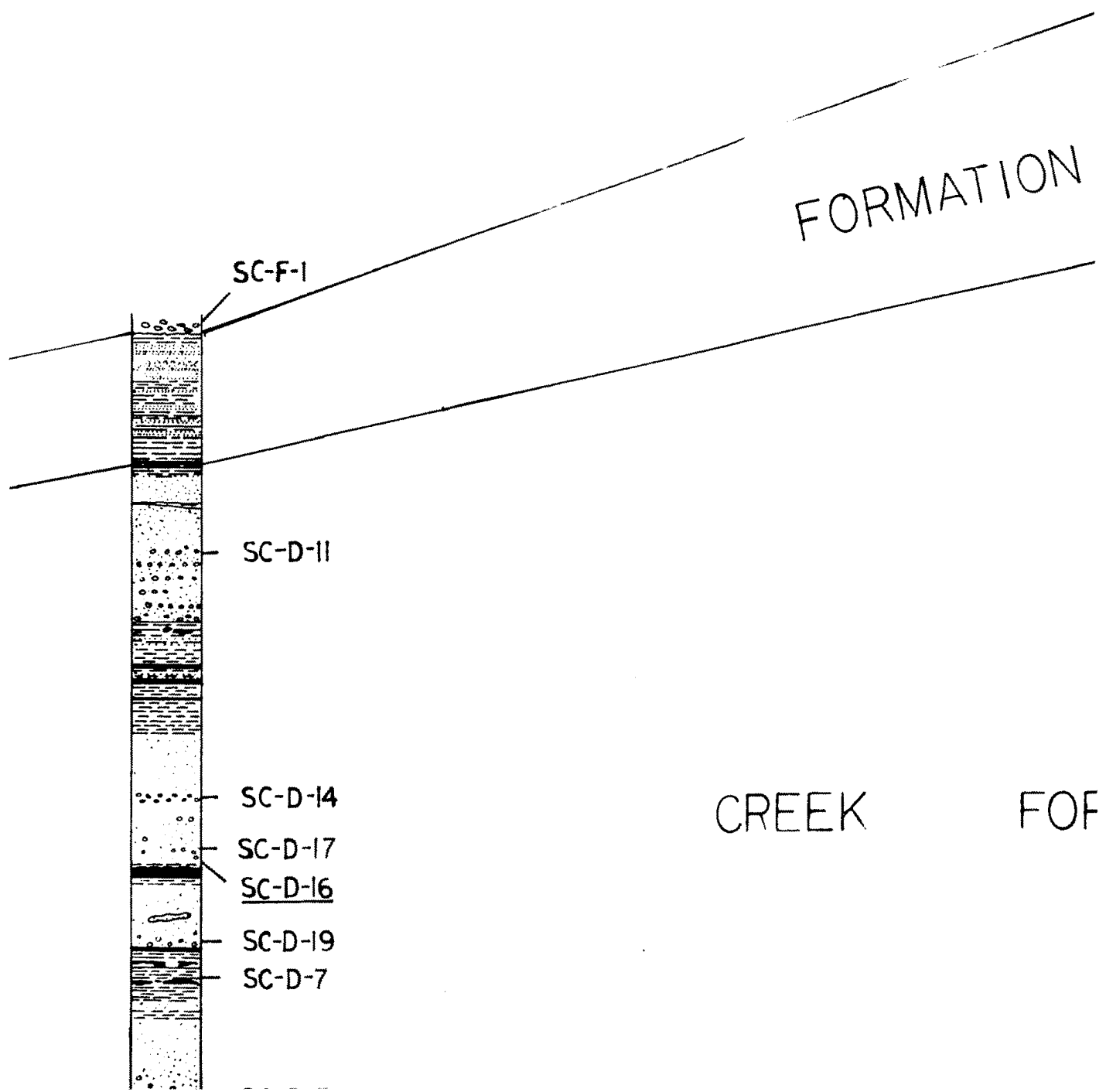
SC-D-16

SC-D-19

SC-D-7

SC-D-5

Reproduced with permission of the copyright owner. Further reproduction prohibited without permission.



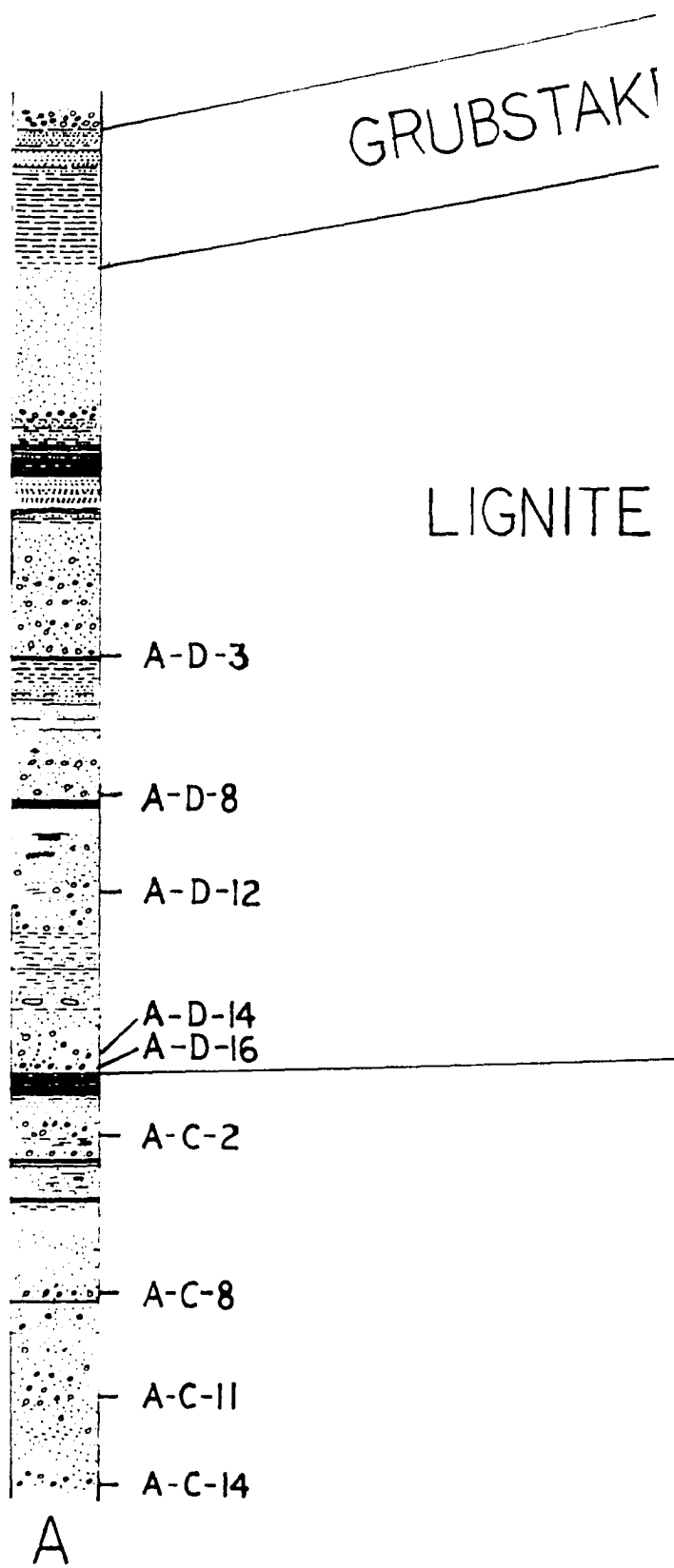
Reproduced with permission of the copyright owner. Further reproduction prohibited without permission.

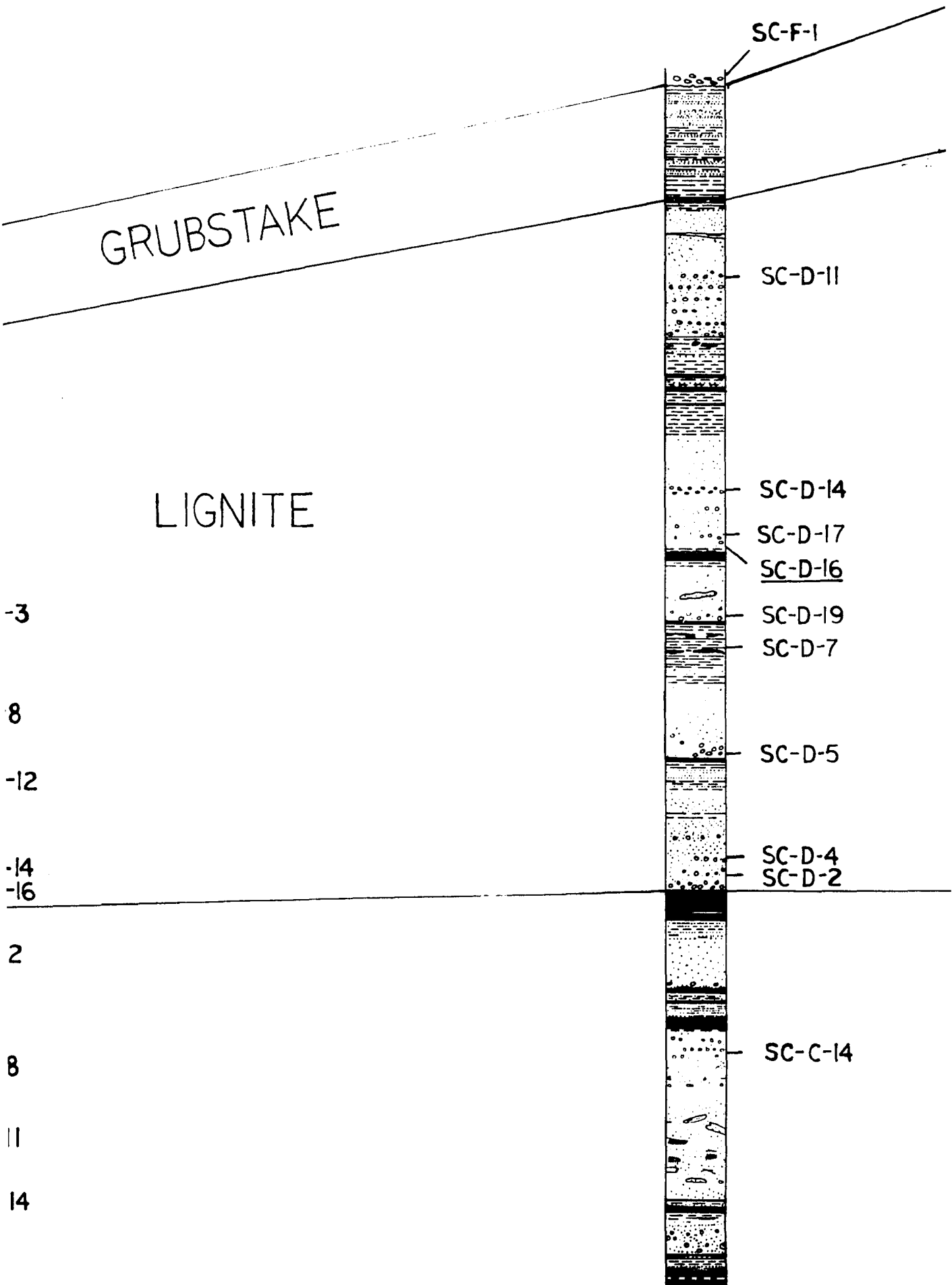


FORMATION

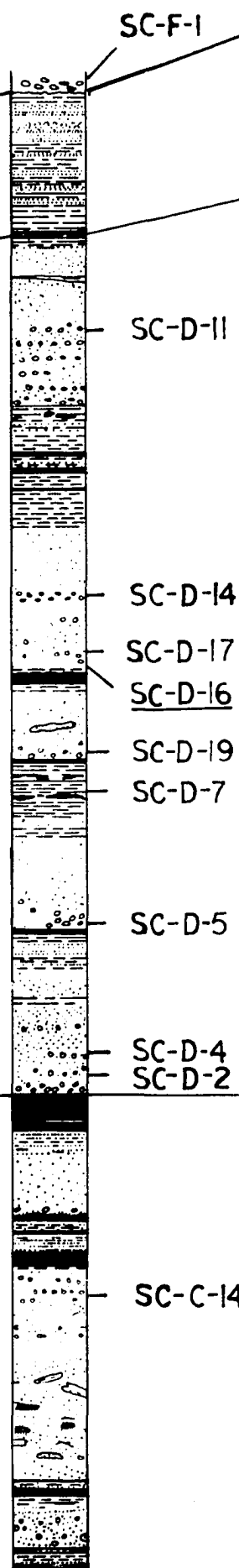
CREEK

FORMATION





FORMATION



CREEK FOR

COAL

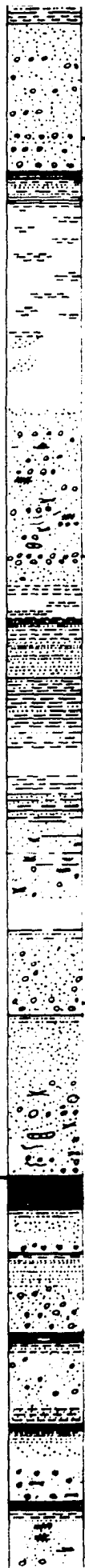


MATION

FORMATION

COAL #6

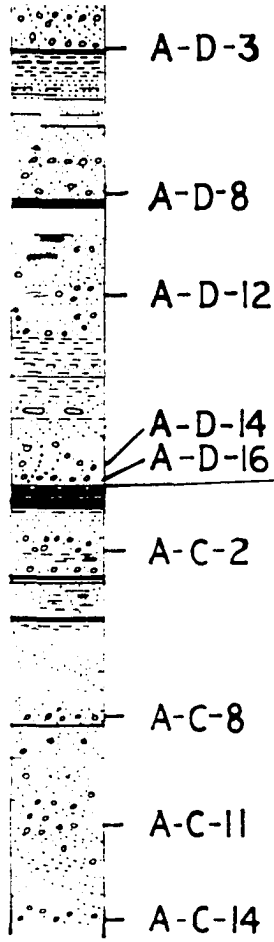




G-2

G-7

G-11

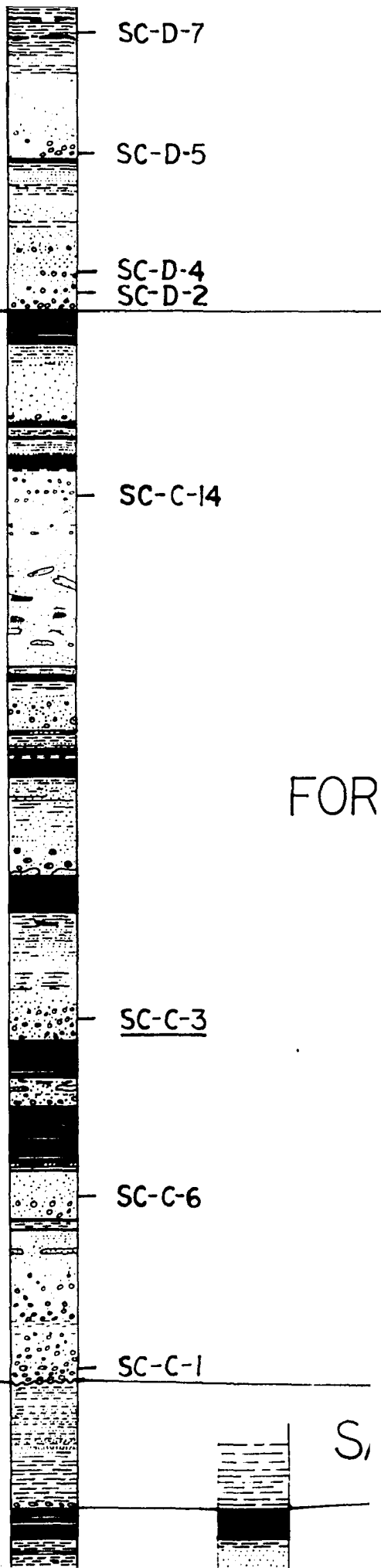


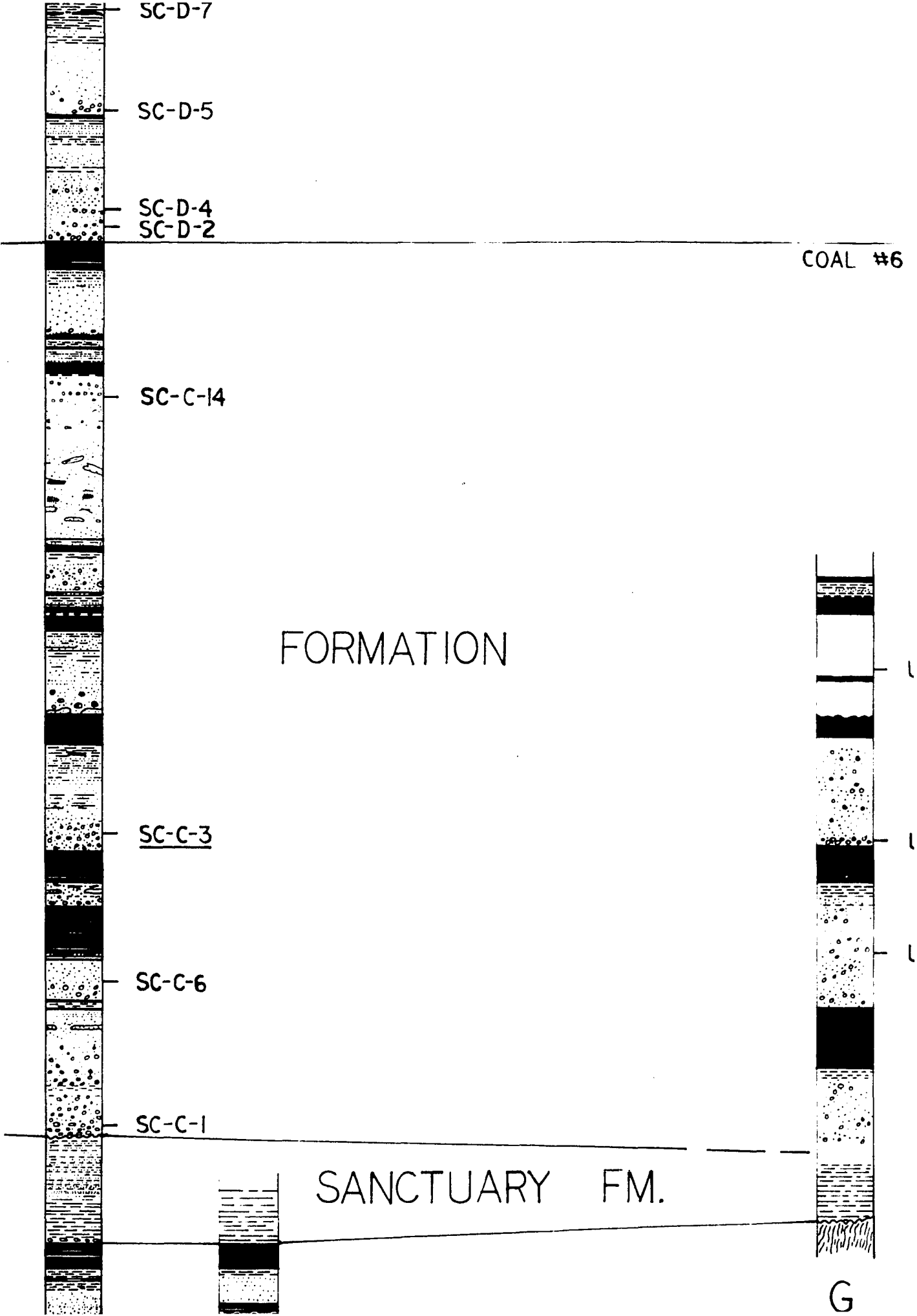
A

SUNTR

SUNTRANA

FOR








G-II

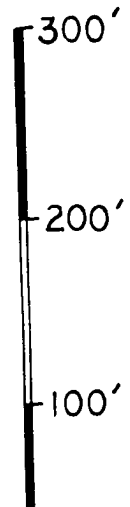
J

LEGEND

 **CROSSBEDDED PEBBLY SANDSTONE**

Reproduced with permission of the copyright owner. Further reproduction prohibited without permission.

HE



SUN TRANA

FORMAT



HEALY CREEK

SANCT

B

C

FORMATION

UV-C-6

UV-C-2

UV-C-13

SANCTUARY FM.

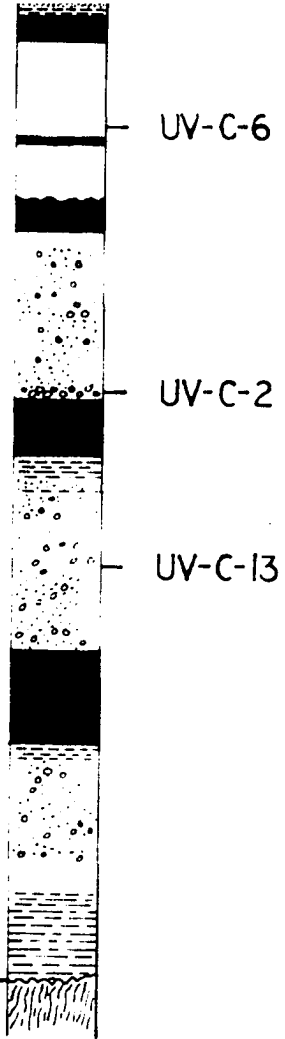
G

SR-A-II

FORMATION

SR-A-7

SR-A-I

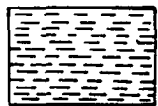


G

LEGEND



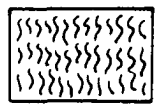
CROSSBEDDED PEBBLY



SHALE



COAL



SCHIST

A-D-4

PEBBLE SAMPLE

A-C-7

SAND SAMPLE

LEGEND

CROSSBEDDED PEBBLY SANDSTONE

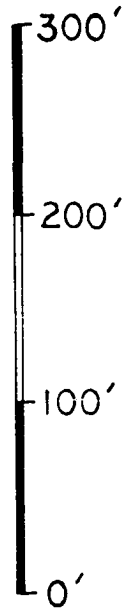
SHALE

COAL

SCHIST

PEBBLE SAMPLE

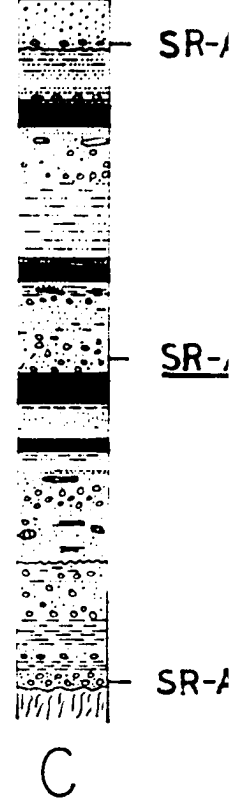
SAND SAMPLE



SCALE

HEALY CREEK

00'
00'
00'
00'
E



HEALY CREEK STRATIGRAPHY

(AFTER WAHRHAUFEN)

K



FORMATION

C

Y CREEK STRATIGRAPHIC SECTIONS —

(AFTER WAHRHAFTIG, ET AL., 1951 and 1969)

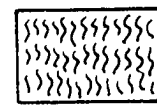
ON



SHALE



COAL



SCHIST

A-D-4

PEBBLE SAM

A-C-7

SAND SAMF

IONS — PLATE I

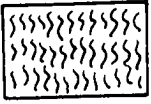
1951 and 1969)



SHALE



COAL



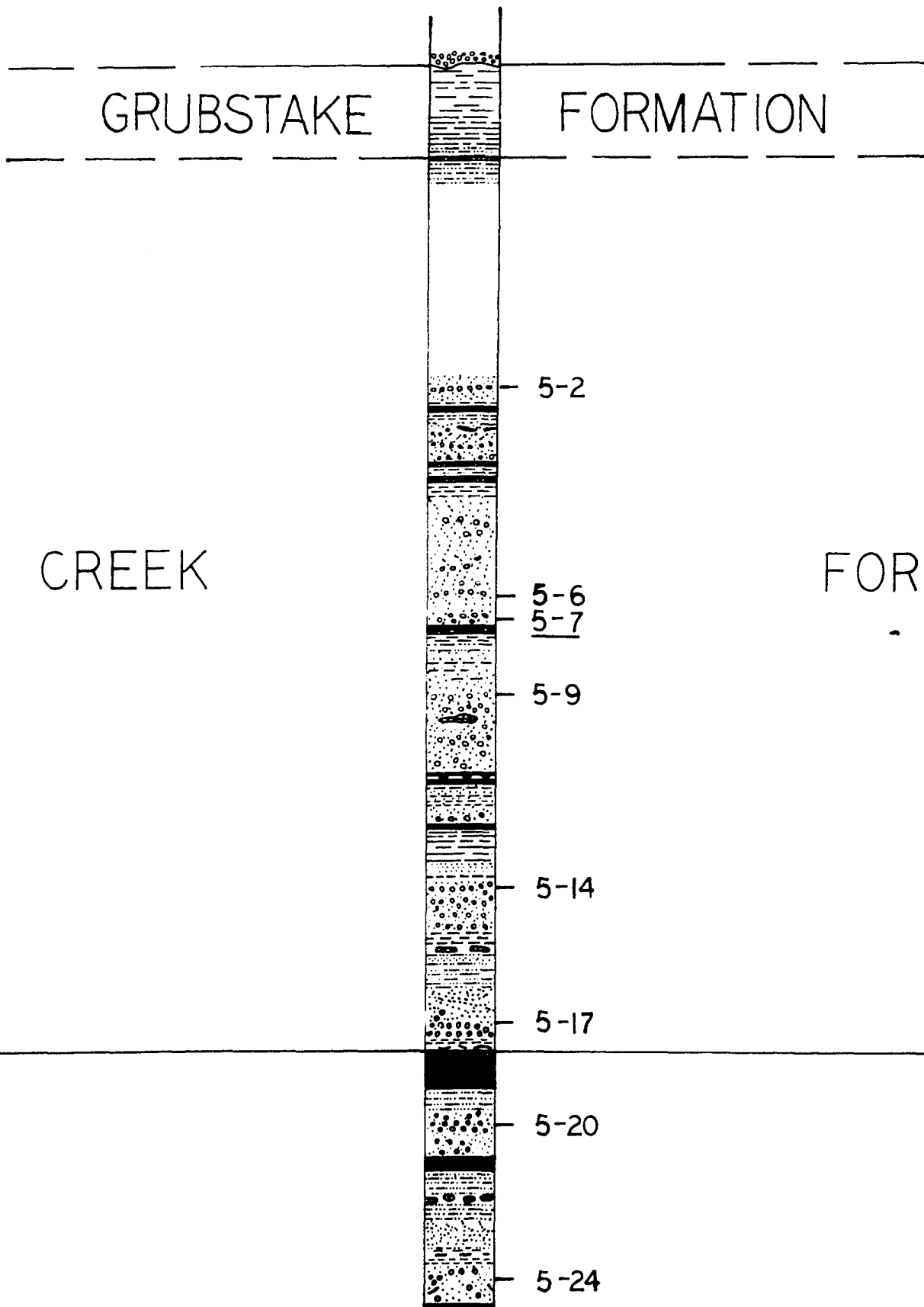
SCHIST

A-D-4

PEBBLE SAMPLE

A-C-7

SAND SAMPLE



Reproduced with permission of the copyright owner. Further reproduction prohibited without permission.

FORMATION

FORMATION

FORMATION

- 5-2

- 5-6
- 5-7

- 5-9

- 5-14

- 5-17

- 5-20

- 5-24



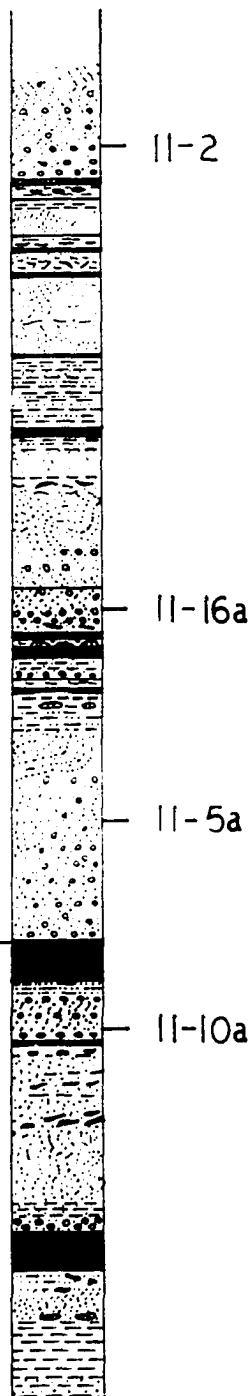
11-2

11-16a

11-5a

11-10a

MATION



FORMATION

IGNITE CREEK

FC

5-6

5-7

5-9

5-14

5-17

5-20

5-24

5-31

5-32

5-34

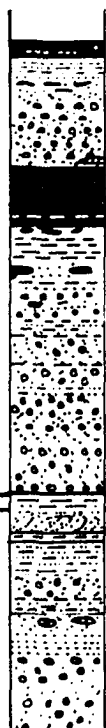
5-37

5-39

SUNTRANA

FC

UARY FM.



4-3

5

FORMATIO

FORMATION

6
7

9

-14

-17

-20

-24

FORMATION

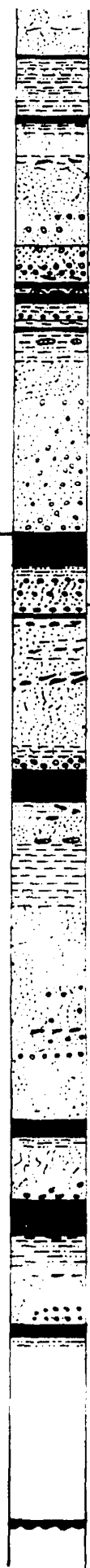
-31

-32

-34

-37

-39



11-16a

11-5a

11-10a

11

FORMATION

ATION

ATION

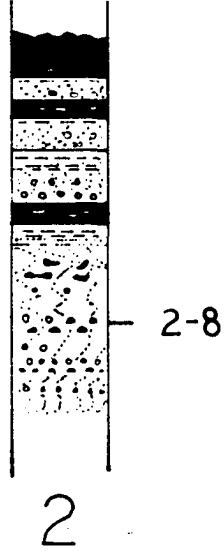


11-16a

11-5a

11-10a

11



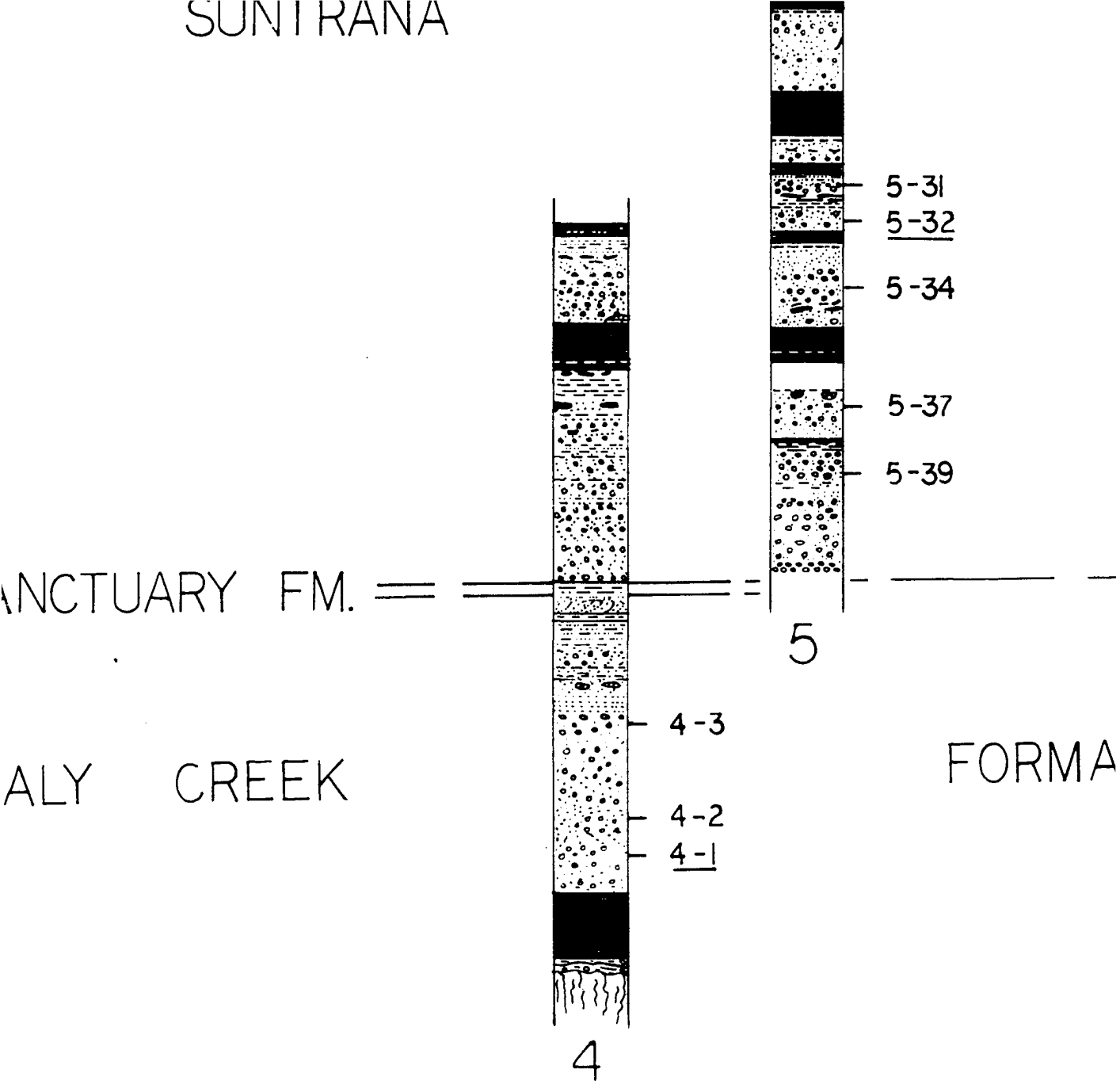
SANCTUARY FM

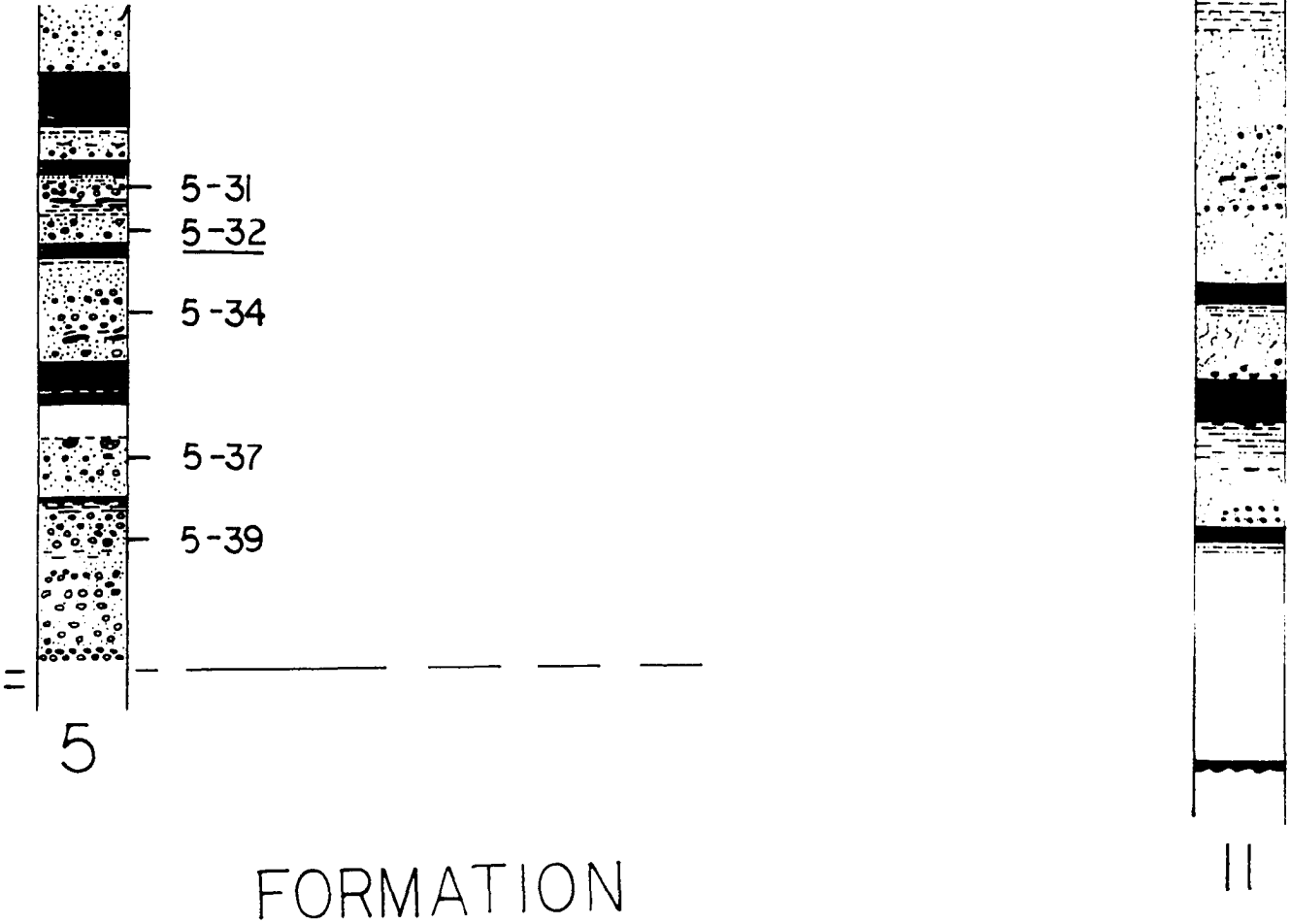
HEALY CREEK



SCALE

SUNIRANA





LEGEND



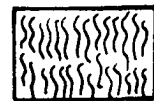
CROSSBEDDED PEBBLY SAND



SHALE



COAL



SCHIST

A-D-4

PEBBLE SAMPLE

A-C-7

SAND SAMPLE



LEGEND

CROSSBEDDED PEBBLY SANDSTONE

SHALE

COAL

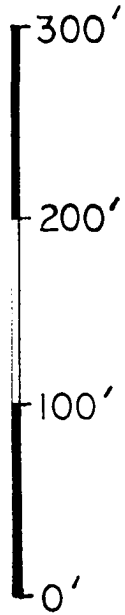
SCHIST

PEBBLE SAMPLE

SAND SAMPLE

SANCTUARY I

HEALY CREEK



SCALE

LIGNITE CREEK

(AF)

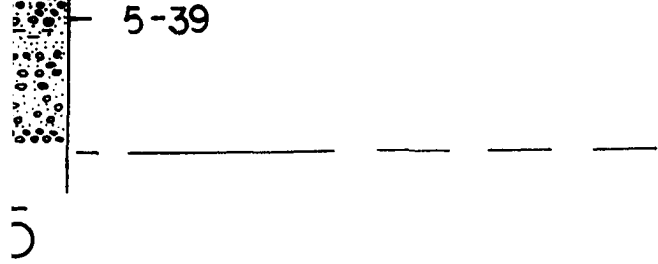
ACTUARY FM.

LY CREEK

FORMAT



NITE CREEK STRATIGRAPHIC SECTIONS
 (AFTER WAHRHAFTIG, ET AL., 1951 and 196



FORMATION

II

LEGEND

	CROSSBEDDED PEBBLY SANDSTONE
	SHALE
	COAL
	SCHIST
A-D-4	PEBBLE SAMPLE
<u>A-C-7</u>	SAND SAMPLE

SECTIONS — PLATE II

AL., 1951 and 1969)



LEGEND

SBEDDED PEBBLY SANDSTONE

LE

ST

BLE SAMPLE

D SAMPLE

I